Statistical Mechanics of MAP Estimation: General Replica Ansatz

Ali Bereyhi, Ralf R. Müller, and Hermann Schulz-Baldes

arXiv:1612.01980v1 [cs.IT] 6 Dec 2016

Abstract

The large-system performance of maximum-a-posterior estimation is studied considering a general distortion function when the observation vector is received through a linear system with additive white Gaussian noise. The analysis considers the system matrix to be chosen from a large class of random ensembles. We take a statistical mechanical approach by introducing a spin glass corresponding to the estimator, and employing the replica method for the large-system analysis. In contrast to earlier replica based studies, our analysis evaluates the general replica ansatz of the corresponding spin glass and determines the asymptotic distortion of the estimator for any structure of the replica correlation matrix. Consequently, the replica symmetric as well as the replica symmetry breaking ansatz with b steps of breaking is deduced from the given general replica ansatz. The generality of our distortion function lets us derive a more general form of the maximum-a-posterior decoupling principle. Based on the general replica ansatz, we show that for any structure of the replica correlation matrix, the vector-valued system decouples into a bank of equivalent decoupled linear systems followed by maximum-a-posterior estimators. The structure of the decoupled linear system is further studied under both the replica symmetry and the replica symmetry breaking assumptions. For b steps of symmetry breaking, the decoupled system is found to be an additive system with a noise term given as the sum of an independent Gaussian random variable with b correlated impairment terms. The general decoupling property of the maximum-a-posterior estimator leads to the idea of a replica simulator which represents the replica ansatz through the state evolution of a transition system described by its corresponding decoupled system. As an application of our study, we investigate large compressive sensing systems by considering the ℓ_p norm minimization recovery schemes. Our numerical investigations show that the replica symmetric predicted performance of the ℓ_0 norm recovery scheme fails as the compression rate grows, and therefore, the replica symmetry breaking ansätze are needed in order to assess the performance precisely.

Index Terms

Maximum-a-posterior estimation, linear vector channel, decoupling principle, equivalent single-user system, compressive sensing, zero norm, replica method, statistical physics, replica symmetry breaking, replica simulator

This work was supported by the German Research Foundation, Deutsche Forschungsgemeinschaft (DFG), under Grant No. MU 3735/2-1.

Ali Bereyhi and Ralf R. Müller are with the Institute for Digital Communications (IDC), Friedrich Alexander University of Erlangen-Nürnberg (FAU), Konrad-Zuse-Straße 5, 91052, Erlangen, Bavaria, Germany (e-mails: ali.bereyhi@fau.de, ralf.r.mueller@fau.de).

Hermann Schulz-Baldes is with the Department of Mathematics, FAU, Cauerstraße 11, 91058, Erlangen, Bavaria, Germany (e-mail: schuba@mi.uni-erlangen.de).

I. Introduction

Consider a vector-valued Additive White Gaussian Noise (AWGN) system specified by

$$\boldsymbol{y} = \mathbf{A}\boldsymbol{x} + \boldsymbol{z} \tag{1}$$

where the independent and identically distributed (i.i.d.) source vector $\boldsymbol{x}_{n\times 1}$, with components in a support set $\mathbb{X} \subset \mathbb{R}$, is measured by the random system matrix $\mathbf{A}_{k\times n} \in \mathbb{A}^{k\times n}$, with $\mathbb{A} \subset \mathbb{R}$, and corrupted by the i.i.d. zero-mean Gaussian noise vector $\boldsymbol{z}_{k\times 1}$, with variance λ_0, i.e., $\boldsymbol{z} \sim \mathcal{N}(\mathbf{0}, \lambda_0 \mathbf{I})$. The source vector can be estimated from the observation vector $\boldsymbol{y}_{k\times 1}$ using a Maximum-A-Posterior (MAP) estimator. For a given system matrix $\mathbf{A}$, the estimator maps the observation vector to the estimated vector $\hat{\boldsymbol{x}}_{n\times 1} \in \mathbb{X}^n$ via the estimation function $\mathbf{g}(\cdot|\mathbf{A})$ defined as

$$\mathbf{g}(\boldsymbol{y}|\mathbf{A}) = \arg\min_{\boldsymbol{v}\in\mathbb{X}^n} \left[\frac{1}{2\lambda}\|\boldsymbol{y} - \mathbf{A}\boldsymbol{v}\|^2 + u(\boldsymbol{v})\right] \tag{2}$$

for some "utility function" $u(\cdot) : \mathbb{R}^n \mapsto \mathbb{R}^+$ and estimation parameter $\lambda \in \mathbb{R}^+$. In (2), $\|\cdot\|^2$ denotes the Euclidean norm, and it is assumed that the minimum is not degenerate so that $\mathbf{g}(\cdot|\mathbf{A})$ is well-defined, at least for almost all $\boldsymbol{y}$ and $\mathbf{A}$. In order to analyze the performance of the system in the large-system limit, i.e., $k, n \uparrow \infty$, one considers a general distortion function $\mathsf{d}(\cdot;\cdot) : \mathbb{X} \times \mathbb{X} \mapsto \mathbb{R}$. For some choices of $\mathsf{d}(\cdot;\cdot)$, the distortion function determines the distance between the source and estimated vector, e.g. $\mathsf{d}(\hat{x}; x) = |\hat{x} - x|^2$; however, in general, it takes different choices. The asymptotic distortion

$$\mathsf{D} = \lim_{n\uparrow\infty} \frac{1}{n} \sum_{i=1}^{n} \mathsf{d}(\hat{x}_i; x_i), \tag{3}$$

then, expresses the large-system performance regarding the distortion function $\mathsf{d}(\cdot;\cdot)$. The performance analysis of the estimator requires (2) to be explicitly computed, and then, $\hat{\boldsymbol{x}} = \mathbf{g}(\boldsymbol{y}|\mathbf{A})$ substituted in the distortion function. This task, however, is not trivial for many choices of the utility function and the source support $\mathbb{X}$, and becomes unfeasible as n grows large. As basic analytic tools fail, we take a statistical mechanical approach and investigate the large-system performance by studying the macroscopic parameters of a corresponding spin glass. This approach enables us to use the replica method which has been developed in the context of statistical mechanics.

A. Corresponding Spin Glass

Consider a thermodynamic system which consists of n particles with each having a microscopic parameter v_i in a state space. The vector $\boldsymbol{v}_{n\times 1} = [v_1, \ldots, v_n]^{\mathsf{T}}$, collecting the microscopic parameters, presents then the microscopic state of the system and is called the "microstate". The main goal of statistical mechanics is to excavate the "macroscopic parameters" of the system, such as energy and entropy through the analysis of the microstate in the thermodynamic limit, i.e., $n \uparrow \infty$. Due to the large dimension of the system, statistical mechanics proposes a stochastic approach in which the microstate is supposed to be randomly distributed over the support $\mathbb{V}^n$ due to some distribution $\mathrm{p}_{\boldsymbol{v}}$. For this system, the Hamiltonian $\mathcal{E}(\cdot) : \mathbb{R}^n \mapsto \mathbb{R}^+$ assigns to each realization of the microstate a non-negative energy level, and $\mathrm{H} \coloneqq -\mathsf{E}_{\mathrm{p}_{\boldsymbol{v}}} \log \mathrm{p}_{\boldsymbol{v}}$ denotes the system's entropy. The "free energy" of

the thermodynamic system at the inverse temperature β is then defined as

$$\mathsf{F}(\beta) \coloneqq \mathsf{E}_{\mathrm{p}_{\boldsymbol{v}}} \mathcal{E}(\boldsymbol{v}) - \beta^{-1}\mathrm{H}. \tag{4}$$

The second law of thermodynamics states that the microstate at thermal equilibrium takes its distribution such that the free energy meets its minimum. Thus, the microstate's distribution at thermal equilibrium reads

$$\mathrm{p}_{\boldsymbol{v}}^{\beta}(\boldsymbol{v}) = [\mathcal{Z}(\beta)]^{-1} e^{-\beta \mathcal{E}(\boldsymbol{v})} \tag{5}$$

where $\mathcal{Z}(\beta)$ is a normalization factor referred to as the "partition function", and the superscript β indicates the distribution's dependence on the inverse temperature. The distribution in (5) is known as the "Boltzmann-Gibbs distribution" and covers many distributions on $\mathbb{V}^n$ by specifying $\mathcal{E}(\cdot)$ and β correspondingly. Substituting the Boltzmann-Gibbs distribution in (4), the free energy at thermal equilibrium and inverse temperature β reads

$$\mathsf{F}(\beta) = -\beta^{-1} \log \mathcal{Z}(\beta). \tag{6}$$

The average energy and entropy of the system at thermal equilibrium are then determined by taking expectation over the distribution in (5), i.e.,

$$\mathcal{E}(\beta) \coloneqq \mathsf{E}_{\mathrm{p}_{\boldsymbol{v}}^{\beta}} \mathcal{E}(\boldsymbol{v}) \tag{7a}$$

$$\mathrm{H}(\beta) \coloneqq -\mathsf{E}_{\mathrm{p}_{\boldsymbol{v}}^{\beta}} \log \mathrm{p}_{\boldsymbol{v}}^{\beta}(\boldsymbol{v}), \tag{7b}$$

which can be calculated in terms of the free energy via

$$\mathcal{E}(\beta) = \frac{\mathrm{d}}{\mathrm{d}\beta} [\beta \mathsf{F}(\beta)] \tag{8a}$$

$$\mathrm{H}(\beta) = \beta^2 \frac{\mathrm{d}}{\mathrm{d}\beta} [\mathsf{F}(\beta)]. \tag{8b}$$

In spin glasses [1], the Hamiltonian assigns the energy levels randomly using some randomizer Q resulting from random interaction coefficients. In fact, each realization of Q specifies a thermodynamic system represented by the deterministic Hamiltonian $\mathcal{E}(\cdot|\mathsf{Q})$. In statistical mechanics, Q is known to have "quenched" randomness while the microstate is an "annealed" random variable. The analysis of spin glasses takes similar steps as above considering a given realization of the randomizer, and therefore, as the system converges to its thermal equilibrium at the inverse temperature β, the microstate's conditional distribution given Q, i.e., $\mathrm{p}_{\boldsymbol{v}|\mathsf{Q}}^{\beta}$, is a Boltzmann-Gibbs distribution specified by $\mathcal{E}(\cdot|\mathsf{Q})$. Therefore, the free energy for this case reads

$$\mathsf{F}(\beta|\mathsf{Q}) = -\beta^{-1} \log \mathcal{Z}(\beta|\mathsf{Q}). \tag{9}$$

where $\mathcal{Z}(\beta|\mathsf{Q})$ is the partition function with respect to the Hamiltonian $\mathcal{E}(\cdot|\mathsf{Q})$. Here, the free energy, as well as other macroscopic parameters of the system, is random; however, the physical intuition behind the analyses suggests that these random macroscopic parameters converge to deterministic values in the thermodynamic limit. This property is known as the "self averaging property" and has been rigorously justified for some particular classes

of Hamiltonians, e.g., [2]–[5]. Nevertheless, in cases where a mathematical proof is still lacking, the property is supposed to hold during the analysis. According to the self averaging property, the free energy of spin glasses converges to its expectation in the thermodynamic limit.

As mentioned earlier, the MAP estimator in (2) can be investigated using a corresponding spin glass. To see that, consider a spin glass in which the microstate is taken from $\mathbb{X}^n$, and the Hamiltonian is defined as

$$\mathcal{E}(\boldsymbol{v}|\boldsymbol{y},\mathbf{A}) = \frac{1}{2\lambda}\|\boldsymbol{y}-\mathbf{A}\boldsymbol{v}\|^2 + u(\boldsymbol{v}). \tag{10}$$

Here, the system matrix $\mathbf{A}$ and the observation vector $\boldsymbol{y}$ are considered to be the randomizers of the spin glass. In this case, given $\mathbf{A}$ and $\boldsymbol{y}$, the conditional distribution of the microstate is given by

$$\mathrm{p}^{\beta}_{\boldsymbol{v}|\boldsymbol{y},\mathbf{A}}(\boldsymbol{v}|\boldsymbol{y},\mathbf{A}) = [\mathcal{Z}(\beta|\boldsymbol{y},\mathbf{A})]^{-1}\, e^{-\beta\mathcal{E}(\boldsymbol{v}|\boldsymbol{y},\mathbf{A})}. \tag{11}$$

Taking the limit when $\beta \uparrow \infty$ and using Laplace method of integration [6], the zero temperature distribution, under the assumption of uniqueness of the minimizer, reduces to

$$\mathrm{p}^{\infty}_{\boldsymbol{v}|\boldsymbol{y},\mathbf{A}}(\boldsymbol{v}|\boldsymbol{y},\mathbf{A}) = \mathbf{1}\{\boldsymbol{v} = \arg\min_{\boldsymbol{v}\in\mathbb{X}^n} \mathcal{E}(\boldsymbol{v}|\boldsymbol{y},\mathbf{A})\} \tag{12a}$$

$$= \mathbf{1}\{\boldsymbol{v} = \mathbf{g}(\boldsymbol{y}|\mathbf{A})\}, \tag{12b}$$

where $\mathbf{1}\{\cdot\}$ denotes the indicator function, and $\mathbf{g}(\cdot|\mathbf{A})$ is defined as in (2). (12b) indicates that the microstate of the spin glass converges to the estimated vector of the MAP estimator, i.e., $\hat{\boldsymbol{x}} = \mathbf{g}(\boldsymbol{y}|\mathbf{A})$, in the zero temperature limit. Invoking this connection, we study the corresponding spin glass instead of the MAP estimator. We represent the input-output distortion of the system regarding a general distortion function $\mathrm{d}(\cdot;\cdot)$ as a macroscopic parameter of the spin glass. Consequently, the replica method developed in statistical mechanics is employed to determine the defined macroscopic parameter of the corresponding spin glass. The replica method is a nonrigorous but effective method developed in the physics literature to study spin glasses. Although the method lacks rigorous mathematical proof in some particular parts, it has been widely accepted as an analysis tool and utilized to investigate a variety of problems in applied mathematics, information processing, and coding [7]–[10].

The use of the replica method for studying multiuser estimators goes back to [11] where Tanaka determined the asymptotic spectral efficiency of Marginal-Posterior-Mode (MPM) estimators by employing the replica method. The results given in [11], in some special cases, recovered known rigorous results, and consequently, the statistical mechanical approach received more attention in the context of multiuser systems. Several works considered different classes of multiuser estimators and employed the replica method to study the performance in the large-system limit regarding different measures, e.g. [12], [13]. The method was also used to analyze the asymptotic properties of Multiple-Input Multiple-Output (MIMO) systems [14] considering an approach similar to [11]. Regarding multiuser estimators, the earlier studies mainly considered the cases in which the entries of the source vector are binary or Gaussian random variables. The results were later shown to hold for a general source distribution in [15]. Replica analyses were further employed in several problems such as vector precoding and compressive sensing [16], [17].

B. Decoupling Principle

Considering the MAP estimator defined in (2), the entries of the estimated vector $\hat{\boldsymbol{x}}$ are correlated in general, since the system matrix couples the entries of $\boldsymbol{x}$ linearly, and $\mathbf{g}(\cdot|\mathbf{A})$ performs several nonlinear operations on $\boldsymbol{y}$. In the large-system performance analysis, the marginal joint distribution of two corresponding input-output entries x_j and $\hat{x}_j$, $1 \leq j \leq n$, is of interest. To clarify our point, consider the case in which a linear estimator is employed instead of (2), i.e., $\hat{\boldsymbol{x}} = \mathbf{G}^{\mathsf{T}}\boldsymbol{y}$. Denote the matrices $\mathbf{A}$ and $\mathbf{G}$ as $\mathbf{A} = [\mathbf{a}_1 \cdots \mathbf{a}_n]$ and $\mathbf{G} = [\mathbf{g}_1 \cdots \mathbf{g}_n]$, respectively, with $\mathbf{a}_i$ and $\mathbf{g}_i$ being $k \times 1$ vectors for $1 \leq i \leq n$. Therefore, $\hat{x}_j$ is written as

$$\hat{x}_j = \mathbf{g}_j^{\mathsf{T}}\boldsymbol{y} \tag{13a}$$

$$= \mathbf{g}_j^{\mathsf{T}}\left[\sum_{i=1}^{n} x_i\mathbf{a}_i + \boldsymbol{z}\right] \tag{13b}$$

$$= (\mathbf{g}_j^{\mathsf{T}}\mathbf{a}_j)\ x_j + \sum_{i=1, i\neq j}^{n} (\mathbf{g}_j^{\mathsf{T}}\mathbf{a}_i)\ x_i + \mathbf{g}_j^{\mathsf{T}}\boldsymbol{z}. \tag{13c}$$

Here, the right hand side of (13c) can be interpreted as the linear estimation of a single-user system indexed by j in which the symbol x_j is corrupted by an additive impairment given by the last two summands in the right hand side of (13c). The impairment term is not necessarily independent and Gaussian. For some classes of matrix ensembles, and under a set of assumptions, it is shown that the dependency of the derived single-user systems on the index j vanishes, and the distribution of the impairment terms converges to a Gaussian distribution in the large-system limit [18]. As a result, one can assume the vector-valued system described by (1) followed by the linear estimator $\mathbf{G}$ to be a set on n additive scalar systems with Gaussian noise which have been employed in parallel. In other words, the vector system can be considered to "decouple" into a set of similar scalar systems. Each of them relates an input entry x_j to its corresponding estimated one $\hat{x}_j$. This asymptotic property of the estimator is referred to as the "decoupling property" and can be investigated through a large-system performance analysis.

The decoupling property was first studied for linear estimators. Tse and Hanly noticed this property while they were determining the multiuser efficiency of several linear multiuser estimators in the large-system limit [19]. They showed that for an i.i.d. system matrix, the effect of impairment is similar to the effect of some modified Gaussian noise when the dimension tends to infinity. This asymptotic property was then investigated further by studying the asymptotics of different linear receivers and their large-system distributions [20], [21]. In an independent work, Verdú and Shamai also studied the linear Minimum Mean Square Error (MMSE) estimator and showed that the conditional output distribution is asymptotically Gaussian [22]. In [23], the authors studied the asymptotics of the impairment term when a family of linear estimators is employed and proved that it converges in distribution to a Gaussian random variable. The latter result was further extended to a larger class of linear estimators in [18].

Regarding linear estimators, the main analytical tool is random matrix theory [24] [25]. In fact, invoking properties of large random matrices and the central limit theorem, the decoupling property is rigorously proved, e.g. [26], [27]. These tools, however, fail for nonlinear estimators as the source symbol and impairment term do not decouple linearly due to nonlinear operations at the estimators. In [28], Müller and Gerstacker employed the replica method and studied the capacity loss due to the separation of detection and decoding. The authors showed that the additive

decoupling of the spectral efficiency, reported in [27] for Gaussian inputs, also holds for binary inputs. As a result, it was conjectured that regardless of input distribution and linearity, the spectral efficiency always decouples in an additive form [29]. In [15], Guo and Verdú justified the conjecture for a family of nonlinear MMSE estimators, and showed that for an i.i.d. system matrix, the estimator decouples into a bank of single-user MMSE estimators under the Replica Symmetry (RS) ansatz. In [30], Rangan et al. studied the asymptotic performance of a class of MAP estimators. Using standard large deviation arguments, the authors represented the MAP estimator as the limit of an indexed MMSE estimators' sequence. Consequently, they determined the estimator's asymptotics employing the results from [15] and justified the decoupling property of MAP estimators under the RS ansatz for an i.i.d. $\mathbf{A}$.

For the MAP estimator, there are still two main issues which have not been considered precisely: 1) the cases in which the system matrix $\mathbf{A}$ is not i.i.d., and 2) the analysis of the estimator under the Replica Symmetry Breaking (RSB) ansätze. The first issue was partially addressed in [31] where the authors studied the asymptotics of a MAP estimator using the RS ansatz employed to recover the support of a source vector from observations received through noisy sparse random measurements. They considered a model in which a sparse Gaussian source vector[1] is first randomly measured by a square matrix $\mathbf{V}$, and then, the measurements are sparsely sampled by a diagonal matrix $\mathbf{B}$ whose non-zero entries are i.i.d. Bernoulli random variables. For this setup, the input-output information rate and support recovery error rate were investigated by considering the measuring matrix $\mathbf{V}$ to belong to a larger set of matrix ensembles. These results, moreover, could address the decoupling principle for the supposed system model. Although the class of system matrices is broadened in [31], it cannot be considered as a complete generalization of [15] and [30], since it is restricted to cases with a sparse Gaussian source and loading factors less than one, i.e., $kn^{-1} < 1$ in (1). Vehkaperä et al. also tried to investigate the first issue by studying large compressive sensing systems via the replica method [32]. In fact, the authors considered the system model as in (1) for a large class of matrix ensembles and, under the RS ansatz, determined the asymptotic Mean Square Error (MSE) for a class of least-square decompressors modeled as the MAP estimator in (2). The large-system results in [32], however, did not address the asymptotic marginal joint input-output distribution, and the emphasis was on the MSE. Regarding the second issue, the MAP estimator has not yet been investigated under RSB ansätze in the literature.

C. Compressive Sensing

The MAP estimation of a source vector from a set of noisy linear observations arises in several applications, such as MIMO and sampling systems. To address one, we consider large compressive sensing systems and employ our asymptotic results to analyze the large-system performance [33]–[35]. In context of compressive sensing, (1) represents a noisy sampling system in which the source vector $\boldsymbol{x}$ is being sampled linearly via $\mathbf{A}$ and corrupted by additive noise $\boldsymbol{z}$. In the "noise free" case, i.e. $\lambda_0 = 0$, the source vector $\boldsymbol{x}$ is exactly recovered from the observation vector $\boldsymbol{y}$, if the number of observations k is as large as the source length n and the sampling matrix $\mathbf{A}$ is full rank. As the number of observations reduces, the possible answers to the exact reconstruction problem may increase regarding the source support $\mathbb{X}$, and therefore, the recovered source vector from the observation vector is

[1]It means that the entries of the source vector are of the form $x_i b_i$ where x_i and b_i are Gaussian and Bernoulli random variables, respectively.

not necessarily unique. In this case, one needs to enforce some extra constraints on the properties of the source vector in order to recover it uniquely among all possible solutions.

In compressive sensing, the source vector is supposed to be sparse, i.e., a certain fraction of entries are zero (or another deterministic scalar). This property of the source imposes an extra constraint on the solution which allows for exact recovery in cases with $k < n$. In fact, in this case, one should find a solution to $\boldsymbol{y} = \mathbf{A}\boldsymbol{v}$ over

$$\mathbb{S} = \{\boldsymbol{v}_{n\times 1} \in \mathbb{X}^n : \ \|\boldsymbol{v}\|_0 < \alpha n\} \tag{14}$$

where $\|\cdot\|_0$ denotes the "ℓ_0 norm" and is defined as $\|\boldsymbol{v}\|_0 \coloneqq \sum_{i=1}^{n} \mathbf{1}\{v_i \neq 0\}$, and $\alpha \leq 1$ is the source's sparsity factor defined as the fraction of non-zero entries. Depending on $\mathbf{A}$ and $\mathbb{X}$, the latter problem can have a unique solution even in cases where $k < n$. Several works studied the properties of the sampling matrix $\mathbf{A}$, such as mutual coherence and restricted isometry property to find tight sufficient conditions for the problem, e.g. [36]–[38].

In noisy sampling systems, exact recovery is only possible for some particular choices of $\mathbb{X}$. Nevertheless, in either case, the noise free recovery procedure gives an invalid reconstruction of the source vector which can result in a large distortion. The strategy in these cases is to find a vector in $\mathbb{S}$ such that the recovery distortion becomes minimal. Therefore, the recovery scheme based on the ℓ_0 norm extends to

$$\hat{\boldsymbol{x}} = \arg\min_{\boldsymbol{v}\in\mathbb{X}^n} \left[\frac{1}{2\lambda}\|\boldsymbol{y} - \mathbf{A}\boldsymbol{v}\|^2 + \|\boldsymbol{v}\|_0\right] \tag{15}$$

which is the MAP estimator defined in (2) with $u(\boldsymbol{v}) = \|\boldsymbol{v}\|_0$. It is straightforward to show that for $\lambda_0 = 0$, i.e., zero noise variance, (15) reduces to the optimal noise free recovery scheme as $\lambda \downarrow 0$.

The reconstruction scheme of (15) results in a non-convex optimization problem due to the ℓ_0 norm cost function, and therefore, is computationally unfeasible. Alternatively, computationally traceable schemes have been introduced by replacing the cost function in (15) with the ℓ_2 norm or the ℓ_1 norm. The former scheme is usually referred to as the linear scheme, while the latter is known as LASSO [39] or basic pursuit denoising [40]. Moreover, several reconstruction schemes based on iterative and greedy algorithms have been introduced taking into account the sparsity pattern of the source and properties of the sampling matrix [41]–[43].

A common strategy for analyzing the performance of the reconstruction schemes is to consider a random sampling matrix and determine the performance metric for a given realization of it. In this case, the average performance is evaluated by taking the expectation over the matrix distribution. In most of the cases, the asymptotic performance is of interest. In fact, due to the self averaging property, for almost any realization of the system matrix the reconstructed vector converges to a deterministic vector in the large-system limit, and therefore, the system can be deterministically characterized. The investigation, however, needs more advanced analytical tools, due to complexity issues mentioned at the beginning of this section. Donoho and Tanner took a combinatorial geometric approach, as one of the few mathematically rigorous approaches, in order to quantify the exact sparsity-sampling rate tradeoff in noise free sensing systems [44]–[46]. Another rigorous analysis approach was introduced in [47] in which the authors used the recently developed conditioning technique [48] to justify the accuracy of describing the dynamics of Approximate Message Passing (AMP) algorithms by "state evolution" in asymptotic regime, when $\mathbf{A}$ is set to be

an i.i.d. matrix with Gaussian entries. Reeves and Gastpar, then, considered the linear and LASSO reconstruction schemes as special cases of the AMP algorithms and employed the results from [47] to study the tradeoff between the sampling rate and reconstruction distortion [49]. The mathematically rigorous results in [46], [47] are given at the expense of addressing a restricted class of system settings. Taking approaches based on statistical mechanics instead, one can study a larger class of system setups by means of commonly accepted tools, such as replica method, in return for lacking the rigorousness in some particular parts of the analysis.

Comparing (15) with (2), one can utilize the asymptotic results for the MAP estimator to study the large-system performance of several reconstruction schemes. This similarity was initially considered in a series of papers, see for example [17], [50], where the authors employed earlier replica analyses to study a family of compressive sensing systems in the large-system limit. The approach was taken further in [30] where the RS decoupling principle of MMSE as stated in [15] was first extended to the MAP estimators and then employed to study the asymptotics of the ℓ_0 norm, LASSO and linear schemes. The aforementioned approach has the disadvantage that the sampling system's specifications are limited to those being considered for the corresponding multiuser estimator. In fact, as the starting point of these analyses is the replica results form the literature, one needs to restrict the sampling system to the model specified in the original estimation problem. The compressive sensing systems, however, may require a wider set of assumptions, and thus, several sampling systems cannot be investigated by the results in the literature. As the result, several works deviated from the earlier approach and studied large compressive sensing systems employing the replica method directly in their analyses [31], [32], [51]–[54].

D. Contribution and Outline

In this paper, we determine the asymptotic distortion for a general distortion function for cases where the MAP estimator is employed to estimate the source vector from the observation given in (1). We represent the asymptotic distortion in (3) as a macroscopic parameter of a corresponding spin glass and study the spin glass via the replica method. The general replica ansatz is then given for an arbitrary replica correlation matrix, and its special cases are studied considering the RS and RSB assumptions. The asymptotic distortion is determined for a wide set of matrix ensembles invoking results for asymptotics of spherical integrals [55], [56]. Using our asymptotic results, we justify a more general form of the decoupling principle by restricting the distortion function to be of a special form and employing the moment method [57], [58]. We show that the vector-valued system in (1) estimated by (2) decouples into a bank of similar noisy single-user systems followed by single-user MAP estimators. This result holds for any replica correlation matrix; however, the structure of the decoupled single-user system depends on the supposed structure of the correlation matrix. Under the RSB assumption with b steps of breaking (bRSB), the noisy single-user is given in the form of an input term added by an impairment term. The impairment term, moreover, is expressed as the sum of an independent Gaussian random variable and b correlated interference terms. By reducing the assumption to RS, the result reduces to the formerly studied RS decoupling principle of the MAP estimators for a wide range of system matrix ensembles [30]. In fact, our investigations collect the previous results regarding the decoupling principle in addition to a new set of setups under a single umbrella given by a more general form of the decoupling principle. More precisely, we extend the scope of the decoupling principle to

- the systems in which the system matrix belongs to a wide set of matrix ensembles, and
- the general replica ansatz including the RS and RSB ansätze.

To address a particular application, we study the large-system performance of a compressive sensing system under the ℓ_p minimization recovery schemes. We address the linear reconstruction, as well as the LASSO and the ℓ_0 norm scheme considering both the sparse Gaussian and finite alphabet sources. Our general distortion function allows to investigate the asymptotic performance with respect to different metrics. Moreover, the generality of our matrix ensembles enables us to study different sensing schemes, such as i.i.d. and random projector sensing. The numerical investigations show that the RS ansatz fails to predict the performance of ℓ_0 norm recovery scheme accurately within relatively large compression rates, and therefore, RSB ansätze are needed to be investigated further. Moreover, it is observed that the better performance of the projector sensing reported in [32] for sparse Gaussian sources extends to the reconstruction of sparse finite alphabet sources as well.

The rest of the manuscript is organized as follows. In Section II, the problem is formulated. We illustrate our statistical mechanical approach in Section III and explain briefly the replica method. The general replica ansatz, as well as the general decoupling principle is given in Section IV. The ansatz under the RS and RSB assumptions are expressed in Sections V and VI. Based on bRSB decoupled system, we propose the idea of a replica simulator in VII and describe the given ansätze in terms of the corresponding decoupled systems. To address an application of our study, we consider large compressive sensing systems in Section VIII and discuss several examples. The numerical investigations of the examples are then given in Section IX. Finally, we conclude the manuscript in Section X.

E. Notations

Throughout the manuscript, we represent scalars, vectors and matrices with lower, bold lower, and bold upper case letters, respectively. The set of real numbers is denoted by $\mathbb{R}$, and $\mathbf{A}^{\mathsf{T}}$ and $\mathbf{A}^{\mathsf{H}}$ indicate the transposed and Hermitian of $\mathbf{A}$. $\mathbf{I}_m$ is the $m \times m$ identity matrix and $\mathbf{1}_m$ is an $m \times m$ matrix with all entries equal to 1. For a random variable x, p_x represents either the Probability Mass Function (PMF) or Probability Density Function (PDF), and F_x represents the Cumulative Distribution Function (CDF). We denote the expectation over x by E_x, and an expectation over all random variables involved in a given expression by E. $\mathbb{Z}$ and $\mathbb{R}$ represent the set of integer and real numbers and the superscript $+$, e.g. $\mathbb{R}^+$, indicates the corresponding subset of all non-negative numbers. For sake of compactness, the set of integers $\{1, \ldots, n\}$ is abbreviated as $[1:n]$, the zero-mean and unit-variance Gaussian PDF is denoted by $\phi(\cdot)$, and the Gaussian averaging is expressed as

$$\int (\cdot)\, \mathrm{D}t \coloneqq \int_{-\infty}^{+\infty} (\cdot)\, \phi(t) \mathrm{d}t. \tag{16}$$

Moreover, in many cases, we drop the set on which a sum, minimization or an integral is taken. Whenever needed, we consider the entries of $\boldsymbol{x}$ to be discrete random variables, namely the support $\mathbb{X}$ to be discrete. The results of this paper, however, are in full generality and hold also for continuous distributions.

F. Announcements

Some of the results of this manuscript were presented at IEEE Information Theory Workshop [59]. Even though the results have a mathematical flavor, the stress is not on investigating the rigorousness of the available tools such as replica method, but rather to employ them for deriving formulas which can be used in different problems.

II. Problem Formulation

Consider the vector-valued linear system described by (1). Let the system satisfy the following properties.

(a) $\boldsymbol{x}_{n\times 1}$ is an i.i.d. random vector with each entry being distributed with the distribution p_x over the support $\mathbb{X}$ where $\mathbb{X} \subseteq \mathbb{R}$.

(b) $\mathbf{A}_{k\times n}$ is randomly generated over $\mathbb{A}^{k\times n}$ with $\mathbb{A} \subseteq \mathbb{R}$, such that its Gramian, i.e., $\mathbf{J} = \mathbf{A}^{\mathsf{T}}\mathbf{A}$, has the eigendecomposition

$$\mathbf{J} = \mathbf{U}\mathbf{D}\mathbf{U}^{\mathsf{T}} \tag{17}$$

where $\mathbf{U}_{n\times n}$ is an orthogonal Haar distributed matrix and $\mathbf{D}_{n\times n}$ is a diagonal matrix with $\lambda_i^{\mathbf{J}}$ denoting its ith diagonal entry for $i \in [1:n]$. For a given n, we denote the empirical CDF of the eigenvalues (cumulative density of states) of the matrix $\mathbf{J}$ with $\mathrm{F}_{\mathbf{J}}^n$ and define it as

$$\mathrm{F}_{\mathbf{J}}^n(\lambda) = \frac{1}{n}\sum_{i=1}^{n} \mathbf{1}\{\lambda_i^{\mathbf{J}} < \lambda\}. \tag{18}$$

We assume that $\mathrm{F}_{\mathbf{J}}^n$ converges, as $n \uparrow \infty$, to a deterministic CDF $\mathrm{F}_{\mathbf{J}}$.

(c) $\boldsymbol{z}_{k\times 1}$ is a real i.i.d. zero-mean Gaussian random vector in which the variance of each entry is λ_0.

(d) The number of observations k is a deterministic function of the transmission length n, such that

$$\lim_{n\uparrow\infty} \frac{k(n)}{n} = \frac{1}{\mathsf{r}} < \infty. \tag{19}$$

For sake of compactness, we drop the explicit dependence of k on n.

(e) $\boldsymbol{x}$, $\mathbf{A}$ and $\boldsymbol{z}$ are independent.

The source vector $\boldsymbol{x}$ is reconstructed from the observation vector $\boldsymbol{y}$ with a system matrix $\mathbf{A}$ that is known at the estimator. Thus, for a given $\mathbf{A}$, the source vector is recovered by

$$\hat{\boldsymbol{x}} = \mathbf{g}(\boldsymbol{y}|\mathbf{A}) = \arg\min_{\boldsymbol{v}} \left[\frac{1}{2\lambda}\|\boldsymbol{y} - \mathbf{A}\boldsymbol{v}\|^2 + u(\boldsymbol{v})\right] \tag{20}$$

where $\boldsymbol{v} \in \mathbb{X}^n$, the non-negative scalar λ is the estimation parameter and the non-negative cost function $u(\cdot)$ is referred to the "utility function". The utility function $u(\cdot)$ is supposed to decouple which means that it takes arguments with different lengths, i.e., $u(\cdot) : \mathbb{R}^{\ell} \mapsto \mathbb{R}^{+}$ for any positive integer ℓ, and

$$u(\boldsymbol{x}) = \sum_{i=1}^{n} u(x_i). \tag{21}$$

In order to use the estimator in (20), one needs to guarantee the uniqueness of the solution of the optimization. Therefore, we impose the following constraint on our problem.

(f) For a given observation vector $\boldsymbol{y}$, the objective function in (20) has a unique minimizer over the support $\mathbb{X}^n$.

A. MAP Estimator

The MAP estimator in (20) can be considered as the optimal estimator in the sense that it minimizes the reconstruction's error probability postulating a source prior distribution proportional to $e^{-u(\boldsymbol{x})}$ and a noise variance λ. To clarify the argument, assume $\mathbb{X}$ is a finite set[1]. In this case, we can define the reconstruction's error probability as

$$\mathsf{P}_{\mathsf{e}} = \Pr\{\boldsymbol{x} \neq \tilde{\mathbf{g}}(\boldsymbol{y}|\mathbf{A})\} \tag{22}$$

for some estimator $\tilde{\mathbf{g}}(\cdot|\mathbf{A})$. In order to minimizes P_{e}, $\tilde{\mathbf{g}}(\cdot|\mathbf{A})$ is chosen to maximize the posterior distribution over the input support $\mathbb{X}^n$, i.e.,

$$\tilde{\mathbf{g}}(\boldsymbol{y}|\mathbf{A}) = \arg\max_{\boldsymbol{v}} \mathrm{p}_{\boldsymbol{x}|\boldsymbol{y},\mathbf{A}}(\boldsymbol{v}|\boldsymbol{y},\mathbf{A}) \tag{23a}$$

$$= \arg\max_{\boldsymbol{v}} \mathrm{p}_{\boldsymbol{y}|\boldsymbol{x},\mathbf{A}}(\boldsymbol{y}|\boldsymbol{v},\mathbf{A})\mathrm{p}_{\boldsymbol{x}|\mathbf{A}}(\boldsymbol{v}|\mathbf{A}) \tag{23b}$$

$$\stackrel{\star}{=} \arg\min_{\boldsymbol{v}} \left[-\log \mathrm{p}_{\boldsymbol{y}|\boldsymbol{x},\mathbf{A}}(\boldsymbol{y}|\boldsymbol{v},\mathbf{A}) - \log \mathrm{p}_{\boldsymbol{x}}(\boldsymbol{v})\right]. \tag{23c}$$

where $\star$ comes from the independency of $\boldsymbol{x}$ and $\mathbf{A}$. Here, $\mathrm{p}_{\boldsymbol{y}|\boldsymbol{x},\mathbf{A}}(\boldsymbol{y}|\boldsymbol{v},\mathbf{A}) = \mathrm{p}_{\boldsymbol{z}}(\boldsymbol{y}-\mathbf{A}\boldsymbol{v})$, and $\mathrm{p}_{\boldsymbol{x}}$ is the prior distribution of the source vector. Now, let the estimator postulate the noise variance to be λ and the prior to be

$$\mathrm{p}_{\boldsymbol{x}}(\boldsymbol{v}) = \frac{e^{-u(\boldsymbol{v})}}{\sum_{\boldsymbol{v}} e^{-u(\boldsymbol{v})}} \tag{24}$$

for some non-negative function $u(\cdot)$. Substituting in (23c), the estimator $\tilde{\mathbf{g}}(\cdot|\mathbf{A})$ reduces to $\mathbf{g}(\cdot|\mathbf{A})$ defined in (20). The estimator in (20) models several particular reconstruction schemes in compressive sensing; some of which we address later on.

Remark II.1. In the case that the entries of $\boldsymbol{x}$ are continuous random variables, the above argument needs some modifications. In fact, in this case the reconstruction's error probability as defined in (22) is always one, and therefore, it cannot be taken as the measure of error. In this case, the MAP estimator is considered to maximize the posterior PDF postulating $\mathrm{p}_{\boldsymbol{x}}(\boldsymbol{v}) \propto e^{-u(\boldsymbol{v})}$ and noise variance λ.

B. Asymptotic Distortion and Conditional Distribution

In many applications, the distortion is given in terms of the average MSE, while in some others the average symbol error rate is considered. In fact, the former takes the ℓ_2 norm as the distortion function, and the latter considers the ℓ_0 norm. The distortion function, however, can be of some other form in general. Here, we study the asymptotic performance by considering a general distortion function which determines the imperfection level of the estimation. Thus, we consider a distortion function $\mathsf{d}(\cdot;\cdot)$ which

$$\mathsf{d}(\cdot;\cdot) : \mathbb{X} \times \mathbb{X} \to \mathbb{R}. \tag{25}$$

[1]i.e., the entries of $\boldsymbol{x}$ are discrete random variables.

The term "average distortion" usually refers to the case when the averaging weight vector is uniform. It means that each tuple of source-estimated entries $(x_i, \hat{x}_i)$ is weighted equally when the distortion is averaged over all the entries' tuples. The distortion, however, can be averaged non-uniformly for some arbitrary weight vector. We define the average distortion in a wider sense which also includes the uniform average distortion.

Definition II.1 (Asymptotic distortion)**.** Consider the vectors $\boldsymbol{x}_{n\times 1}$ and $\hat{\boldsymbol{x}}_{n\times 1}$ defined over $\mathbb{X}^n$, and let $\mathsf{d}(\cdot;\cdot)$ be a distortion function defined in (25). Define the index set $\mathbb{W}(n)$ as a subset of $[1:n]$, and let $|\mathbb{W}(n)|$ grow with n such that

$$\lim_{n\uparrow\infty} \frac{|\mathbb{W}(n)|}{n} = \eta \tag{26}$$

for some $\eta \in [0,1]$. Then, the average distortion of $\hat{\boldsymbol{x}}$ and $\boldsymbol{x}$ over the index set $\mathbb{W}(n)$ regarding the distortion function $\mathsf{d}(\cdot;\cdot)$ is defined as

$$\mathsf{D}^{\mathbb{W}(n)}(\hat{\boldsymbol{x}};\boldsymbol{x}) \coloneqq \frac{1}{|\mathbb{W}(n)|} \sum_{w\in\mathbb{W}(n)} \mathsf{d}(\hat{x}_w; x_w). \tag{27}$$

Assuming the limit of (27) when $n \uparrow \infty$ exists, we denote

$$\mathsf{D}^{\mathbb{W}}(\hat{\boldsymbol{x}};\boldsymbol{x}) \coloneqq \lim_{n\uparrow\infty} \mathsf{D}^{\mathbb{W}(n)}(\hat{\boldsymbol{x}};\boldsymbol{x}) \tag{28}$$

and refer to it as the "asymptotic distortion" over the limit of the index set $\mathbb{W}(n)$. ■

Definition II.1 can, moreover, help to investigate the asymptotic conditional distribution of the estimator which plays a key role in studying the decoupling principle. For further convenience, we define the asymptotic conditional distribution of the MAP estimator as follows.

Definition II.2 (Asymptotic conditional distribution)**.** Consider the source vector $\boldsymbol{x}_{n\times 1}$ passed through the linear system in (1), and let $\hat{\boldsymbol{x}}_{n\times 1}$ be its MAP estimation as given in (20). For a given n, we take an index $j \in [1:n]$ and denote the conditional distribution of $\hat{x}_j$ given x_j by $\mathrm{p}^{j(n)}_{\hat{x}|x}$ which at the mass point $(\hat{v}, v) \in \mathbb{X}\times\mathbb{X}$ reads

$$\mathrm{p}^{j(n)}_{\hat{x}|x}(\hat{v}|v) \coloneqq \big[\mathrm{p}_{x_j}(v)\big]^{-1} \mathrm{p}_{\hat{x}_j, x_j}(\hat{v}, v) \tag{29}$$

with $\mathrm{p}_{\hat{x}_j,x_j}(\hat{v},v)$ being the marginal joint distribution of x_j and $\hat{x}_j$ at the mass point $(\hat{v},v)$. Then, in the large-system limit, we define the asymptotic conditional distribution of $\hat{x}_j$ given x_j at $(\hat{v},v)$ as

$$\mathrm{p}^{j}_{\hat{x}|x}(\hat{v}|v) \coloneqq \lim_{n\uparrow\infty} \mathrm{p}^{j(n)}_{\hat{x}|x}(\hat{v}|v). \tag{30}$$

■

We study the asymptotic distortion over the limit of a desired index set $\mathbb{W}(n)$ and distortion function $\mathsf{d}(\cdot;\cdot)$ by defining it as a macroscopic parameter of the corresponding spin glass and employing the replica method to evaluate it. Using the result for the asymptotic distortion, we determine then the asymptotic conditional distribution and investigate the decoupling property of the estimator.

III. Statistical Mechanical Approach

The Hamiltonian in (10) introduces a spin glass which corresponds to the MAP estimator. The spin glass at zero temperature describes the asymptotics of the MAP estimator. For further convenience, we formally define the "corresponding spin glass" as follows.

Definition III.1 (Corresponding spin glass)**.** Consider the integer $n \in \mathbb{Z}^+$. The corresponding spin glass with the microstate $\boldsymbol{v}_{n\times 1} \in \mathbb{X}^n$ and the quenched randomizers $\boldsymbol{y}_{n\times 1}$ and $\mathbf{A}$ is given by the followings:

- $\mathbf{A}$ is a random matrix satisfying the constraints in Section II, and $\boldsymbol{y}$ is constructed as in (1) for some $\boldsymbol{x}$.
- For any realization of $\mathbf{A}$ and $\boldsymbol{y}$, the Hamiltonian reads

$$\mathcal{E}(\boldsymbol{v}|\boldsymbol{y},\mathbf{A}) = \frac{1}{2\lambda}\|\boldsymbol{y}-\mathbf{A}\boldsymbol{v}\|^2 + u(\boldsymbol{v}), \tag{31}$$

  fore $\boldsymbol{v} \in \mathbb{X}^n$.

■

For the corresponding spin glass, at the inverse temperature β, the following properties are directly concluded.

- The conditional distribution of the microstate reads

$$\mathrm{p}^{\beta}_{\boldsymbol{v}|\boldsymbol{y},\mathbf{A}}(\boldsymbol{v}|\boldsymbol{y},\mathbf{A}) = \frac{e^{-\beta\mathcal{E}(\boldsymbol{v}|\boldsymbol{y},\mathbf{A})}}{\mathcal{Z}(\beta|\boldsymbol{y},\mathbf{A})} \tag{32}$$

  with $\mathcal{Z}(\beta|\boldsymbol{y},\mathbf{A})$ being the partition function

$$\mathcal{Z}(\beta|\boldsymbol{y},\mathbf{A}) = \sum_{\boldsymbol{v}} e^{-\beta\mathcal{E}(\boldsymbol{v}|\boldsymbol{y},\mathbf{A})}. \tag{33}$$

- The normalized free energy is given by

$$\mathsf{F}(\beta) = -\frac{1}{\beta n}\mathsf{E}\log\mathcal{Z}(\beta|\boldsymbol{y},\mathbf{A}), \tag{34}$$

  where the expectation is taken over the quenched randomizers.
- The entropy of the spin glass is determined as

$$\mathrm{H}(\beta) = \beta^2\frac{\mathrm{d}}{\mathrm{d}\beta}\left[\mathsf{F}(\beta)\right]. \tag{35}$$

Regarding the MAP estimator, one can represent the asymptotic distortion as a macroscopic parameter of the corresponding spin glass. More precisely, using Definition II.2, the asymptotic distortion reads

$$\mathsf{D}^{\mathsf{W}}(\hat{\boldsymbol{x}};\boldsymbol{x}) = \lim_{\beta\uparrow\infty}\lim_{n\uparrow\infty}\mathsf{E}^{\beta}_{\boldsymbol{v}}\mathsf{D}^{\mathsf{W}(n)}(\boldsymbol{v};\boldsymbol{x}) \tag{36}$$

where $\mathsf{E}^{\beta}_{\boldsymbol{v}}$ indicates the expectation over $\boldsymbol{v} \in \mathbb{X}^n$ with respect to the conditional Boltzmann-Gibbs distribution

$\mathsf{p}^{\beta}_{\boldsymbol{v}|\boldsymbol{y},\mathbf{A}}$ defined in (32). In fact, by introducing the macroscopic parameter $\mathsf{D}^{\mathbb{W}}(\beta)$[1] at the temperature β^{-1} as

$$\mathsf{D}^{\mathbb{W}}(\beta) \coloneqq \lim_{n\uparrow\infty} \mathsf{E}^{\beta}_{\boldsymbol{v}} \mathsf{D}^{\mathbb{W}(n)}(\boldsymbol{v};\boldsymbol{x}), \tag{37}$$

the asymptotic distortion can be interpreted as the macroscopic parameter at zero temperature. Here, we take a well-known strategy in statistical mechanics which modifies the partition function to

$$\mathcal{Z}(\beta,h) = \sum_{\boldsymbol{v}} e^{-\beta\mathcal{E}(\boldsymbol{v}|\boldsymbol{y},\mathbf{A})+hn\mathsf{D}^{\mathbb{W}(n)}(\boldsymbol{v};\boldsymbol{x})}. \tag{38}$$

In this case, the expectation in (37) is taken as

$$\mathsf{D}^{\mathbb{W}}(\beta) = \lim_{n\uparrow\infty}\lim_{h\downarrow 0} \frac{1}{n}\frac{\partial}{\partial h}\log \mathcal{Z}(\beta,h). \tag{39}$$

The macroscopic parameter defined in (37) is random, namely depending on the quenched randomizer $\{\boldsymbol{y},\mathbf{A}\}$. As discussed in Section I-A, under the self averaging property, the macroscopic parameter is supposed to converge in the large-system limit to its expected value over the quenched random variables. For the corresponding spin glass defined in Definition III.1, the self averaging property has not been rigorously justified, and the proof requires further mathematical investigations as in [4]. However, as it is widely accepted in the literature, we assume that the property holds at least for the system setup we have specified here. Therefore, we state the following assumption.

Assumption 1 (Self Averaging Property)**.** Consider the corresponding spin glass defined in Definition III.1. For almost all realizations of the quenched randomizers $\mathbf{A}$ and $\boldsymbol{y}$,

$$\mathsf{D}^{\mathbb{W}}(\beta) = \mathsf{E}_{\boldsymbol{y},\mathbf{A}}\mathsf{D}^{\mathbb{W}}(\beta). \tag{40}$$

■

Using the self averaging property of the system, the asymptotic distortion is written as

$$\mathsf{D}^{\mathbb{W}}(\hat{\boldsymbol{x}};\boldsymbol{x}) = \lim_{\beta\uparrow\infty}\lim_{n\uparrow\infty}\lim_{h\downarrow 0} \frac{1}{n}\frac{\partial}{\partial h}\mathsf{E}\log \mathcal{Z}(\beta,h). \tag{41}$$

Evaluation of (41), as well as the normalized free energy defined in (34), confronts the nontrivial problem of determining the logarithmic expectation. The task can be bypassed by using the Riesz equality [60] which for a given random variable t states that

$$\mathsf{E}\,\log t = \lim_{m\downarrow 0}\frac{1}{m}\log \mathsf{E}\,t^m. \tag{42}$$

Using the Riesz equality, the asymptotic distortion can be finally written as

$$\mathsf{D}^{\mathbb{W}}(\hat{\boldsymbol{x}};\boldsymbol{x}) = \lim_{\beta\uparrow\infty}\lim_{n\uparrow\infty}\lim_{h\downarrow 0}\lim_{m\downarrow 0} \frac{1}{m}\frac{1}{n}\frac{\partial}{\partial h}\log \mathsf{E}[\mathcal{Z}(\beta,h)]^m. \tag{43}$$

(43) expresses the asymptotic distortion in terms of the moments of the modified partition function; however, it

[1]In general, $\mathsf{D}^{\mathbb{W}}(\beta)$ is a function of β, $\boldsymbol{y}$, $\boldsymbol{x}$ and $\mathbf{A}$. However, we drop the other arguments for sake of compactness.

does not yet simplify the problem. In fact, one faces two main difficulties when calculating the right hand side of (43): 1) the moment needs to be evaluated for real values of m (at least in a vicinity of 0), and 2) the limits need to be taken in the order stated. Here is where the replica method plays its role. The replica method suggests to determine the moment for an arbitrary non-negative integer m as an analytic function in m and then assume the two following statements:

1) The moment function analytically continues from the set of integer numbers onto the real axis (at least for some m at a right neighborhood of 0) which means that an analytic expression found for integer moments directly extends to all (or some) real moments. Under this assumption, the expression determined for integer moments can be replaced in (43), and the limit with respect to m taken when $m \downarrow 0$. This assumption is the main part where the replica method lacks rigor and is known as the "replica continuity".
2) In (43), the limits with respect to m and n exchange. We refer to this assumption as the "limit exchange".

In order to employ the replica method, we need to suppose the validity of the above two statements; therefore, we state the following assumption.

Assumption 2 (Replica Continuity and Limit Exchange)**.** For the spin glass defined in Definition III.1, the replica continuity and limit exchange assumptions hold. ■

By means of Assumption 2, the calculation of asymptotic distortion reduces to the evaluation of integer moments of the modified partition function which is written as

$$\mathsf{Z}(m) \coloneqq \mathsf{E}[\mathcal{Z}(\beta, h)]^m \tag{44a}$$

$$= \mathsf{E} \prod_{a=1}^{m} \sum_{\boldsymbol{v}_a} e^{-\beta \mathcal{E}(\boldsymbol{v}_a|\boldsymbol{y},\mathbf{A}) + hn \mathsf{D}^{\mathbb{W}(n)}(\boldsymbol{v}_a;\boldsymbol{x})} \tag{44b}$$

$$= \mathsf{E}_{\boldsymbol{x}} \mathsf{E}_{\mathbf{A}} \mathsf{E}_{\boldsymbol{z}} \sum_{\{\boldsymbol{v}_a\}} e^{-\beta \sum_{a=1}^{m} \mathcal{E}(\boldsymbol{v}_a|\boldsymbol{y},\mathbf{A}) + hn \sum_{a=1}^{m} \mathsf{D}^{\mathbb{W}(n)}(\boldsymbol{v}_a;\boldsymbol{x})}. \tag{44c}$$

Here, we refer to $\boldsymbol{v}_a \in \mathbb{X}^n$ for $a \in [1:m]$ as the replicas, and define $\{\boldsymbol{v}_a\} \coloneqq \{\boldsymbol{v}_1, \ldots, \boldsymbol{v}_m\} \in \mathbb{X}^n \times \cdots \times \mathbb{X}^n$ as the set of replicas. After taking the expectation with respect to $\boldsymbol{z}$ and $\mathbf{A}$, it is further observed that, in the large limit, the expectation with respect to $\boldsymbol{x}$ can be dropped due to the law of large numbers. By inserting the final expression for $\mathsf{Z}(m)$ in (43) and taking the limits, the asymptotic distortion is determined as in Proposition IV.1 given below.

IV. Main Results

Proposition IV.1 states the general replica ansatz. The term "general" is emphasized here, in order to indicate that no further assumption needs to be considered in the derivation. Using Proposition IV.1 along with results in the classical moment problem [58], a general form of the decoupling principle is justified for the MAP estimator.

Before stating the general replica ansatz, let us define the R-transform of a probability distribution. Considering a random variable t, the corresponding Stieltjes transform over the upper complex half plane is defined as

$$\mathrm{G}_t(s) = \mathsf{E}\,(t - s)^{-1}. \tag{45}$$

Denoting the inverse with respect to composition by $\mathrm{G}_t^{-1}(\cdot)$, the R-transform is given by

$$\mathrm{R}_t(\omega) = \mathrm{G}_t^{-1}(-\omega) - \omega^{-1} \tag{46}$$

such that $\lim_{\omega\downarrow 0} \mathrm{R}_t(\omega) = \mathsf{E}\, t$.

The definition can also be extended to matrix arguments. Assume the matrix $\mathbf{M}_{n\times n}$ to have the decomposition $\mathbf{M} = \mathbf{U}\mathbf{\Lambda}\mathbf{U}^{-1}$ where $\mathbf{\Lambda}_{n\times n}$ is a diagonal matrix with the nonzero elements given by the eigenvalues of $\mathbf{M}$, i.e., $\mathbf{\Lambda} = \mathrm{diag}[\lambda_1, \ldots, \lambda_n]$, and $\mathbf{U}_{n\times n}$ is the matrix of eigenvectors. $\mathrm{R}_t(\mathbf{M})$ is then an $n \times n$ matrix defined as

$$\mathrm{R}_t(\mathbf{M}) = \mathbf{U}\ \mathrm{diag}[\mathrm{R}_t(\lambda_1), \ldots, \mathrm{R}_t(\lambda_n)]\ \mathbf{U}^{-1}. \tag{47}$$

A. General Replica Ansatz

Proposition IV.1 expresses the macroscopic parameters of the corresponding spin glass, including the asymptotic distortion, in terms of the parameters of a new spin glass of finite dimension. It is important to note that the new spin glass, referred to as "spin glass of replicas", is different from the corresponding spin glass defined in Definition III.1. In fact, the spin glass of replicas is the projection of the corresponding spin glass on the reduced support $\mathbb{X}^m$ with m indicating the number of replicas. The macroscopic parameters of the spin glass of replicas can therefore readily be determined.

Definition IV.1 (Spin glass of replicas)**.** For the finite integer m, the spin glass of replicas with the microstate $\mathbf{v}_{m\times 1} \in \mathbb{X}^m$ and quenched randomizer $\mathbf{x}_{m\times 1}$ is defined as follows.

- All the entries of $\mathbf{x}$ equal to x where x is a random variable distributed with the source distribution p_x.
- For a given realization of $\mathbf{x}$, the Hamiltonian reads

$$\mathcal{E}^{\mathsf{R}}(\mathbf{v}|\mathbf{x}) = (\mathbf{x}-\mathbf{v})^{\mathsf{T}}\mathbf{T}\mathrm{R}_{\mathbf{J}}(-2\beta\mathbf{T}\mathbf{Q})(\mathbf{x}-\mathbf{v}) + u(\mathbf{v}) \tag{48}$$

  where $\mathrm{R}_{\mathbf{J}}(\cdot)$ is the R-transform corresponding to $\mathrm{F}_{\mathbf{J}}$, $\mathbf{T}_{m\times m}$ is defined as

$$\mathbf{T} \coloneqq \frac{1}{2\lambda}\left[\mathbf{I}_m - \frac{\beta\lambda_0}{\lambda + m\beta\lambda_0}\mathbf{1}_m\right], \tag{49}$$

  and $\mathbf{Q}_{m\times m}$ is the so-called replica correlation matrix defined as

$$\mathbf{Q} = \mathsf{E}\,(\mathbf{x}-\mathbf{v})(\mathbf{x}-\mathbf{v})^{\mathsf{T}}. \tag{50}$$

  with the expectation taken over $\mathbf{x}$ and $\mathbf{v}$ at thermal equilibrium.
- At thermal equilibrium, the microstate is distributed according to the Boltzmann-Gibbs distribution $\mathrm{p}^{\beta}_{\mathbf{v}|\mathbf{x}}$

$$\mathrm{p}^{\beta}_{\mathbf{v}|\mathbf{x}}(\mathbf{v}|\mathbf{x}) = \frac{e^{-\beta\mathcal{E}^{\mathsf{R}}(\mathbf{v}|\mathbf{x})}}{\mathcal{Z}^{\mathsf{R}}(\beta|\mathbf{x})} \tag{51}$$

  where $\mathcal{Z}^{\mathsf{R}}(\beta|\mathbf{x})$ denotes the partition function of the system defined as

$$\mathcal{Z}^{\mathsf{R}}(\beta|\mathbf{x}) \coloneqq \sum_{\mathbf{v}} e^{-\beta\mathcal{E}^{\mathsf{R}}(\mathbf{v}|\mathbf{x})}. \tag{52}$$

- The normalized free energy of the system at the inverse temperature β is given by

$$\mathsf{F}^{\mathsf{R}}(\beta, m) = -\frac{1}{\beta m}\mathsf{E}\log \mathcal{Z}^{\mathsf{R}}(\beta|\mathbf{x}), \tag{53}$$

  where the expectation is taken over $\mathbf{x}$ with respect to p_x. The average energy and entropy at the inverse temperature β are further found using (8a) and (8b).
- For the system at thermal equilibrium, the replicas' average distortion regarding the distortion function $\mathsf{d}(\cdot,\cdot)$ at the inverse temperature β is

$$\mathsf{D}^{\mathsf{R}}(\beta, m) = \frac{1}{m}\mathsf{E}\sum_{a=1}^{m}\mathsf{d}(\mathrm{v}_a, x), \tag{54}$$

  with expectation being taken over $\mathbf{x}$ and $\mathbf{v}$ with respect to $\mathrm{p}_{\mathbf{x}}\mathrm{p}_{\mathbf{v}|\mathbf{x}}$.

■

Considering Definition IV.1, the evaluation of the system parameters such as the replicas' average distortion $\mathsf{D}^{\mathsf{R}}(\beta, m)$ or the normalized free energy $\mathsf{F}^{\mathsf{R}}(\beta, m)$ needs the replica correlation matrix $\mathbf{Q}$ to be explicitly calculated first. In fact, (50) describes a fixed point equation in terms of $\mathbf{Q}$ when one writes out the expectation using the conditional distribution in (51). The solution can then be substituted in the distribution and the parameters of the system can be calculated via (52)-(54). The fixed point equation, however, may have several solutions and thus result in multiple outputs for the system. Nevertheless, we express the asymptotic distortion of the MAP estimator in terms of a single output of the spin glass of replicas which minimizes the free energy.

Proposition IV.1. *Let the linear system* (1) *fulfill the constraints of Section II. Suppose Assumptions 1 and 2 hold, and consider the spin glass of replicas as defined in Definition IV.1 for a finite integer m. Then, the free energy of the corresponding spin glass defined in Definition III.1 is given by*

$$\mathsf{F}(\beta) = \lim_{m\downarrow 0}\frac{1}{m}\left[\int_0^1 \mathrm{Tr}\{\mathbf{TQ}\mathrm{R}_{\mathbf{J}}(-2\beta\omega\mathbf{TQ})\}\mathrm{d}\omega - \mathrm{Tr}\{\mathbf{Q}^{\mathsf{T}}\mathbf{T}\mathrm{R}_{\mathbf{J}}(-2\beta\mathbf{TQ})\}\right] + \mathsf{F}^{\mathsf{R}}(\beta, m) \tag{55}$$

where $\mathbf{Q}$ is the replica correlation matrix satisfying (50)*. The asymptotic distortion of the MAP estimator regarding the distortion function $\mathsf{d}(\cdot;\cdot)$ is then determined as*

$$\mathsf{D}^{\mathsf{W}}(\hat{\boldsymbol{x}}; \boldsymbol{x}) = \lim_{\beta\uparrow\infty}\lim_{m\downarrow 0}\mathsf{D}^{\mathsf{R}}(\beta, m). \tag{56}$$

In case that multiple solutions are available for the replica correlation matrix, the replica's average distortion in (56) *is evaluated via a correlation matrix which minimizes the free energy at zero temperature, i.e., $\beta\uparrow\infty$.* ■

Proof. The proof is given in Appendix A. However, we explain briefly the strategy in the following. Starting from (44c), the expectation with respect to the noise term is straightforwardly taken. Using the results from [56], the expectation with respect to the system matrix is further taken as discussed in Appendix D. Then, by considering the following variable exchange,

$$[\mathbf{Q}]_{ab} = \frac{1}{n}(\boldsymbol{x} - \boldsymbol{v}_a)^{\mathsf{T}}(\boldsymbol{x} - \boldsymbol{v}_b). \tag{57}$$

$\mathsf{Z}(m)$ is determined in terms of the replica correlation matrix $\mathbf{Q}$. Finally, by employing the law of large numbers, the mth moment of the partition function is given as

$$\mathsf{Z}(m) = \mathsf{E}_{\boldsymbol{x}} \int e^{-n[\mathcal{G}(\mathbf{TQ})-\mathcal{I}(\mathbf{Q})]+\epsilon_n} \mathrm{d}\mathbf{Q} \tag{58}$$

where $\mathrm{d}\mathbf{Q} \coloneqq \prod_{a,b=1}^{m} \mathrm{d}[\mathbf{Q}]_{ab}$ with the integral being taken over $\mathbb{R}^{m\times m}$, ϵ_n tends to zero as $n \uparrow \infty$ and $\mathbf{T}$ is as in (49). Moreover, $e^{n\mathcal{I}(\mathbf{Q})}$ denotes the non-normalized probability weight of the vectors of replicas with a same correlation matrix and is explicitly determined in (199b) in Appendix A, and $\mathcal{G}(\cdot)$ reads

$$\mathcal{G}(\mathbf{M}) = \int_0^{\beta} \mathrm{Tr}\{\mathbf{M}\mathrm{R}_{\mathbf{J}}(-2\omega\mathbf{M})\}\mathrm{d}\omega \tag{59}$$

for some diagonal matrix $\mathbf{M}$ with $\mathrm{Tr}\{\cdot\}$ denoting the trace operator, and $\mathrm{R}_{\mathbf{J}}(\cdot)$ being the R-transform with respect to $\mathrm{F}_{\mathbf{J}}$. In (58), the term $e^{n\mathcal{I}(\mathbf{Q})}\mathrm{d}\mathbf{Q}$ is a probability measure which satisfies the large deviations property. Using results from large deviations [61], the integral in (58) for large values of n can be written as the integrand at the saddle point $\tilde{\mathbf{Q}}$ multiplied by some bounded coefficient K_n which results in

$$\mathsf{Z}(m) \doteq \mathsf{K}_n e^{-n\left[\mathcal{G}(\mathbf{T}\tilde{\mathbf{Q}})-\mathcal{I}(\tilde{\mathbf{Q}})\right]} \tag{60}$$

with $\doteq$ denoting the asymptotic equivalence in exponential scale[1]. Consequently, by substituting $\mathsf{Z}(m)$ in (43), and exchanging the limits with respect to n and m, as suggested in Assumption 2, the asymptotic distortion is found as in Proposition IV.1 where (50) determines the saddle point of the integrand function in (58). The free energy is further determined as in (55) by substituting (60) in (34). Finally by noting the fact that the free energy is minimized at the equilibrium, the proof is concluded. ▲

Proposition IV.1 introduces a feasible way to determine the asymptotics of the MAP estimator; its validity depends only on Assumptions 1 and 2 and has no further restriction. To pursue the analysis, one needs to solve the fixed point equation (50) for the replica correlation matrix $\mathbf{Q}$ and calculate the parameters of the spin glass of replicas explicitly. The direct approach to find $\mathbf{Q}$, however, raises both complexity and analyticity issues. In fact, finding the saddle point by searching over the set of all possible choices of $\mathbf{Q}$ is a hard task to do; moreover, several solutions may not be of use since they do not lead to analytic $\mathsf{F}^{\mathsf{R}}(\beta, m)$ and $\mathsf{D}^{\mathsf{R}}(\beta, m)$ in the variable m, and thus, they cannot be continued analytically to the real axis via Assumption 2.

To overcome both the issues, the approach is to restrict our search into a parameterized set of replica correlation matrices and find the solution within this set. Clearly, the asymptotics found via this approach may fail as several other solutions are missed by restriction. The result, in this case, becomes more trustable by extending the restricted set of replica correlation matrices. Several procedures of restrictions can be considered. The procedures introduced in the literature are roughly divided into RS and RSB schemes. The former considers the m replicas to interact symmetrically while the latter recursively breaks this symmetry in a systematic manner. In fact, the RS scheme was first introduced due to some symmetric properties observed in the analysis of the spin glasses [62]. The properties,

[1] $a(\cdot)$ and $b(\cdot)$ are asymptotically equivalent in exponential scale over a non-bounded set $\mathbb{X}$, if for $x \in \mathbb{X}$ we have $\lim\limits_{x\uparrow\infty} \log|\frac{a(x)}{b(x)}| = 0$.

however, do not force the correlation matrix to have a symmetric structure, and later several examples were found showing that RS leads to wrong conclusions. For these examples, the RSB scheme was further considered as an extension of the symmetric structure of the correlation matrix to a larger set. We consider both the RS and RSB schemes in this manuscript; however, before pursuing our study, let us first investigate the general decoupling property of the estimator which can be concluded from Proposition IV.1.

B. General Decoupling Property of MAP Estimator

Regardless of any restriction on $\mathbf{Q}$, the general ansatz leads to the decoupling property of the MAP estimator. In fact using Proposition IV.1, it can be shown that for almost any tuple of input-output entries, the marginal joint distribution converges to a deterministic joint distribution which does not depend on the entries' index. The explicit term for the joint distribution, however, depends on the assumptions imposed on the correlation matrix.

Proposition IV.2 (General Decoupling Principle)**.** *Let the linear system* (1) *fulfill the constraints of Section II. Suppose Assumptions 1 and 2 hold, and consider the spin glass of replicas as defined in Definition IV.1 with the replica correlation matrix* $\mathbf{Q}$*. Then, for* $j \in [1:n]$*, the asymptotic conditional distribution of the MAP estimator* $\mathrm{p}^{j}_{\hat{x}|x}$ *defined in Definition II.2 is, almost sure in* $\mathbf{A}$*, independent of* j*, namely*

$$\mathrm{p}^{j}_{\hat{x}|x}(\hat{v}|v) = \mathrm{p}_{\hat{\mathrm{x}}|\mathrm{x}}(\hat{v}|v) \tag{61}$$

for some conditional distribution $\mathrm{p}_{\hat{\mathrm{x}}|\mathrm{x}}$ *at the mass point* $(\hat{v}, v) \in \mathbb{X} \times \mathbb{X}$*. Consequently, the marginal joint distribution of the entries* x_j *and* $\hat{x}_j$ *is described by the input-output joint distribution of the single-user system specified by the conditional distribution* $\mathrm{p}_{\hat{\mathrm{x}}|\mathrm{x}}$ *and the input* $\mathrm{x} \sim \mathrm{p}_x$*. The explicit form of* $\mathrm{p}_{\hat{\mathrm{x}}|\mathrm{x}}$ *depends on* $\mathbf{Q}$*.* ■

Proof. The proof follows from Proposition IV.1 and the moment method [57], [58]. From the classical moment problem, we know that the joint probability of the tuple of random variables (t_1, t_2) are uniquely specified with the sequence of integer joint moments, if the joint moments are uniformly bounded. More precisely, by defining the (k, ℓ)-joint moment of the tuple (t_1, t_2) as

$$\mathsf{M}_{k,\ell} \coloneqq \mathsf{E}\, t_1^k t_2^\ell, \tag{62}$$

the sequence of $\{\mathsf{M}_{k,\ell}\}$ for $(k, \ell) \in \mathbb{Z}^+ \times \mathbb{Z}^+$ is uniquely mapped to the probability distribution p_{t_1,t_2}, if $\mathsf{M}_{k,\ell}$ is uniformly bounded for all integers k and ℓ. Consequently, one can infer that any two tuples of the random variables (t_1, t_2) and $(\hat{t}_1, \hat{t}_2)$ with the same sequences of the joint moments are identical in distribution.

To determine the joint moment of input and output entries, consider the distortion function

$$\mathsf{d}(\hat{x}, x) = \hat{x}^k x^\ell \tag{63}$$

in Proposition IV.1, and evaluate the asymptotic distortion over the limit of $\mathbb{W}(n) = [j : j + \eta n]$ for some η in a right neighborhood of zero. The (k, ℓ)-joint moment of $(\hat{x}_j, x_j)$ is then determined by taking the limit $\eta \downarrow 0$.

Substituting the distortion function and the index set in Proposition IV.1, it is clear that the asymptotic distortion is independent of η and j, and therefore, the limit with respect to η exists and is independent of j as well. Noting

that the evaluated moments are uniformly bounded, it is inferred that the asymptotic joint distribution of $(\hat{x}_j, x_j)$ is uniquely specified and does not depend on the index j. Finally, by using the fact that the source vector is i.i.d. and the distribution of the entry j is independent of the index, we conclude that the asymptotic conditional distribution $\mathrm{p}^{j}_{\hat{x}|x}$ is independent of j. The exact expression for $\mathrm{p}^{j}_{\hat{x}|x}$ is then found by determining the solution $\mathbf{Q}$ to the fixed point equation and determining the joint moments. ▲

Proposition IV.2 is a generalized form of the RS decoupling principle for the MAP estimators studied in [30]. In fact, Proposition IV.2 indicates that a vector system followed by a MAP estimator always decouples into a bank of identical single-user systems regardless of any restriction on the replica correlation matrix.

C. Consistency Test

If one restricts the replica correlation matrix $\mathbf{Q}$ to be of a special form, the asymptotics determined under the assumed structure do not necessarily approximate true asymptotics accurately. Several methods were introduced in the literature to check the consistency of the solution. A primary method is based on the entropy of the system at zero temperature. As the temperature tends to zero, the distribution of the microstate tends to an indicator function at the point of the estimated vector, and consequently, the entropy of the corresponding spin glass converges to zero. One consistency check is, therefore, the zero temperature entropy of a given solution.

In several cases in which the RS ansatz clearly fails, the zero temperature entropy not only does not converge to zero, but it also takes negative values; on the other hand, the RSB ansätze take values near to zero; see for example [63]. This observation illustrates the invalidity of the RS assumption and hints at RSB ansätz giving better approximations. Inspired by the aforementioned results, we evaluate the zero temperature entropy of the corresponding spin glass as a measure of consistency.

In order to determine the zero temperature entropy, we invoke (35) which determines the entropy in terms of the free energy at inverse temperature β. Considering the free energy of the corresponding spin glass as given in Proposition IV.1, the entropy $\mathrm{H}(\beta)$ reads

$$\mathrm{H}(\beta) = \lim_{m\downarrow 0} \frac{\beta^2}{m} \frac{\partial}{\partial \beta} \left[\int_0^1 \mathrm{Tr}\{\mathbf{TQ}\mathrm{R}_{\mathbf{J}}(-2\beta\omega\mathbf{TQ})\}\mathrm{d}\omega - \mathrm{Tr}\{\mathbf{Q}^{\mathsf{T}}\mathbf{T}\mathrm{R}_{\mathbf{J}}(-2\beta\mathbf{TQ})\} \right] + \mathrm{H}^{\mathsf{R}}(\beta, m) \tag{64}$$

where $\mathrm{H}^{\mathsf{R}}(\beta, m)$ denotes the normalized entropy of the spin glass of replicas. As $\mathrm{H}^{\mathsf{R}}(\beta, m)$ determines the entropy of a thermodynamic system, for any $m \in \mathbb{R}^+$ we have

$$\lim_{\beta\uparrow\infty} \mathrm{H}^{\mathsf{R}}(\beta, m) = 0, \tag{65}$$

and therefore, the zero temperature entropy is given by

$$\mathrm{H}^0 = \lim_{\beta\uparrow\infty} \lim_{m\downarrow 0} \frac{\beta^2}{m} \frac{\partial}{\partial \beta} \left[\int_0^1 \mathrm{Tr}\{\mathbf{TQ}\mathrm{R}_{\mathbf{J}}(-2\beta\omega\mathbf{TQ})\}\mathrm{d}\omega - \mathrm{Tr}\{\mathbf{Q}^{\mathsf{T}}\mathbf{T}\mathrm{R}_{\mathbf{J}}(-2\beta\mathbf{TQ})\} \right], \tag{66}$$

which obviously depends on the structure of the replica correlation matrix. In [63], the authors determined the zero temperature entropy for their study of a spin glass under the RS and 1RSB assumptions, and observed that it takes the same form under both assumptions. They then conjectured that the zero temperature entropy takes similar form

under the general RSB structure regardless of the number of breaking steps[1]. Using (66), we later show that the conjecture in [63] is true.

V. RS Ansatz and RS Decoupling Principle

The most elementary structure which can be imposed on the replica correlation matrix is RS. Here, one assumes the correlation matrix to be of a symmetric form which means that the replicas of the spin glass defined in Definition IV.1 are invariant under any permutation of indices. Using the definition of the replica correlation matrix as given in (50), it consequently reads that

$$(x-\mathrm{v}_a)(x-\mathrm{v}_b)=\begin{cases} q_0 & \text{if } a\neq b \\ q_1 & \text{if } a=b. \end{cases} \tag{67}$$

Assumption 3 (RS Structure)**.** Considering the spin glass of replicas as defined in Definition IV.1, the replica correlation matrix is of the form

$$\mathbf{Q}=\frac{\chi}{\beta}\mathbf{I}_m+q\mathbf{1}_m \tag{68}$$

where χ and q are some non-negative real scalars. ■

Considering (67), Assumption 3 supposes $q_0=q$ and $q_1=\chi\beta^{-1}+q$. Substituting (68) in Definition IV.1, the spin glass of replicas is then specified by the scalars χ and q. The scalars are moreover related via a set of saddle point equations which are obtained from (50). Finally, using Proposition IV.1, the asymptotics of the system are found.

Proposition V.1 (RS Ansatz)**.** *Let the linear system* (1) *fulfill the constraints of Section II. Suppose Assumptions 1 and 2, as well as Assumption 3 hold. Let* $x\sim \mathrm{p}_x$*, and*

$$\mathrm{g}=\arg\min_{v}\left[\frac{1}{2\lambda^{\mathsf{s}}}(x+\sqrt{\lambda_0^{\mathsf{s}}}z-v)^2+u(v)\right] \tag{69}$$

with $v\in\mathbb{X}$*, and* λ_0^{s} *and* λ^{s} *being defined as*

$$\lambda_0^{\mathsf{s}}\coloneqq\left[\mathrm{R}_{\mathbf{J}}(-\frac{\chi}{\lambda})\right]^{-2}\frac{\partial}{\partial\chi}\left\{[\lambda_0\chi-\lambda q]\,\mathrm{R}_{\mathbf{J}}(-\frac{\chi}{\lambda})\right\} \tag{70a}$$

$$\lambda^{\mathsf{s}}\coloneqq\left[\mathrm{R}_{\mathbf{J}}(-\frac{\chi}{\lambda})\right]^{-1}\lambda \tag{70b}$$

for some non-negative real χ *and* q *and the real variable* z*. Then, the asymptotic distortion defined in* (28) *reads*

$$\mathsf{D}^{\mathsf{W}}=\mathsf{E}\int\mathsf{d}(\mathrm{g},x)\mathrm{D}z, \tag{71}$$

[1]In fact in this case, the dependence of the zero temperature entropy on the correlation matrix is completely described via the scalar χ which corresponds to the diagonal entries of the correlation matrix. See Assumption 3-5 for more illustrations.

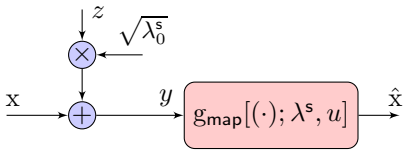


Fig. 1: The decoupled single-user system under the RS ansatz.

for χ and q which satisfy

$$\sqrt{\lambda_0^{\mathsf{s}}}\ \chi = \lambda^{\mathsf{s}}\ \mathsf{E}\int(\mathrm{g}-x)z\ \mathrm{D}z \tag{72a}$$

$$q = \mathsf{E}\int(\mathrm{g}-x)^2\ \mathrm{D}z \tag{72b}$$

and minimize the zero temperature free energy $\mathsf{F}_{\mathsf{rs}}^0$ where

$$\mathsf{F}_{\mathsf{rs}}^0 = \frac{1}{2\lambda}\left[\int_0^1 \mathrm{F}(\omega)\mathrm{d}\omega - \mathrm{F}(1)\right] + \mathsf{E}\int\frac{1}{2\lambda^{\mathsf{s}}}\left[(x+\sqrt{\lambda_0^{\mathsf{s}}}z-\mathrm{g})^2-\lambda_0^{\mathsf{s}}z^2\right]+u(\mathrm{g})\ \mathrm{D}z \tag{73}$$

with $\mathrm{F}(\cdot)$ being defined by

$$\mathrm{F}(\omega) = \left[q-\frac{\lambda_0}{\lambda}\chi\right]\frac{\mathrm{d}}{\mathrm{d}\omega}\left[\omega\mathrm{R}_{\mathbf{J}}(-\frac{\chi}{\lambda}\omega)\right]. \tag{74}$$

■

Proof. See Appendix B. ▲

The asymptotic distortion under the RS ansatz is equivalent to the average distortion of a scalar AWGN channel followed by a single-user estimator as shown in Fig. 1. In this block diagram, the single-user estimator $\mathrm{g}_{\mathsf{map}}[(\cdot);\lambda^{\mathsf{s}},u]$ maximizes the posterior probability over a postulated scalar AWGN channel. We refer to this estimator as the "decoupled MAP estimator" and define it as follows.

Definition V.1 (Decoupled MAP estimator)**.** The decoupled MAP estimator $\mathrm{g}_{\mathsf{map}}[(\cdot);\lambda^{\mathsf{s}},u]$ with the estimation parameter λ^{s} and the utility function $u(\cdot)$ is defined as

$$\mathrm{g}_{\mathsf{map}}[(y);\lambda^{\mathsf{s}},u] \coloneqq \arg\max_v\ \mathrm{q}_{\lambda^{\mathsf{s}}}(v|y) \tag{75a}$$

$$= \arg\min_v\left[\frac{1}{2\lambda^{\mathsf{s}}}(y-v)^2+u(v)\right], \tag{75b}$$

where $\mathrm{q}_{\lambda^{\mathsf{s}}}(v|y)$ denotes the "decoupled posterior distribution" postulated by the estimator which reads

$$\mathrm{q}_{\lambda^{\mathsf{s}}}(v|y) = \mathsf{K}\ e^{-\left[\frac{1}{2\lambda^{\mathsf{s}}}(y-v)^2+u(v)\right]} \tag{76}$$

for some real constant K. ■

Using the definition of the decoupled MAP estimator, the RS decoupled system is defined next.

Definition V.2 (RS decoupled system)**.** Define the RS decoupled system to be consistent with the block diagram in Fig. 1 in which

- the source symbol x is distributed with p_{x} over the support $\mathbb{X}$,
- z is a zero-mean and unit-variance Gaussian random variable,
- x and z are independent,
- $\hat{\mathrm{x}}$ is estimated from the observation $y \coloneqq \mathrm{x} + \sqrt{\lambda_0^{\mathsf{s}}} z$ as

$$\hat{\mathrm{x}} = \mathrm{g}_{\mathsf{map}}[(y); \lambda^{\mathsf{s}}, u]. \tag{77}$$

- $\mathrm{g}_{\mathsf{map}}[(\cdot); \lambda^{\mathsf{s}}, u]$ is the decoupled MAP estimator with the estimation parameter λ^{s} and the utility function $u(\cdot)$ as defined in Definition V.1.
- λ_0^{s} and λ^{s} are defined as in Proposition V.1.

■

Using Proposition IV.2, the equivalency in the asymptotic distortion can be extended to the asymptotic conditional distribution as well. In fact, by considering the decoupling principle, Definition V.2 describes the structure of the decoupled single-user system under the RS ansatz.

Proposition V.2 (RS Decoupling Principle)**.** *Let the linear system* (1) *fulfill the constraints of Section II and be estimated via the MAP estimator in* (20)*. Consider the RS decoupled system as defined in Definition V.2, and suppose Assumptions 1, 2 and 3 hold. Then, for any* $j \in [1:n]$*, the tuple* $(\hat{x}_j, x_j)$ *converges in distribution to* $(\hat{\mathrm{x}}, \mathrm{x})$ *if* $\mathrm{p}_x = \mathrm{p}_{\mathrm{x}}$*, almost sure in* $\mathbf{A}$*.* ■

Proof. Using Proposition IV.2, for any two different indices $j, q \in [1:n]$ we have

$$\mathrm{p}^{j}_{\hat{x}|x}(\hat{v}|v) = \mathrm{p}^{q}_{\hat{x}|x}(\hat{v}|v) \tag{78}$$

at the mass point $(\hat{v}, v)$. Therefore for any index j, we have

$$\mathsf{E}\, \hat{x}_j^k x_j^\ell = \lim_{n\uparrow\infty} \frac{1}{n} \mathsf{E} \sum_{i=1}^{n} \hat{x}_i^k x_i^\ell. \tag{79}$$

Consequently, the asymptotic (k,ℓ)-joint moment of $(\hat{x}_j, x_j)$ under the RS assumption is determined by letting $\mathbb{W}(n) = [1:n]$ and the distortion function in the RS ansatz

$$\mathsf{d}(\hat{x}; x) = \hat{x}^k x^\ell \tag{80}$$

and determining the asymptotic distortion. Substituting in Proposition V.1, the asymptotic joint moment reads

$$\mathsf{M}^{j}_{k,\ell} = \mathsf{E} \int \mathrm{g}^k x^\ell \mathrm{D}z \tag{81}$$

where g is defined in (69). Considering Definition V.2 and assuming $\mathrm{p}_{\mathrm{x}} = \mathrm{p}_x$, (81) describes the (k,ℓ)-joint moment of $(\hat{\mathrm{x}}, \mathrm{x})$ as well. Noting that $\mathsf{M}^{j}_{k,\ell}$ is uniformly bounded for any pair of integers k and ℓ, it is concluded that the

asymptotic joint distribution of $(\hat{x}_j, x_j)$ and the joint distribution of $(\hat{\mathrm{x}}, \mathrm{x})$ are equivalent. ▲

Proposition V.2 gives a more general form of the RS decoupling principles investigated in [30] and [31]. In fact, by restricting the system matrix and source distribution as in [30] and [31], one can recover the formerly studied RS decoupling principles.

RS Zero Temperature

To have a basic measure of RS ansatz's consistency, we evaluate the zero temperature entropy under the RS assumption following the discussion in Section IV-C. Substituting (68) in (66) and taking the same steps as in Appendix B, the RS zero temperature entropy is determined as

$$\mathrm{H}^0_{\mathsf{rs}} = \lim_{\beta\uparrow\infty} \frac{\beta^2}{2\lambda}\frac{\partial}{\partial\beta}\left[\int_0^1 \mathrm{F}^{\beta}(\omega)\mathrm{d}\omega - \mathrm{F}^{\beta}(1)\right] \tag{82}$$

where the function $\mathrm{F}^{\beta}(\cdot)$ is defined as

$$\mathrm{F}^{\beta}(\omega) = \frac{\chi}{\beta}\mathrm{R}_{\mathbf{J}}(-\frac{\chi}{\lambda}\omega) + \left[q - \frac{\lambda_0}{\lambda}\chi\right]\frac{\mathrm{d}}{\mathrm{d}\omega}\left[\omega\mathrm{R}_{\mathbf{J}}(-\frac{\chi}{\lambda}\omega)\right]. \tag{83}$$

Taking the derivative first and then the limit, it finally reads

$$\mathrm{H}^0_{\mathsf{rs}} = \frac{\chi}{2\lambda}\left[\mathrm{R}_{\mathbf{J}}(-\frac{\chi}{\lambda}) - \int_0^1 \mathrm{R}_{\mathbf{J}}(-\frac{\chi}{\lambda}\omega)\mathrm{d}\omega\right]. \tag{84}$$

We later on see that the zero temperature entropy takes the same form under the RSB assumptions.

VI. RSB Ansatz and RSB Decoupling Principle

In [64], Parisi introduced a breaking scheme to broaden the restricted set of correlation matrices. The scheme recursively extends the set of matrices to larger sets. The breaking scheme was then employed to broaden the RS structure of the correlation matrices, and therefore, the obtained structure was identified as the broken RS or, RSB structure. The key feature of Parisi's breaking scheme is that, by starting from the RS structure, the new structure after breaking can be reduced to the structure before breaking. Thus, the set of fixed point solutions found by assuming the broken structure includes the solutions of the previous structure as well.

Definition VI.1 (Parisi's breaking scheme)**.** Let m be a multiple of the integer ξ, and $\mathbf{Q}^{[\ell]}$ represent an $\frac{m}{\xi}\times\frac{m}{\xi}$ correlation matrix. Parisi's breaking scheme then constructs a new $m\times m$ correlation matrix $\mathbf{Q}^{[\ell+1]}$ as

$$\mathbf{Q}^{[\ell+1]} = \mathbf{I}_{\xi}\otimes\mathbf{Q}^{[\ell]} + \kappa\mathbf{1}_m \tag{85}$$

for some real scalar κ. ■

By choosing $\mathbf{Q}^{[0]}$ to be an RS correlation matrix in Definition VI.1, the matrix $\mathbf{Q}^{[1]}$ finds the RSB structure with one step of breaking (1RSB) structure. The steps of breaking can be further increased recursively by inserting $\mathbf{Q}^{[1]}$ in the next breaking scheme, determining the new correlation matrix $\mathbf{Q}^{[2]}$, and repeating the procedure. We start by the 1RSB correlation matrix, and then, extend the result to higher RSB ansätze with more steps of breaking.

Assumption 4 (1RSB Structure)**.** Considering the spin glass of replicas as defined in Definition IV.1, the replica correlation matrix is of the form

$$\mathbf{Q} = \frac{\chi}{\beta}\mathbf{I}_m + p\mathbf{I}_{\frac{m\beta}{\mu}} \otimes \mathbf{1}_{\frac{\mu}{\beta}} + q\mathbf{1}_m \tag{86}$$

where χ, p, q and μ are some non-negative real scalars. ■

Regarding Parisi's breaking scheme, Assumption 4 considers $\mathbf{Q} = \mathbf{Q}^{[1]}$ by letting $\mathbf{Q}^{[0]}$ have the RS structure with parameters $\chi\beta^{-1}$ and p, $\xi = \mu\beta^{-1}$ and $\kappa = q$. Here, the 1RSB structure reduces to RS by setting $p = 0$. Therefore, the set of 1RSB correlation matrices contains the one considered in Assumption 3.

Proposition VI.1 (1RSB Ansatz)**.** *Let the linear system* (1) *fulfill the constraints of Section II. Suppose Assumptions 1 and 2, as well as Assumption 4 hold. Let* $x \sim \mathrm{p}_x$ *and*

$$\mathrm{g} = \arg\min_{v} \left[\frac{1}{2\lambda^{\mathsf{s}}}(x + \sqrt{\lambda_0^{\mathsf{s}}}z_0 + \sqrt{\lambda_1^{\mathsf{s}}}z_1 - v)^2 + u(v)\right] \tag{87}$$

with $v \in \mathbb{X}$ *and* λ_0^{s}, λ_1^{s} *and* λ^{s} *being defined by*

$$\lambda_0^{\mathsf{s}} = \left[\mathrm{R}_{\mathbf{J}}(-\frac{\chi}{\lambda})\right]^{-2} \frac{\partial}{\partial\chi}\left\{[\lambda_0(\chi + \mu p) - \lambda q]\,\mathrm{R}_{\mathbf{J}}(-\frac{\chi + \mu p}{\lambda})\right\}, \tag{88a}$$

$$\lambda_1^{\mathsf{s}} = \left[\mathrm{R}_{\mathbf{J}}(-\frac{\chi}{\lambda})\right]^{-2}\left[\mathrm{R}_{\mathbf{J}}(-\frac{\chi}{\lambda}) - \mathrm{R}_{\mathbf{J}}(-\frac{\chi + \mu p}{\lambda})\right]\lambda\mu^{-1}, \tag{88b}$$

$$\lambda^{\mathsf{s}} = \left[\mathrm{R}_{\mathbf{J}}(-\frac{\chi}{\lambda})\right]^{-1}\lambda \tag{88c}$$

for some non-negative real χ, p, q *and* μ *and real variables* z_0 *and* z_1*. Then, the asymptotic distortion in* (28) *reads*

$$\mathsf{D}^{\mathbb{W}} = \mathsf{E}\int \mathsf{d}(\mathrm{g}, x)\ \tilde{\Lambda}\mathrm{D}z_1\mathrm{D}z_0, \tag{89}$$

with $\tilde{\Lambda} \coloneqq \left[\int \Lambda \mathrm{D}z_1\right]^{-1}\Lambda$ *and* Λ *being defined by*

$$\Lambda = e^{-\mu\left[\frac{1}{2\lambda^{\mathsf{s}}}(x + \sqrt{\lambda_0^{\mathsf{s}}}z_0 + \sqrt{\lambda_1^{\mathsf{s}}}z_1 - \mathrm{g})^2 - \frac{1}{2\lambda^{\mathsf{s}}}(\sqrt{\lambda_0^{\mathsf{s}}}z_0 + \sqrt{\lambda_1^{\mathsf{s}}}z_1)^2 + u(\mathrm{g})\right]}. \tag{90}$$

The scalars χ, p *and* q *satisfy*

$$\sqrt{\lambda_0^{\mathsf{s}}}\,[\chi + \mu p] = \lambda^{\mathsf{s}}\mathsf{E}\int(\mathrm{g} - x)z_0\ \tilde{\Lambda}\mathrm{D}z_1\mathrm{D}z_0 \tag{91a}$$

$$\sqrt{\lambda_1^{\mathsf{s}}}\,[\chi + \mu q + \mu p] = \lambda^{\mathsf{s}}\mathsf{E}\int(\mathrm{g} - x)z_1\ \tilde{\Lambda}\mathrm{D}z_1\mathrm{D}z_0 \tag{91b}$$

$$q + p = \mathsf{E}\int(\mathrm{g} - x)^2\ \tilde{\Lambda}\mathrm{D}z_1\mathrm{D}z_0 \tag{91c}$$

and μ *is a solution of the fixed point equation*

$$\frac{\mu}{2\lambda^{\mathsf{s}}}\left[\mu\frac{\lambda_1^{\mathsf{s}}}{\lambda^{\mathsf{s}}}q + p\right] - \frac{1}{2\lambda}\int_0^{\mu p}\mathrm{R}_{\mathbf{J}}(-\frac{\chi + \omega}{\lambda})\mathrm{d}\omega = \mathsf{E}\int\log\tilde{\Lambda}\ \tilde{\Lambda}\mathrm{D}z_1\mathrm{D}z_0. \tag{92}$$

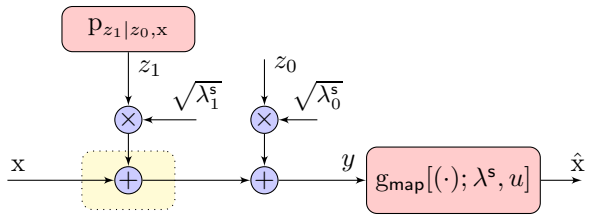


Fig. 2: The decoupled scalar system under the 1RSB ansatz.

Moreover, χ, p, q and μ minimize the zero temperature free energy $\mathsf{F}_{\mathsf{rsb}}^{0[1]}$ which reads

$$\mathsf{F}_{\mathsf{rsb}}^{0[1]} = \frac{1}{2\lambda}\left[\int_0^1 \mathrm{F}(\omega)\mathrm{d}\omega - \mathrm{F}(1)\right] - \frac{1}{\mu}\mathsf{E}\int \log\left[\int \Lambda \mathrm{D}z_1\right]\,\mathrm{D}z_0 \tag{93}$$

with $\mathrm{F}(\cdot)$ being defined as

$$\mathrm{F}(\omega) = \frac{1}{\mu}\frac{\mathrm{d}}{\mathrm{d}\omega}\left[\int_{\chi\omega}^{[\chi+\mu p]\omega} \mathrm{R}_{\mathbf{J}}(-\frac{t}{\lambda})\mathrm{d}t\right] + \left[q - \lambda_0\frac{\chi+\mu p}{\lambda}\right]\frac{\mathrm{d}}{\mathrm{d}\omega}\left[\omega \mathrm{R}_{\mathbf{J}}(-\frac{\chi+\mu p}{\lambda}\omega)\right]. \tag{94}$$

■

Proof. See Appendix C. ▲

Similar to our approach under the RS ansatz, we employ Proposition VI.1 to introduce the decoupled 1RSB single-user system which describes the statistical behavior of the MAP estimator's input-output entries under 1RSB assumption. The decoupled system under 1RSB differs from RS within a new impairment term which is correlated with the source and noise symbols through a joint distribution. The impairment term intuitively plays the role of a correction factor which compensates the possible inaccuracy of the RS ansatz. The decoupled MAP estimator, however, follows the same structure as for RS.

Definition VI.2 (1RSB decoupled system)**.** Fig. 2 defines the 1RSB decoupled system in which

- the source symbol x is distributed with p_{x} over the support $\mathbb{X}$,
- z_0 is a zero-mean and unit-variance Gaussian random variable,
- z_1 is a random variable correlated with x and z_0,
- x and z_0 are independent, and

$$\mathrm{p}_{z_1|\mathrm{x},z_0} = \tilde{\Lambda}\phi(z_1) \tag{95}$$

  with $\tilde{\Lambda}$ defined in Proposition VI.1.
- $\hat{\mathrm{x}}$ is estimated from the observation $y \coloneqq \mathrm{x} + \sqrt{\lambda_0^{\mathsf{s}}}z_0 + \sqrt{\lambda_1^{\mathsf{s}}}z_1$ as

$$\hat{\mathrm{x}} = \mathsf{g}_{\mathsf{map}}[(y);\lambda^{\mathsf{s}},u]. \tag{96}$$

- $\mathsf{g}_{\mathsf{map}}[(\cdot);\lambda^{\mathsf{s}},u]$ is the decoupled MAP estimator with the estimation parameter λ^{s} and the utility function $u(\cdot)$ as defined in Definition V.1.

- λ_0^{s}, λ_1^{s} and λ^{s} are defined as in Proposition VI.1.

■

Proposition VI.2 (1RSB Decoupling Principle)**.** *Let the linear system* (1) *fulfill the constraints of Section II and be estimated via the MAP estimator in* (20)*. Consider the 1RSB decoupled system as defined in Definition VI.2, and suppose Assumptions 1, 2 and 4 hold. Then, for all* $j \in [1:n]$*, the tuple* $(\hat{x}_j, x_j)$ *converges in distribution to* $(\hat{\mathrm{x}}, \mathrm{x})$ *if* $\mathrm{p}_x = \mathrm{p}_{\mathrm{x}}$. ■

Proof. The proof takes exactly same steps as for the RS decoupling principle using Proposition VI.1. ▲

The 1RSB decoupled system, in general, provides a more accurate approximation of the estimator's asymptotics by searching over a larger set of solutions which include the RS ansatz. To investigate the latter statement, consider the case of $p = 0$. In this case, the 1RSB structure reduces to RS. Setting $p = 0$ in Proposition VI.1, λ_1 becomes zero, and consequently $\tilde{\Lambda} = 1$. Moreover, the fixed point equations in (92) hold for any choice of μ, and the scalars χ and q couple through the same set of equations as in the RS ansatz. The zero temperature free energy of the system, furthermore, reduces to its RS form under the assumption of $p = 0$. Denoting the parameters of the RS ansatz by $[\chi_{\mathsf{rs}}, q_{\mathsf{rs}}]$, it is then concluded that $[\chi, p, q, \mu] = [\chi_{\mathsf{rs}}, 0, q_{\mathsf{rs}}, 0]$ is a solution to the 1RSB fixed point equations. The solution, however, does not give necessarily the 1RSB ansatz, since the $\mathsf{F}_{\mathsf{rsb}}^{0[1]}$ may meet the minimum at another solution. We investigate the impact of replica breaking for some examples later through numerical results.

Parisi's breaking scheme can be employed to extend the structure of the correlation matrix to the RSB structure with more steps of breaking by recursively repeating the scheme. In fact, one can start from $\mathbf{Q}^{[0]}$ having RS structure and employ the breaking scheme for b steps to determine the correlation matrix $\mathbf{Q}^{[b]}$. In this case, the replica correlation matrix is referred to as the bRSB correlation matrix.

Assumption 5 (bRSB Structure)**.** Considering the spin glass of replicas as defined in Definition IV.1, the replica correlation matrix is of the form

$$\mathbf{Q} = \frac{\chi}{\beta}\mathbf{I}_m + \sum_{\kappa=1}^{b} p_\kappa \mathbf{I}_{\frac{m\beta}{\mu_\kappa}} \otimes \mathbf{1}_{\frac{\mu_\kappa}{\beta}} + q\mathbf{1}_m \tag{97}$$

where scalars χ and q, and the sequences $\{p_\kappa\}$ and $\{\mu_\kappa\}$ with $\kappa \in [1:b]$ are non-negative reals, and $\{\mu_\kappa\}$ satisfies the following constraint

$$\frac{\mu_{\kappa+1}}{\mu_\kappa} \in \mathbb{Z}^+ \tag{98}$$

for $\kappa \in [1 : b-1]$. ■

Considering the correlation matrix in Proposition IV.1 to be of the form indicated in Assumption 5 the previous ansätze are extended to a more general ansatz which can reduce to the 1RSB as well as RS ansatz. Proposition VI.3 expresses the replica ansatz under the bRSB assumption.

Proposition VI.3 (bRSB Ansatz)**.** *Let the linear system* (1) *fulfill the constraints of Section II. Suppose Assumptions*

1 and 2, as well as Assumption 5 hold. For $\kappa \in [0:b]$, define the sequence $\{\tilde{\chi}_\kappa\}$, such that $\tilde{\chi}_0 = \chi$ and

$$\tilde{\chi}_\kappa \coloneqq \chi + \sum_{\varsigma=1}^{\kappa} \mu_\varsigma p_\varsigma \tag{99}$$

for $\kappa \in [1:b]$. Let $x \sim \mathrm{p}_x$, and

$$\mathrm{g} = \arg\min_{v} \left[\frac{1}{2\lambda^{\mathsf{s}}} (x + \sum_{\kappa=0}^{b} \sqrt{\lambda_\kappa^{\mathsf{s}}} z_\kappa - v)^2 + u(v) \right] \tag{100}$$

with $v \in \mathbb{X}$ and λ_0^{s}, $\{\lambda_\kappa^{\mathsf{s}}\}$ and λ^{s} being defined as

$$\lambda_0^{\mathsf{s}} = \left[\mathrm{R}_{\mathbf{J}}(-\frac{\tilde{\chi}_0}{\lambda}) \right]^{-2} \frac{\partial}{\partial \tilde{\chi}_b} \left\{ [\lambda_0 \tilde{\chi}_b - \lambda q] \, \mathrm{R}_{\mathbf{J}}(-\frac{\tilde{\chi}_b}{\lambda}) \right\}, \tag{101a}$$

$$\lambda_\kappa^{\mathsf{s}} = \left[\mathrm{R}_{\mathbf{J}}(-\frac{\tilde{\chi}_0}{\lambda}) \right]^{-2} \left[\mathrm{R}_{\mathbf{J}}(-\frac{\tilde{\chi}_{\kappa-1}}{\lambda}) - \mathrm{R}_{\mathbf{J}}(-\frac{\tilde{\chi}_\kappa}{\lambda}) \right] \lambda \mu_\kappa^{-1}, \tag{101b}$$

$$\lambda^{\mathsf{s}} = \left[\mathrm{R}_{\mathbf{J}}(-\frac{\tilde{\chi}_0}{\lambda}) \right]^{-1} \lambda \tag{101c}$$

for some non-negative real scalar q, sequences $\{\tilde{\chi}_\kappa\}$ and $\{\mu_\kappa\}$ and sequence of real variables $\{z_\kappa\}$. Then, the asymptotic distortion defined in (28) reads

$$\mathsf{D}^{\mathbb{W}} = \mathsf{E} \int \mathsf{d}(\mathrm{g}; x) \prod_{\kappa=1}^{b} \tilde{\Lambda}_\kappa \, \mathrm{D}z_\kappa \mathrm{D}z_0, \tag{102}$$

where $\tilde{\Lambda}_\kappa$ for $\kappa \in [1:b]$ is defined as $\tilde{\Lambda}_\kappa = \left[\int \Lambda_\kappa \mathrm{D}z_\kappa \right]^{-1} \Lambda_\kappa$ with

$$\Lambda_1 \coloneqq e^{-\mu_1 \left[\frac{1}{2\lambda^{\mathsf{s}}} (x + \sum_{\kappa=0}^{b} \sqrt{\lambda_\kappa^{\mathsf{s}}} z_\kappa - \mathrm{g})^2 - \frac{1}{2\lambda^{\mathsf{s}}} (\sum_{\kappa=0}^{b} \sqrt{\lambda_\kappa^{\mathsf{s}}} z_\kappa)^2 + u(\mathrm{g}) \right]} \tag{103}$$

and $\{\Lambda_\kappa\}$ for $\kappa \in [2:b]$ being recursively determined by

$$\Lambda_\kappa \coloneqq \left[\int \Lambda_{\kappa-1} \, \mathrm{D}z_{\kappa-1} \right]^{\frac{\mu_\kappa}{\mu_{\kappa-1}}}. \tag{104}$$

The scalar q and sequences $\{\tilde{\chi}_\kappa\}$ and $\{p_\kappa\}$ satisfy

$$\sum_{\kappa=1}^{b} p_\kappa + q = \mathsf{E} \int (\mathrm{g} - x)^2 \prod_{\kappa=1}^{b} \tilde{\Lambda}_\kappa \, \mathrm{D}z_\kappa \mathrm{D}z_0, \tag{105a}$$

$$\tilde{\chi}_{\kappa-1} + \mu_\kappa \left(\sum_{\varsigma=\kappa}^{b} p_\varsigma + q \right) = \frac{\lambda^{\mathsf{s}}}{\sqrt{\lambda_\kappa^{\mathsf{s}}}} \mathsf{E} \int (\mathrm{g} - x) z_\kappa \prod_{\kappa=1}^{b} \tilde{\Lambda}_\kappa \, \mathrm{D}z_\kappa \mathrm{D}z_0, \tag{105b}$$

$$\tilde{\chi}_b = \frac{\lambda^{\mathsf{s}}}{\sqrt{\lambda_0^{\mathsf{s}}}} \mathsf{E} \int (\mathrm{g} - x) z_0 \prod_{\kappa=1}^{b} \tilde{\Lambda}_\kappa \, \mathrm{D}z_\kappa \mathrm{D}z_0, \tag{105c}$$

and the sequence $\{\mu_\kappa\}$ is given by

$$\{\mu_\kappa\} = \arg\min_{\{\tilde{\mu}_\kappa\}} \left[\frac{1}{2\lambda} \int_0^1 \mathrm{F}(\omega; \{\tilde{\mu}_\kappa\}) \mathrm{d}\omega - \frac{1}{\tilde{\mu}_b} \mathsf{E} \int \log \left[\int \Lambda_b \mathrm{D}z_b \right] \mathrm{D}z_0 - \frac{1}{2\lambda^{\mathsf{s}}} \Delta(\{\tilde{\mu}_\kappa\}) \right] \tag{106}$$

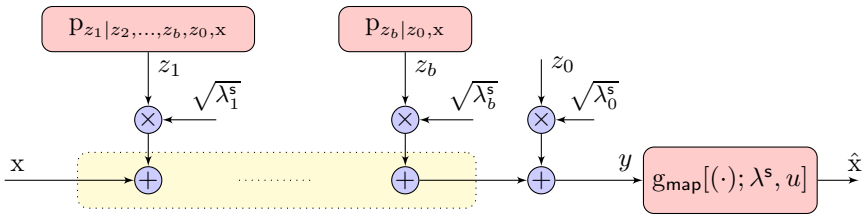


Fig. 3: The decoupled scalar system under the bRSB ansatz.

where the function $\mathrm{F}(\cdot;\{\mu_\kappa\})$ *is defined as*

$$\mathrm{F}(\omega;\{\mu_\kappa\}) \coloneqq \sum_{\kappa=1}^{b} \frac{1}{\mu_\kappa} \frac{\mathrm{d}}{\mathrm{d}\omega} \int_{\tilde{\chi}_{\kappa-1}\omega}^{\tilde{\chi}_\kappa \omega} \mathrm{R}_{\mathbf{J}}(-\frac{t}{\lambda})\mathrm{d}t + \left[q - \frac{\lambda_0}{\lambda}\tilde{\chi}_b\right] \frac{\mathrm{d}}{\mathrm{d}\omega}\left[\omega \mathrm{R}_{\mathbf{J}}(-\frac{\tilde{\chi}_b}{\lambda}\omega)\right], \tag{107}$$

$\Delta(\cdot)$ *is defined as*

$$\Delta(\{\mu_\kappa\}) = \sum_{\kappa=1}^{b} \frac{1}{\mu_\kappa}\left[\zeta_\kappa \tilde{\chi}_\kappa - \zeta_{\kappa-1}\tilde{\chi}_{\kappa-1}\right] + \zeta_b q - \frac{\lambda_0^{\mathsf{s}}}{\lambda^{\mathsf{s}}}\tilde{\chi}_b \tag{108}$$

with $\zeta_0 = 1$, *and* ζ_κ *for* $\kappa \in [1:b]$ *denoting*

$$\zeta_\kappa \coloneqq 1 - \sum_{\varsigma=1}^{\kappa} \mu_\varsigma \frac{\lambda_\varsigma^{\mathsf{s}}}{\lambda^{\mathsf{s}}}, \tag{109}$$

and $\{\tilde{\mu}_\kappa\} \in \mathbb{S}_{\boldsymbol{\mu}}$ *in which*

$$\mathbb{S}_{\boldsymbol{\mu}} \coloneqq \left\{ \{\mu_1,\ldots,\mu_b\} \ni \mu_\kappa \in \mathbb{R}^+ \ \wedge \ \frac{\mu_{\kappa+1}}{\mu_\kappa} \in \mathbb{Z}^+ \ \forall \kappa \in [1:b-1] \right\}. \tag{110}$$

In the case of multiple solutions for χ, q, $\{p_\kappa\}$ *and* $\{\mu_\kappa\}$, *the ansatz is chosen such that the free energy at zero temperature*

$$\mathsf{F}_{\mathsf{rsb}}^{0[b]} = \frac{1}{2\lambda}\left[\int_0^1 \mathrm{F}(\omega;\{\mu_\kappa\})\mathrm{d}\omega - \mathrm{F}(1;\{\mu_\kappa\})\right] - \frac{1}{\mu_b}\mathsf{E}\int \log\left[\int \Lambda_b \mathrm{D}z_b\right] \mathrm{D}z_0 \tag{111}$$

is minimized. ■

Proof. See Appendix D. ▲

One can simply observe that Proposition VI.3 reduces to Propositions VI.1 and V.1 by letting $b = 1$ and $p_\kappa = 0$ for $\kappa \in [1:b]$, respectively. The ansatz, moreover, extends the corresponding decoupled single-user system of the estimator considering the general decoupling principle investigated in Proposition IV.2. By taking the same steps as in Proposition VI.2, the decoupled bRSB single-user system is found which represents the extended version of the 1RSB system with b number of additive impairment taps. In fact, considering the impairment terms to intuitively play the role of correction factors, the bRSB ansatz takes more steps of correction into account. The decoupled MAP estimator, moreover, remains unchanged.

Definition VI.3 (bRSB decoupled system)**.** Define the bRSB decoupled system as a single-user system illustrated

in Fig. 3 in which

- the source symbol x is distributed with p_{x} over the support $\mathbb{X}$,
- z_0 is a zero-mean and unit-variance Gaussian random variable,
- z_κ is a random variable correlated with x, z_0 and $\{z_{\kappa+1}, \ldots, z_b\}$
- x and z_0 are independent, and

$$\mathrm{p}_{z_\kappa|z_{\kappa+1},\ldots,z_b,z_0,\mathrm{x}} = \tilde{\Lambda}_\kappa \phi(z_\kappa) \tag{112}$$

  with $\tilde{\Lambda}$ defined in Proposition VI.3.
- $\hat{\mathrm{x}}$ is estimated from the observation $y \coloneqq \mathrm{x} + \sum_{\kappa=0}^{b} \sqrt{\lambda_\kappa^{\mathsf{s}}} z_\kappa$ as

$$\hat{\mathrm{x}} = \mathrm{g}_{\mathsf{map}}[(y); \lambda^{\mathsf{s}}, u]. \tag{113}$$

- $\mathrm{g}_{\mathsf{map}}[(\cdot); \lambda^{\mathsf{s}}, u]$ is the decoupled MAP estimator with the estimation parameter λ^{s} and the utility function $u(\cdot)$ as defined in Definition V.1, and
- λ_0^{s}, $\{\lambda_\kappa^{\mathsf{s}}\}$ and λ^{s} for $\kappa \in [1:b]$ are as in Proposition VI.3.

■

Proposition VI.4 (bRSB Decoupling Principle)**.** *Let the linear system* (1) *fulfill the constraints of Section II and be estimated via the MAP estimator in* (20)*. Consider the bRSB decoupled system as defined in Definition VI.3, and suppose Assumptions 1, 2 and 5 hold. Then, for all $j \in [1:n]$, the tuple $(\hat{x}_j, x_j)$ converges in distribution to $(\hat{\mathrm{x}}, \mathrm{x})$ if $\mathrm{p}_x = \mathrm{p}_{\mathrm{x}}$.* ■

Proof. Using Proposition VI.1, it takes same steps as for Proposition V.2. ▲

RSB Zero Temperature

In Appendix D, it is shown that under the bRSB assumption on the replica correlation matrix the free energy of the corresponding spin glass at the inverse temperature β reads

$$\mathsf{F}(\beta) = \frac{1}{2\lambda}\left[\int_0^1 \mathrm{F}^\beta(\omega)\mathrm{d}\omega - \mathrm{F}^\beta(1)\right] + \mathsf{F}^{\mathsf{R}}(\beta). \tag{114}$$

Here, $\mathsf{F}^{\mathsf{R}}(\beta)$ denotes the normalized free energy of the spin glass of replicas defined in (53) in the limit $m \downarrow 0$, and the function $\mathrm{F}^\beta(\cdot)$ is defined as

$$\mathrm{F}^\beta(\omega) = \sum_{\kappa=1}^{b} \frac{1}{\mu_\kappa} \frac{\mathrm{d}}{\mathrm{d}\omega} \int_{\tilde{\chi}_{\kappa-1}\omega}^{\tilde{\chi}_\kappa \omega} \mathrm{R}_{\mathbf{J}}(-\frac{t}{\lambda})\mathrm{d}t + \frac{\chi}{\beta}\mathrm{R}_{\mathbf{J}}(-\frac{\chi}{\lambda}\omega) + \left[q - \frac{\lambda_0}{\lambda}\tilde{\chi}_b\right] \frac{\mathrm{d}}{\mathrm{d}\omega}\left[\omega \mathrm{R}_{\mathbf{J}}(-\frac{\tilde{\chi}_b}{\lambda}\omega)\right]. \tag{115}$$

Following the discussion in Section IV-C, the entropy at the zero temperature reads

$$\mathrm{H}_{\mathsf{rsb}}^{0[b]} = \lim_{\beta\uparrow\infty} \frac{\beta^2}{2\lambda}\frac{\partial}{\partial\beta}\left[\int_0^1 \mathrm{F}^\beta(\omega)\mathrm{d}\omega - \mathrm{F}^\beta(1)\right] \tag{116}$$

which reduces to

$$\mathrm{H}_{\mathsf{rsb}}^{0[b]} = \frac{\chi}{2\lambda}\left[\mathrm{R}_{\mathbf{J}}(-\frac{\chi}{\lambda}) - \int_0^1 \mathrm{R}_{\mathbf{J}}(-\frac{\chi}{\lambda}\omega)\mathrm{d}\omega\right]. \tag{117}$$

(117) justifies the conjecture in [63] and states that the zero temperature entropy under any number of breaking steps, including the RS case, is of the similar form and only depends on the scalar χ. In fact, the Hamiltonian in (10) reduces to the one considered in vector precoding by considering $\boldsymbol{x}$ to be the deterministic vector of zeros, $\lambda_0 = 0$, $\lambda = 1$ and $u(\boldsymbol{v}) = 0$. Substituting in (117), the zero temperature entropy reduces to the one determined in [63] within a factor of 2. The factor comes from the difference in the priory assumption on the support of microstate[1].

VII. Replica Simulator: Characterization via the Single-User Representation

The general bRSB decoupling principle determines an equivalent single-user system which describes the input-output statistics of the MAP estimator under the bRSB ansatz. In order to specify the exact parameters of the decoupled single-user system, the set of fixed point equations needs to be solved explicitly. In this section, we propose an alternative approach which describes an ansatz in terms of the corresponding decoupled system's input-output statistics. We define the exact form of the decoupled system as the "steady state" of a transition system named "replica simulator". The proposed approach enables us to investigate the properties of the RS and RSB ansätze through the study of the replica simulator.

In order to clarify the idea of the replica simulator, let us define a set of input-output statistics regarding the bRSB decoupled system.

Definition VII.1. Consider the single-user system consistent with the block diagram in Fig. 3. Denote the joint distribution of the source and impairment terms with $\mathrm{p}_{\mathrm{x},z_0,\ldots,z_b}$. For this system,

- the κth noise-error correlation is defined as

$$\mathsf{C}_\kappa = \frac{1}{\sqrt{\lambda_\kappa^{\mathsf{s}}}}\mathsf{E}\left(\hat{\mathrm{x}} - \mathrm{x}\right)z_\kappa \tag{118}$$

  for $\kappa \in [0:b]$, and
- the MSE is denoted by

$$\mathsf{MSE} = \mathsf{E}\left(\hat{\mathrm{x}} - \mathrm{x}\right)^2. \tag{119}$$

■

Invoking Definition VII.1, the bRSB ansatz can be completely represented in terms of the input-output statistics of the decoupled system. In fact, by means of Definition VII.1, the fixed point equations in (105a)-(105c) can be

[1] In [63], the authors considered $\boldsymbol{v}$ to be a complex vector.

expressed as

$$\sum_{\kappa=1}^{b} p_\kappa + q = \mathsf{MSE}, \tag{120a}$$

$$\tilde{\chi}_{\kappa-1} + \mu_\kappa \left(\sum_{\varsigma=\kappa}^{b} p_\varsigma + q \right) = \lambda^{\mathsf{s}} \mathsf{C}_\kappa, \tag{120b}$$

$$\tilde{\chi}_b = \lambda^{\mathsf{s}} \mathsf{C}_0, \tag{120c}$$

for $\kappa \in [1:b]$; moreover, the factor Λ_1 is given as

$$\Lambda_1 = e^{-\mu_1 \left[\frac{1}{2\lambda^{\mathsf{s}}} (y-\hat{\mathrm{x}})^2 - \frac{1}{2\lambda^{\mathsf{s}}} (y-\mathrm{x})^2 + u(\hat{\mathrm{x}}) \right]}, \tag{121}$$

which reduces to

$$\Lambda_1 = \mathrm{p_x}(\mathrm{x})^{\mu_1} \left[\frac{\mathrm{q}_{\lambda^{\mathsf{s}}}(\hat{\mathrm{x}}|y)}{\mathrm{q}_{\lambda^{\mathsf{s}}}(\mathrm{x}|y)} \right]^{\mu_1} \tag{122}$$

with $\mathrm{q}_{\lambda^{\mathsf{s}}}(x|y)$ indicating the decoupled posterior distribution defined in Definition V.1. The second term on the right hand side of (122) is an extended form of the likelihood ratio. By defining

$$\Gamma_1 = \left[\frac{\mathrm{q}_{\lambda^{\mathsf{s}}}(\hat{\mathrm{x}}|y)}{\mathrm{q}_{\lambda^{\mathsf{s}}}(\mathrm{x}|y)} \right]^{\mu_1}, \tag{123}$$

(122) reads

$$\Lambda_1 = \mathrm{p_x}(\mathrm{x})^{\mu_1} \Gamma_1, \tag{124}$$

and Λ_κ for $\kappa \in [2:b]$ are determined by

$$\Lambda_\kappa = \mathrm{p_x}(\mathrm{x})^{\mu_\kappa} \Gamma_\kappa \tag{125}$$

where Γ_κ are recursively defined as

$$\Gamma_\kappa = \left[\int \Gamma_{\kappa-1} \, \mathrm{D}z_{\kappa-1} \right]^{\frac{\mu_\kappa}{\mu_{\kappa-1}}}. \tag{126}$$

The fixed point in (106) is therefore rewritten accordingly.

The above alternative representation of the bRSB ansatz leads us to a new interpretation. In fact, one can define a transition system in which the vector of replica parameters denotes the state, and the decoupled single-user system defines the transition rule [65], [66]. We refer to this transition system as the "replica simulator", and define it formally as the following.

Definition VII.2 (Replica simulator)**.** Let b be a non-negative integer. Consider the vector $\mathbf{s}$ as

$$\mathbf{s} \coloneqq [\chi, \mu_1, \ldots, \mu_b, p_1, \ldots, p_b, q] \tag{127}$$

with entries satisfying the corresponding constraints in Proposition VI.3, and denote its support by $\mathbb{S}_b$. The transition

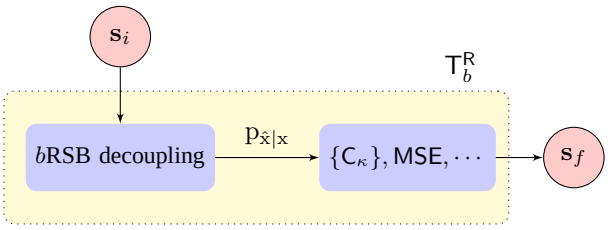


Fig. 4: Replica Simulator of breaking order b

rule $\mathsf{T}_b^{\mathsf{R}} : \mathbb{S}_b \mapsto \mathbb{S}_b$ maps the prior state $\mathbf{s}_i \in \mathbb{S}_b$ to the posterior state $\mathbf{s}_f \in \mathbb{S}_b$ in the following way:

$\mathsf{T}_b^{\mathsf{R}}$ *realizes the bRSB decoupled system considering the entries of $\mathbf{s}_i$ as the replica parameters. It then constructs the entries of $\mathbf{s}_f$ by determining a new set of replica parameters from the statistics of the decoupled system using the equivalent representation of the fixed point equations given in* (120a)-(126).

The replica simulator of breaking order b is then defined as the transition system $\mathsf{Sim}^{\mathsf{R}}[b] \coloneqq \big(\mathbb{S}_b, \mathsf{T}_b^{\mathsf{R}}\big)$. ■

The structure of the replica simulator is illustrated in Fig. 4. For the replica simulator of breaking order b, a sequence of states $\{\mathbf{s}_t\}$ is considered to be a "process", if for $t \in [1 : \infty]$

$$\mathbf{s}_t \xrightarrow{\mathsf{T}_b^{\mathsf{R}}} \mathbf{s}_{t+1}. \tag{128}$$

The state $\mathbf{s}^\star$ is then called the "steady state", if setting $\mathbf{s}_t = \mathbf{s}^\star$ results in $\mathbf{s}_{t+1} = \mathbf{s}^\star$. Regarding Proposition VI.3, the bRSB ansatz is in fact the steady state of the replica simulator which minimizes the free energy function. Our conclusion also extends to the RS case, if we set $b = 0$.

Considering Definition VII.2, as well as the above discussions, the bRSB ansatz can be numerically investigated using the methods developed in the literature of transition systems. This approach may reduce the complexity of numerical analysis; however, it does not impact the computational complexity[1]. In fact, assuming that one realizes the bRSB decoupled system for any desired state vector denoted in (127) via some methods of realization, e.g., Monte Carlo simulation, the bRSB ansatz can be found by means of an iterative algorithm which has been designed to find the steady state of a transition system. The latter statement can be clarified as in Scheme 1.

In Scheme 1, $\mathsf{T}_b^{\mathsf{R}}$ in step A can be realized via different methods. One may determine the input-output distribution of the single-user system analytically or simulate the system by generating impairment and source samples numerically via Monte Carlo technique. Another degree of freedom is in step B where different mapping rules with different convergence speeds can be employed. For algorithms designed based on Scheme 1, the computational complexity depends on the realization method while the convergence speed is mainly restricted with some given mapping rule $\mathsf{IM}(\cdot, \cdot)$.

The replica simulator introduces a systematic approach for investigating the replica anätze based on the decoupling principle. Moreover, it gives an intuition about the impact of symmetry breaking. To clarify the latter statement, let

[1]We conjecture that in some cases, our bRSB decoupled system represents the asymptotic of a decision-feedback system. The validity of this conjecture can further reduce the computation complexity.

Scheme 1 Analysis via Replica Simulator

begin
set replica simulator of breaking order b, $\mathsf{Sim}^{\mathsf{R}}[b]$
  if $b=0$ **then**
    $\mathsf{T}_b^{\mathsf{R}}$ corresponds to the RS decoupled system
  else
    $\mathsf{T}_b^{\mathsf{R}}$ corresponds to the bRSB decoupled system
  end if
initiate initial state $\mathbf{s}^0 \in \mathbb{S}_b$
evaluate $\mathbf{s}^0 \xrightarrow{\mathsf{T}_b^{\mathsf{R}}} \mathbf{s}$ ▷ A
  if $\mathbf{s}=\mathbf{s}^0$ **then**
    $\mathbf{s}^\star \leftarrow \mathbf{s}$
    break
  else
    consider mapping rule $\mathsf{IM}(\cdot,\cdot) : \mathbb{S}_b \times \mathbb{S}_b \mapsto \mathbb{S}_b$ ▷ B
    $\mathbf{s}^0 \leftarrow \mathsf{IM}(\mathbf{s},\mathbf{s}^0)$
    return A
  end if
output $\mathbf{s}^\star$
end

us consider an example.

Example. (RS vs. 1RSB ansatz) Let $b=0$; thus, the RS fixed point equations read

$$q = \mathsf{MSE}, \tag{129a}$$

$$\chi = \lambda^{\mathsf{s}}\mathsf{C}_0. \tag{129b}$$

The equations under the 1RSB assumption are moreover given by

$$q+p = \mathsf{MSE}, \tag{130a}$$

$$\chi+\mu p = \lambda^{\mathsf{s}}\mathsf{C}_0, \tag{130b}$$

$$\chi+\mu p+\mu q = \lambda^{\mathsf{s}}\mathsf{C}_1, \tag{130c}$$

and μ is determined through the fixed point equation

$$\frac{\mu}{2\lambda^{\mathsf{s}}}\left[\mu\frac{\lambda_1^{\mathsf{s}}}{\lambda^{\mathsf{s}}}q+p\right]-\frac{1}{2\lambda}\int_0^{\mu p}\mathrm{R}_{\mathbf{J}}(-\frac{\chi+\omega}{\lambda})\mathrm{d}\omega = \mathrm{I}(z_1;z_0,\mathrm{x})+\mathsf{D}_{\mathsf{KL}}(\mathrm{p}_{z_1}\|\phi) \tag{131}$$

where $\mathrm{I}(\cdot;\cdot)$ and $\mathsf{D}_{\mathsf{KL}}(\cdot\,\|\,\cdot)$ denote the mutual information and Kullback-Leibler divergence, respectively. Assuming the system matrix to be i.i.d. and setting z_1 to be independent of z_0 and x, the right hand side of (131) tends to zero, and therefore, the solutions $\mu=0$ and $p=0$ are concluded. Consequently, (130c) becomes ineffective, and the fixed point equations reduce to RS. The latter observation can be interpreted in terms of the "state evolution" of the replica simulator. More precisely, assume that the initial state of the replica simulator with breaking order one is chosen such that in the corresponding decoupled system, z_1 is sufficiently correlated with the source and noise symbols. In this case, by assuming the mapping rule $\mathsf{IM}(\cdot,\cdot)$ to be converging, the correlation in each iteration of

Scheme 1 reduces, and thus, at the steady state, z_1 becomes independent of z_0 and x.

The above discussion can be extended to replica simulators with larger breaking orders. Moreover, further properties of the RSB ansätze could be studied using methods developed in the literature of transition systems. We leave the further investigations as a possible future work.

VIII. Large Compressive Sensing Systems

Regarding the system setup represented in Section II, a large compressive sensing system can be studied through our results by restricting the source's CDF to be of the form

$$\mathrm{F}_x(x) = (1-\alpha)\mathbf{1}\left\{x \geq x_0\right\} + \alpha \breve{\mathrm{F}}_x(x). \tag{132}$$

In the large limit, the source vector distributed as (132) has $(1-\alpha)n$ entries equal to x_0 while the remaining αn entries are distributed with $\breve{\mathrm{F}}_x$. In this case, $\boldsymbol{x}$ is an αn-sparse vector, and thus, (1) is considered to represent a large compressive sensing system with the sensing matrix $\mathbf{A}$.

Considering the prior as in (132), different recovery schemes are then investigated by restricting the priory setup of the system, correspondingly. In this section, we study the asymptotics of several recovery schemes using our bRSB decoupling principle for both the cases of continuous and finite alphabet sources.

A. Continuous Alphabet Sources

Assuming $\mathbb{X} = \mathbb{R}$ and $x_0 = 0$, (132) describes a continuous random variable multiplied by an α-Bernoulli random variable. In this case, by varying the utility function $u(\cdot)$, different reconstruction schemes are considered. Here, we address the linear, LASSO and zero-mean recovery schemes.

Example 1. (linear recovery scheme) The MAP estimation is reduced to the linear recovery scheme when the utility function is set to be

$$u(v) = \frac{v^2}{2}. \tag{133}$$

In fact, in this case, the MAP estimator postulates the prior distribution to be a zero-mean and unit-variance Gaussian and performs considerably inefficient when the source is sparse. Using the bRSB decoupling principle, we conclude that in the large-system limit the source entry x_j and the estimated entry $\hat{x}_j$, for any $j \in [1:n]$, converge in probability to a sparse random variable x distributed as in (132) and the estimated symbol $\hat{\mathrm{x}} \coloneqq \mathsf{g}_{\mathsf{map}}[(y); \lambda^{\mathsf{s}}, u]$ where the decoupled system reduces to

$$\mathsf{g}_{\mathsf{map}}[(y); \lambda^{\mathsf{s}}, u] = \frac{y}{1+\lambda^{\mathsf{s}}}, \tag{134}$$

with y being given as

$$y = \mathrm{x} + \sum_{\kappa=0}^{b} \sqrt{\lambda_\kappa^{\mathsf{s}}} z_\kappa, \tag{135}$$

and the scalars λ^{s} and $\{\lambda^{\mathsf{s}}_{\kappa}\}$ for $\kappa \in [0:b]$ are defined as in Proposition VI.3. By letting $b=0$, the result reduces to the RS decoupling principle reported in the literature, see [30], [31]; however, the result here holds for a wider set of sensing matrices and source distributions.

Example 2. (LASSO recovery scheme) To study the LASSO recovery scheme, we set

$$u(v) = |v|. \tag{136}$$

Regarding the bRSB decoupling principle, the prior distribution of the decoupled system's input x is postulated to be "Laplacian" or "double exponential" with unit variance. This postulation results in a better performance of the recovery scheme in many cases, since the Laplacian PDF could be a more realistic approximation of the sparse source distribution. Consequently, the decoupled system's output is found as $\hat{\mathrm{x}} = \mathrm{g}_{\mathsf{map}}[(y);\lambda^{\mathsf{s}},u]$ with

$$\mathrm{g}_{\mathsf{map}}[(y);\lambda^{\mathsf{s}},u] = [y - \lambda^{\mathsf{s}}\ \mathsf{sgn}(y)]\ w_{\lambda^{\mathsf{s}}}(y) \tag{137}$$

where y is denoted as in (135), $w_{\lambda^{\mathsf{s}}}(\cdot)$ is the null window function with window width λ^{s} defined as

$$w_{\lambda^{\mathsf{s}}}(y) = \begin{cases} 1 & |y| > \lambda^{\mathsf{s}} \\ 0 & |y| \leq \lambda^{\mathsf{s}} \end{cases}, \tag{138}$$

and $\mathsf{sgn}(y)$ is the sign indicator. The decoupled single-user estimator in (138) which is often referred to as the "soft-thresholding" operator recovers the earlier RS results by setting $b=0$ and the sensing matrix to be i.i.d. [30].

Example 3. (ℓ_0 norm recovery scheme) The ℓ_0 norm recovery scheme which considers

$$u(v) = \|v\|_0 \tag{139}$$

can perform significantly better that the latter schemes when the sparsity increases. In this case, the prior distribution of the bRSB decoupled system's input x is found as the limit of

$$\mathrm{p}_{\mathrm{x}}^{\theta,\delta}(\mathrm{x}) = \frac{1}{2\theta + 2\delta\,(e-1)} \begin{cases} e & 0 \leq |\mathrm{x}| \leq \delta \\ 1 & \delta < |\mathrm{x}| < \theta \end{cases}, \tag{140}$$

when $\theta \uparrow \infty$ and $\delta \downarrow 0$. For finite values of θ and δ, $\mathrm{p}_{\mathrm{x}}^{\theta,\delta}$ can be considered as a sparse distribution in which non-zero symbols occur uniformly. The prior explains the better performance of the ℓ_0 norm recovery scheme compared to the linear and LASSO schemes. For this case, the output of the decoupled single-user system reads $\hat{\mathrm{x}} = \mathrm{g}_{\mathsf{map}}[(y);\lambda^{\mathsf{s}},u]$, such that

$$\mathrm{g}_{\mathsf{map}}[(y);\lambda^{\mathsf{s}},u] = y w_{\vartheta}(y) \tag{141}$$

where y is denoted as in (135), and $w_{\vartheta}(\cdot)$ is the null window function with $\vartheta = \sqrt{2\lambda^{\mathsf{s}}}$. Here, $\mathrm{g}_{\mathsf{map}}[(\cdot);\lambda^{\mathsf{s}},u]$ is the hard limiting operator and recovers the analysis in [30] for a wider ensemble of sensing matrices by setting $b=0$.

The above examples have been also studied in earlier replica based studies, e.g., [30], [32]. The given results

can be analytically derived from the above expressions by considering the RS ansatz and properly substituting the corresponding R-transforms. We address the results of two important cases reported in the literature in following.

Special Case 1: In [30], the authors addressed the case of which an i.i.d. sparse source is sampled by an i.i.d. sensing matrix where the matrix entries are zero-mean random variables with the variance vanishing proportional to k^{-1}. The asymptotic performance of the estimator was then addressed when the linear, LASSO, and ℓ_0 norm recovery schemes are employed using the RS MAP decoupling principle. The results reported in [30] can be derived directly by setting the R-transform in Proposition V.2 to be

$$\mathrm{R}_{\mathbf{J}}(\omega) = \frac{1}{1-\mathsf{r}\omega}. \tag{142}$$

Special Case 2: The results of [30] extended in [32] to a larger set of sensing matrices, and the RS prediction of the asymptotic MSE was determined for sparse Gaussian sources. The given results can be recovered by considering the distortion function

$$\mathsf{d}(\hat{\boldsymbol{x}};\boldsymbol{x}) = \|\hat{\boldsymbol{x}}-\boldsymbol{x}\|^2, \tag{143}$$

and the source distribution to be (132) with $\breve{\mathrm{F}}_x$ representing the zero-mean and unit-variance Gaussian CDF.

B. Finite Alphabet Sources

Our result can be further employed to study the sampling problem of finite alphabet sources. Assuming the source's support $\mathbb{X}$ to be of the form

$$\mathbb{X} = \{0, t_1, \ldots, t_{\ell-1}\}, \tag{144}$$

the symbol 0 occurs with probability $1-\alpha$, and the other $\ell-1$ outcomes are distributed due to p_t. Therefore, the source distribution reads

$$\mathrm{p}_x(x) = (1-\alpha)\,\mathbf{1}\{x=0\} + \alpha\mathbf{1}\{x\neq 0\}\mathrm{p}_t(x) \tag{145}$$

which can be interpreted as the multiplication of the random variable t distributed with p_t and an α-Bernoulli random variable. Without loss of generality, we denote the symbols in $\mathbb{X}$ with $\mathrm{c}_1, \ldots, \mathrm{c}_\ell$, such that

$$-\infty < \mathrm{c}_1 < \mathrm{c}_2 < \ldots < \mathrm{c}_\ell < +\infty. \tag{146}$$

For notational compactness, we further define c_0 and $\mathrm{c}_{\ell+1}$ to be $-\infty$ and $+\infty$, respectively. Similar to the continuous case, different choices of the utility function $u(\cdot)$ address different types of reconstruction schemes which we investigate in the sequel.

Example 4. (linear recovery scheme) We consider the case in which the finite alphabet source is reconstructed via the linear recovery scheme as introduced in Example 1. Using the bRSB decoupling principle, the source and

estimated symbols $(x_j, \hat{x}_j)$ converge to the random variables x and $\hat{\mathrm{x}}$ for all $j \in [1:n]$ where x is distributed with p_x defined in (145), and $\hat{\mathrm{x}}$ is found as $\hat{\mathrm{x}} = \mathrm{g}_{\mathsf{map}}[(y); \lambda^{\mathsf{s}}, u]$ with

$$\mathrm{g}_{\mathsf{map}}[(y); \lambda^{\mathsf{s}}, u] = \mathrm{c}_k \qquad \text{if} \qquad y \in \left(v_k^{\ell_2}, v_{k+1}^{\ell_2}\right] \tag{147}$$

for $k \in [1:\ell]$. The scalar y indicates the observation symbol in the equivalent decoupled system, and the boundary point $v_k^{\ell_2}$ is defined as

$$v_k^{\ell_2} \coloneqq \frac{1+\lambda^{\mathsf{s}}}{2}\left(\mathrm{c}_{k-1} + \mathrm{c}_k\right). \tag{148}$$

Example 5. (LASSO recovery scheme) Replacing the reconstruction scheme in Example 4 with the LASSO, the single-user estimator of the bRSB decoupled system is of the form

$$\mathrm{g}_{\mathsf{map}}[(y); \lambda^{\mathsf{s}}, u] = \mathrm{c}_k \qquad \text{if} \qquad y \in \left(v_k^{\ell_1}, v_{k+1}^{\ell_1}\right] \tag{149}$$

for $k \in [1:\ell]$ where the boundary point $v_k^{\ell_l}$ reads

$$v_k^{\ell_1} \coloneqq \frac{1}{2}\left(\mathrm{c}_{k-1} + \mathrm{c}_k\right) + \lambda^{\mathsf{s}} \frac{|\mathrm{c}_k| - |\mathrm{c}_{k-1}|}{\mathrm{c}_k - \mathrm{c}_{k-1}}. \tag{150}$$

Example 6. (ℓ_0 norm recovery scheme) For finite alphabet sources, the ℓ_0 norm recovery scheme is optimal, since it realizes the sparse uniform distribution. In fact, for the case of which the non-zero symbols of the source are uniformly distributed, the ℓ_0 norm utility function exactly models the source's true prior, and therefore, can be considered as the optimal scheme. Under the ℓ_0 norm recovery scheme, the bRSB decoupled system reduces to

$$\mathrm{g}_{\mathsf{map}}[(y); \lambda^{\mathsf{s}}, u] = \mathrm{c}_k \qquad \text{if} \qquad y \in \left(v_k^{\ell_0}, v_{k+1}^{\ell_0}\right] \tag{151}$$

with the boundary point $v_k^{\ell_0}$ being defined as

$$v_k^{\ell_0} \coloneqq \frac{1}{2}\left(\mathrm{c}_{k-1} + \mathrm{c}_k\right) + \lambda^{\mathsf{s}} \frac{\mathbf{1}\{\mathrm{c}_k \neq 0\} - \mathbf{1}\{\mathrm{c}_{k-1} \neq 0\}}{\mathrm{c}_k - \mathrm{c}_{k-1}}. \tag{152}$$

for $k \in [1:\ell]$.

IX. Numerical Results for Large Compressive Sensing Systems

In this section, we numerically investigate the examples of large compressive sensing systems for some known setups. For this purpose, we simulate the decoupled systems by setting the source distribution and sensing matrix to a specific form and determine the expected distortion of the equivalent scalar system. We, then, discuss the validity of RS and RSB assumptions for these examples.

A. Simulation Setups

The variations of the system model and distortion function being considered in the numerical investigations are described in the following.

1) Sensing Matrices: The sensing matrix $\mathbf{A}_{k\times n}$ can in general be of any structural or random form. In our numerical investigations, we consider the two important cases of random "i.i.d." and "projector" matrices.

- **i.i.d. Random Matrix:** In this case, the entries of $\mathbf{A}_{k\times n}$ are supposed to be generated i.i.d. from an arbitrary distribution p_a. Without loss of generality, we assume that the entries are zero-mean random variables with variance k^{-1}. This structure is the most primary and also the most discussed case in random matrix theory. For this matrix, regardless of p_a, it is well known that the asymptotic empirical eigenvalue CDF of the Gramian $\mathbf{J}$ follows the Marcenko-Pastur law which states

$$\mathrm{F}_{\mathbf{J}}(\lambda) = \left[1-\mathsf{r}^{-1}\right]^{+}\mathbf{1}\{\lambda>0\} + \int_{-\infty}^{\lambda}\frac{\sqrt{\mathsf{r}-(1-u)^2}}{2\pi\mathsf{r}u}\mathrm{d}u \tag{153}$$

  where $[x]^{+}$ returns x when x is non-negative and is zero otherwise [24], [25], [67]. Using the definition of R-transform, it is straightforward to show that $\mathrm{R}_{\mathbf{J}}(\cdot)$ reads

$$\mathrm{R}_{\mathbf{J}}(\omega) = \frac{1}{1-\mathsf{r}\omega}. \tag{154}$$

- **Projector Matrix:** Here, the only constraint on the sensing matrix is that the row vectors are orthogonal. The matrices are also referred to as the "row orthogonal" matrices. For the sensing matrix $\mathbf{A}_{k\times n}$, we assume the case that the row vectors are normalized by the number of rows and $k\leq n$; thus, the outer product $\mathbf{A}\mathbf{A}^{\mathsf{T}}$ reads

$$\mathbf{A}\mathbf{A}^{\mathsf{T}} = \frac{n}{k}\mathbf{I}_k. \tag{155}$$

  Consequently, the Gram matrix $\mathbf{J}$ takes two different eigenvalues: $\lambda=0$ with multiplicity $n-k$, and $\lambda=nk^{-1}$ with multiplicity k. Considering the definition of the factor r in (19), the asymptotic empirical CDF of the eigenvalues read

$$\mathsf{F}_{\mathbf{J}}(\lambda) = \left[1-\mathsf{r}^{-1}\right]\mathbf{1}\{\lambda>0\} + \mathsf{r}^{-1}\mathbf{1}\{\lambda>\mathsf{r}\} \tag{156}$$

  which results in the R-transform of the form

$$\mathrm{R}_{\mathbf{J}}(\omega) = \frac{\omega-1+\sqrt{(\mathsf{r}\omega-1)^2+4\omega}}{2\omega}. \tag{157}$$

2) Source Model: Through our numerical investigations, we consider the continuous and finite alphabet sources to be distributed with "sparse Gaussian" and "sparse uniform" distributions, respectively. More precisely, we assume the entries of the continuous and finite alphabet sources to be generated from a Gaussian and uniform distribution, respectively, and multiplied by a Bernoulli random variable with probability α to take 1 and $1-\alpha$ to take 0. Moreover, we assume the nonzero outcomes of the finite alphabet source to be of the symmetric form

$$\{\pm a,\ldots,\pm\kappa a\} \tag{158}$$

for some positive real a and integer κ.

3) Distortion Function: Regarding the continuous sources, we determine the performance of different estimators by considering the MSE as the distortion function, i.e.,

$$\mathsf{d}(\hat{\boldsymbol{x}};\boldsymbol{x}) = \|\hat{\boldsymbol{x}} - \boldsymbol{x}\|^2. \tag{159}$$

For the finite alphabet sources, however, we determine the probability of the error as the measure and consider

$$\mathsf{d}(\hat{\boldsymbol{x}};\boldsymbol{x}) = \sum_{i=1}^{n} \mathbf{1}\left\{\hat{x}_i \neq x_i\right\}. \tag{160}$$

B. Numerical Results for Continuous Alphabet Sources

Considering Examples 1-3, we consider the case in which a sparse Gaussian source with sparsity factor $\alpha = 0.1$ is sampled via a random sensing matrix. Fig. 5 shows the RS prediction of normalized MSE, defined as

$$\mathsf{MSE}^0 = \frac{\mathsf{MSE}}{\mathsf{E}\,|x|^2} = \alpha^{-1}\mathsf{MSE}, \tag{161}$$

as a function of the estimation parameter λ. The compression rate is set to be $\mathsf{r} = 2$, and both the i.i.d. random and projector sensing matrices are considered. The curves match the results reported in [32] and [30]. As it is seen, the ℓ_0-norm recovery scheme with the optimal choice of parameter estimation outperform the LASSO scheme; however, the non-optimal choice of the estimation parameter can make the ℓ_0 norm's performance even worse than the LASSO. Moreover, in contrast to the noiseless case, the projector matrix is always outperforming the i.i.d. matrix in the noisy case; this fact has been also reported in [32].

In [53], the authors showed that in the noiseless sampling case with an i.i.d. Gaussian matrix, the RS ansatz for linear and LASSO recovery schemes is locally stable against perturbations that break the symmetry of the replica correlation matrix. This result in fact agrees with the general belief that convex optimization problems do not exhibit RSB [68]. The result in [53], however, indicated that for the ℓ_0 norm reconstruction, the RS ansatz fails to give a valid prediction, and therefore the RSB ansätze are needed for accurately assessing the performance.

In order to investigate the observation of [53], we have plotted the normalized MSE of the LASSO recovery scheme predicted by the RS ansatz in terms of the estimation parameter λ in Fig. 6 considering different compression rates. It is observed that for a given estimation parameter λ, the normalized MSE increases as the compression rate grows. For large compression rates, the normalized MSE converges to 0 dB which agrees with the fact that for asymptotically large compression rates, the source and observation vectors are independent, and thus, the MSE converges to the source power. To investigate the ℓ_0 norm recovery scheme, we plot the corresponding curves for the ℓ_0 norm scheme considering Fig. 6 as the reference.

For the setup given in Example 3, Fig. 7 shows the normalized MSE predicted by the RS ansatz as a function of the estimation parameter for two different compression rates. The system setup has been set to be similar to the one considered in Example 2 and Fig. 6, and the curves have been plotted for both the i.i.d. and projector sampling

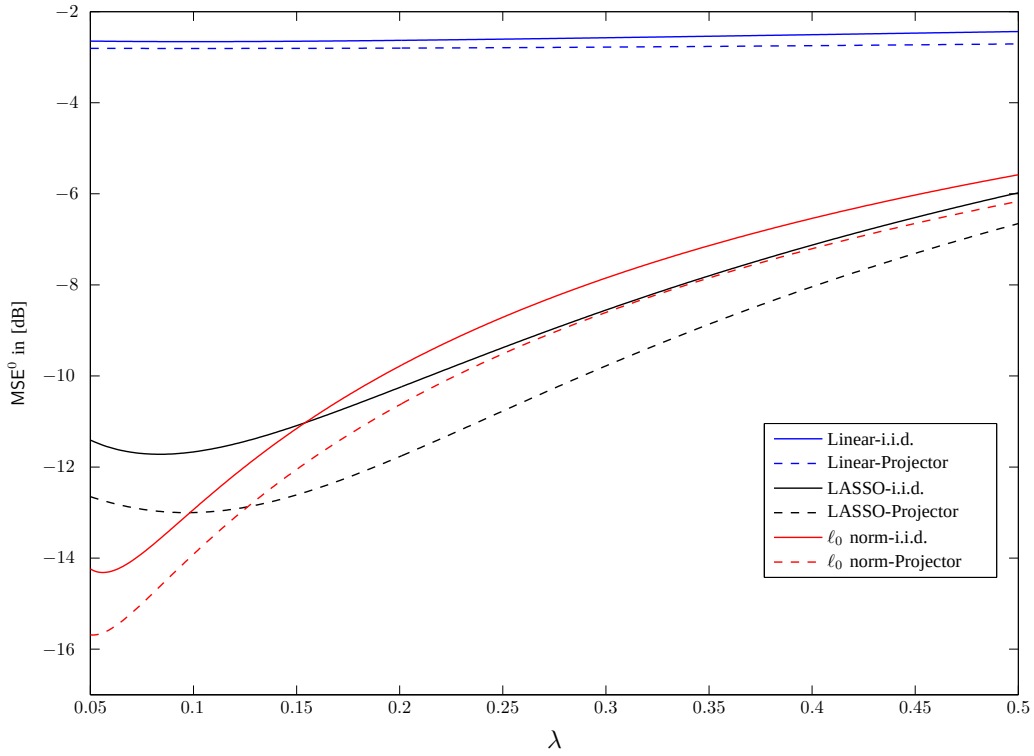


Fig. 5: RS predicted normalized MSE MSE^0 defined in (161) versus the estimation parameter λ as given in Examples 1-3 for the compression rate $\mathsf{r} = 2$. The sparsity factor is set to be $\alpha = 0.1$ and the true noise variance λ_0 is set such that the source power to noise power ratio becomes 10 dB. The dashed and solid lines respectively indicate the cases of which a random projector and i.i.d. matrix has been employed for sampling. The curves match the numerical results reported in [30], [32].

cases. In contrast to the LASSO recovery scheme, the RS ansatz starts to give invalid predictions for the ℓ_0 norm scheme as the compression rate increases. As it is observed, the normalized MSE drops unexpectedly down for an interval of the estimation parameters when the compression rate is intermediate.

In fact, in this interval, the RS fixed point equations have either an invalid solution or no solution. To illustrate this result further, let us consider Examples 2 and 3 under the RS ansatz when an i.i.d. sensing matrix is employed. In this case, the equivalent noise power and estimation parameter λ_0^{s} and λ^{s} read

$$\lambda^{\mathsf{s}} = \lambda + \mathsf{r}\chi \tag{162a}$$

$$\lambda_0^{\mathsf{s}} = \lambda_0 + \mathsf{r}q. \tag{162b}$$

By increasing the compression rate, the interference increases, and thus, the MSE takes larger values. Therefore, for small λ and λ_0, one can consider $\mathsf{r}\chi \gg \lambda$ and $\mathsf{r}q \gg \lambda_0$ as r takes large values and write

$$\lambda^{\mathsf{s}} \approx \mathsf{r}\chi \tag{163a}$$

$$\lambda_0^{\mathsf{s}} \approx \mathsf{r}q. \tag{163b}$$

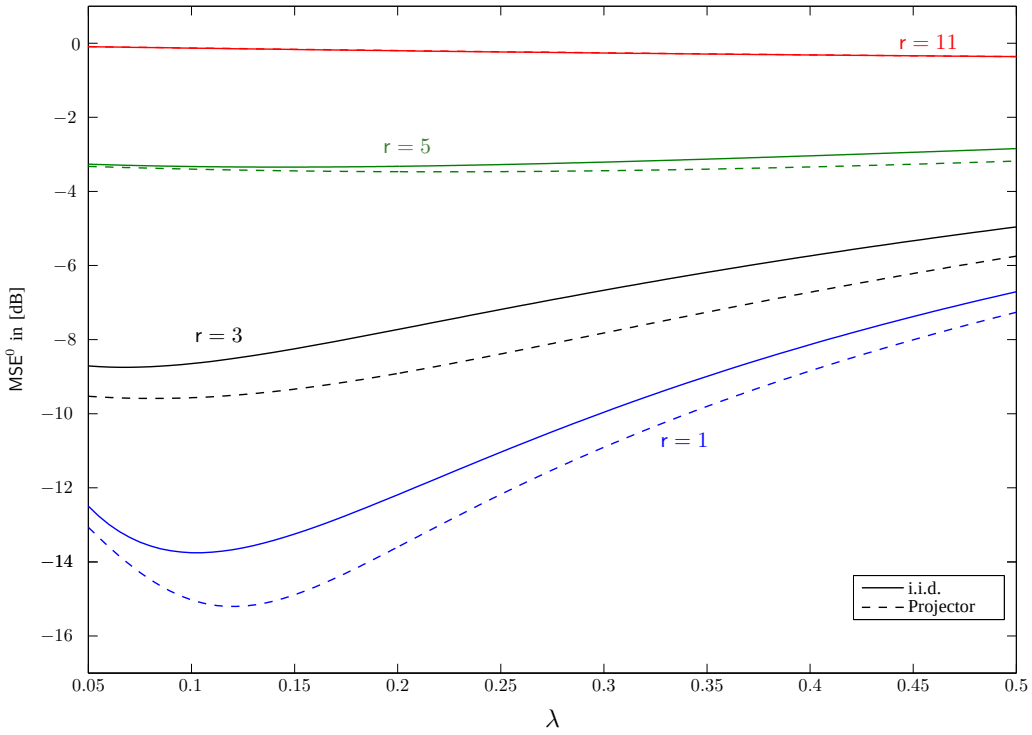


Fig. 6: RS predicted normalized MSE MSE^0 defined in (161) versus the estimation parameter λ as given in Example 2 for different compression rates. The sparsity factor is set to be $\alpha = 0.1$ and the true noise variance λ_0 is set to be 0.01. The dashed and solid lines respectively indicate the random projector and i.i.d. matrices. As the compression rate increases, MSE^0 converges to 0 dB. In fact, for asymptotically large compression rates, the source and observation vectors become independent and the MSE meets the source power. The curves match the corresponding curves in [32].

Considering Example 2, by substituting (163a) and (163b) in the RS ansatz, the fixed point equations, as r grows large, is written in the following form

$$u\sqrt{\mathsf{r}}\ \phi(u\sqrt{\mathsf{r}}) \approx \int_{u\sqrt{\mathsf{r}}}^{\infty} z^2\ \mathrm{D}z + \epsilon_r \tag{164a}$$

$$q \approx 2\alpha \int_{0}^{u\sqrt{\mathsf{r}}} \mathrm{D}z + \epsilon_r. \tag{164b}$$

for some ϵ_r tending to zero as $r \uparrow \infty$, and the bounded real scalar u defined as

$$u := \frac{\chi}{\sqrt{q}}. \tag{165}$$

Taking the limit $\mathsf{r} \uparrow \infty$, (164a) is valid for any bounded real value of u and (164b) reduces to $q \approx \alpha$ for large compression rates. Noting that for this setup $q = \mathsf{MSE}$, one concludes that $\mathsf{MSE}^0 \approx 1$ which agrees with the results given in Fig. 6. A similar approach for the ℓ_0 norm recovery scheme in Example 3, however, results in the following

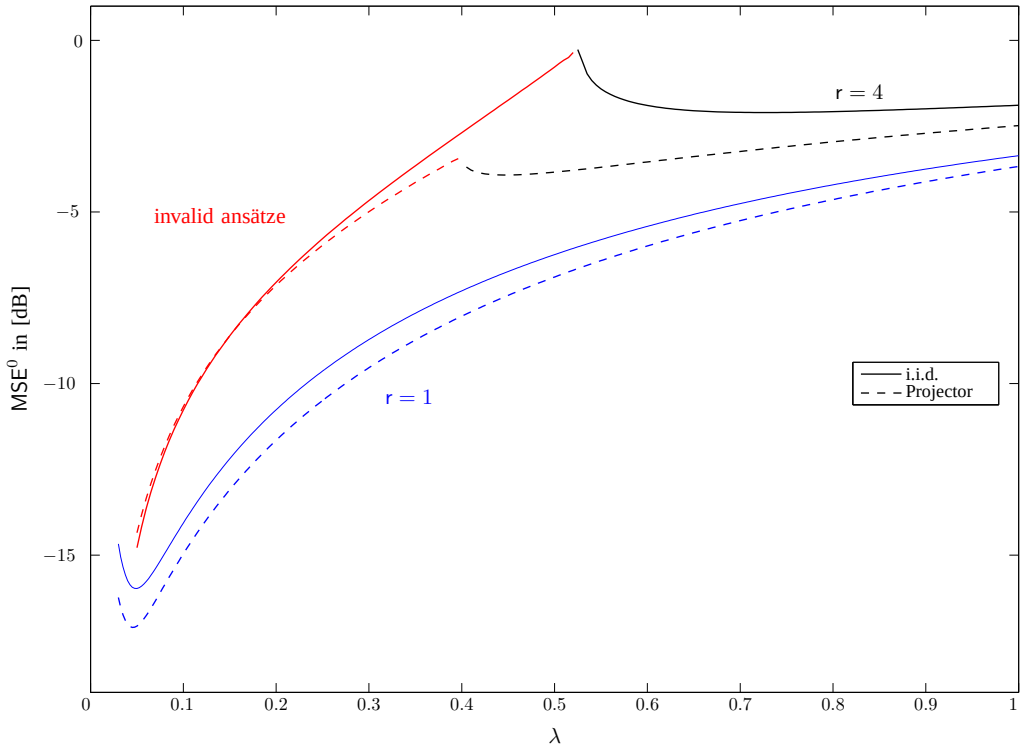


Fig. 7: RS prediction of normalized MSE as a function of the estimation parameter λ for different compression rates considering the ℓ_0 norm recovery scheme illustrated in Example 3. The sparsity factor and the noise variance are considered to be $\alpha = 0.1$ and $\lambda_0 = 0.01$, respectively. The dashed and solid lines respectively indicate the random projector and i.i.d. matrices. As the compression rate increases, the RS ansatz starts to give invalid predictions within an interval of estimation parameters. In fact, as r grows, the RS fixed point equations have no valid solutions for an interval of λ's. The interval becomes larger as the compression rate increases.

contradicting equations

$$\int_u^\infty z^2 \, \mathrm{D}z \approx \epsilon_r \tag{166a}$$

$$\int_0^u \mathrm{D}z \approx \epsilon_r. \tag{166b}$$

for the scalar u defined as

$$u \coloneqq \sqrt{2\frac{\chi}{q}}. \tag{167}$$

Clearly, the set of equations in (166a) and (166b) have no solution as $\mathsf{r} \uparrow \infty$. The approximated fixed point equations explain the invalidity of the RS predicted performance of the ℓ_0 norm recovery scheme for large compression rates.

In order to further investigate the RS ansätze, we plot the optimal normalized MSE as a function of the compression rate in Fig. 8. Here, we consider the case with i.i.d. sensing matrix when the sparsity factor is set to be $\alpha = 0.1$ and source to noise power ratio to be 10 dB. The normalized MSE is minimized numerically over the estimation parameter λ. As the figure illustrates, the MSE of the RS ansatz starts to drop in moderate compression

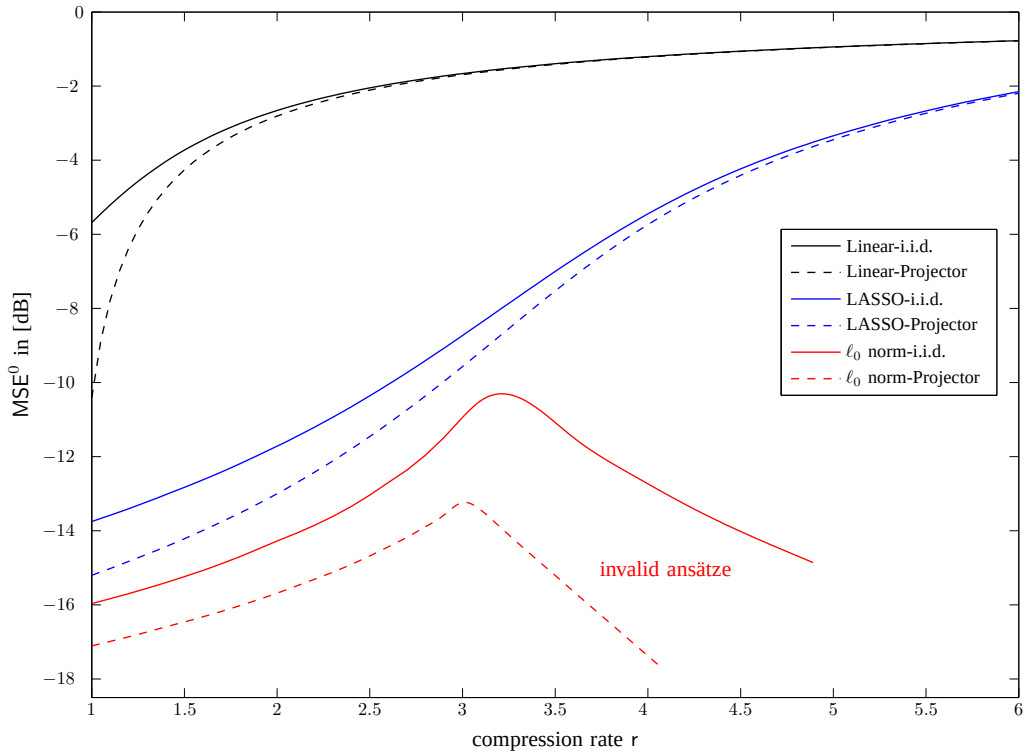


Fig. 8: RS prediction of optimal normalized MSE versus the compression rate r considering the LASSO and ℓ_0-norm recovery schemes illustrated in Examples 2 and 3. The sparsity factor and the source to noise power ratio are considered to be $\alpha = 0.1$ and 10 dB respectively. MSE^0 has been minimized numerically over the estimation parameter λ. As the compression rate grows, the RS ansatz for ℓ_0 norm starts to give invalid predictions. The figure match the numerical results in [30], [32] where the RS predicted curves are plotted within the interval of $\mathsf{r} \in [1, 3]$.

rates. The observation confirms the discussion on the stability of the RS saddle point given in [53]. In fact, the unexpected drop of the RS ansatz is caused by the limited stability region of the RS fixed point solutions. More precisely, for a given source to noise power ratio and estimation parameter, the RS fixed point equations have stable solutions within a certain interval of compression rates. The interval widens as λ grows.

Fig. 9 compares the RS and 1RSB ansätze for the ℓ_0 norm scheme. In this figure, the optimal normalizes MSE is plotted for the case with i.i.d. sensing matrix. The sparsity factor is considered to be $\alpha = 0.1$ and the noise variance is set to be $\lambda_0 = 0.01$. For the RS ansatz, we have considered two cases, namely when MSE^0 is minimized over 1) all possible estimation parameters and 2) the interval of λ's which the RS ansatz is valid within[1]. The latter case is called the "RS restricted" curve and is shown in Fig. 9 with the red dashed line. As the figure depicts, the 1RSB prediction deviates from RS at larger compression rates. This observation indicates that the performance analysis of the ℓ_0 norm recovery exhibits RSB. For sake of comparison, we also plot the curve for the LASSO recovery scheme which is an upper bound on the 1RSB predicted curve. The RS restricted ℓ_0 norm's curve, moreover, crosses the

[1]In fact, we consider $\lambda > \lambda_{\mathrm{d}}$, where λ_{d} is the point in Fig. 7 in which the normalized MSE curve is not differentiable.

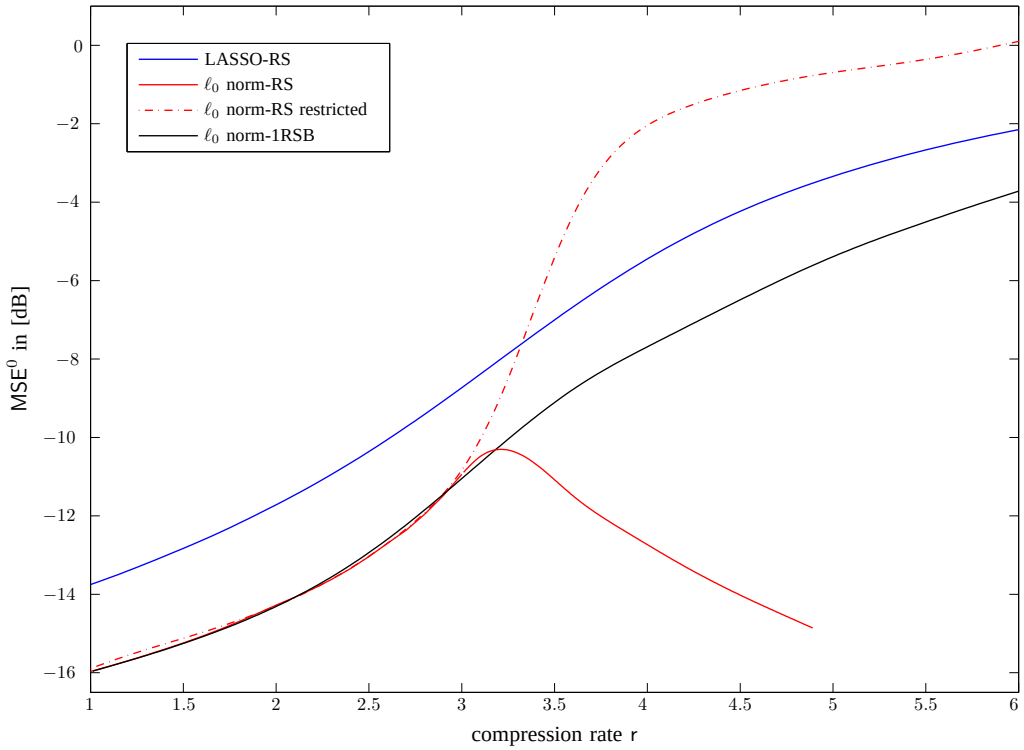


Fig. 9: RS versus 1RSB prediction of the optimal normalized MSE considering the ℓ_0 norm recovery scheme illustrated in Example 3. The sparsity factor and the source to noise power ratio are considered to be $\alpha = 0.1$ and 10 dB respectively. The red solid line shows the RS prediction of optimal MSE^0 when it is minimized over all $\lambda \in \mathbb{R}^+$; however, the red dashed line indicates the restricted RS predicted MSE^0 minimized numerically over the intervals of λ which the RS ansatz gives valid predictions. The black solid line denotes the 1RSB ansatz which deviates both the RS and restricted RS curves.

LASSO curve. This deviation indicates the suboptimality of the intervals in which the RS ansatz returns a valid approximation of MSE^0.

To check the consistency of the solutions under the RS and 1RSB ansätze, we also sketch the zero temperature entropy of the corresponding spin glass as a function of the compression rate in Fig. 10, considering the same setup as in Fig. 8 and Fig. 9. The zero temperature entropy also confirms the better accuracy of the 1RSB ansatz.

Based on the above investigations, the exact performance of the ℓ_0 norm recovery scheme needs the RSB ansätze to be accurately studied. It is however useful to see the validity region of the system parameters in which the prediction given by the RS ansatz lies approximately on the 1RSB curve. For this purpose, we define for the ℓ_0 norm recovery, the "RS break compression rate" $\mathsf{r}_{\mathsf{br}}^{\mathsf{RS}}(\cdot)$ as a function of system parameters to be the compression rate that the prediction via the RS ansatz starts to deviate from 1RSB. More precisely, for a given system setup denoted by the set $\mathbb{P}$, the "RS ϵ-validity region" for a given $\epsilon \in \mathbb{R}^+$ is defined as

$$\mathbb{V}_{\mathsf{br}}^{\mathsf{RS}}(\mathbb{P};\epsilon) \coloneqq \left\{ \mathsf{r} \ni |\mathsf{MSE}_{\mathsf{RS}}^0(\mathsf{r},\mathbb{P}) - \mathsf{MSE}_{\mathsf{1RSB}}^0(\mathsf{r},\mathbb{P})| < \epsilon \right\}. \tag{168}$$

where $\mathsf{MSE}_{\mathsf{RS}}^0(\mathsf{r},\mathbb{P})$ and $\mathsf{MSE}_{\mathsf{1RSB}}^0(\mathsf{r},\mathbb{P})$ indicate, respectively, the RS and 1RSB prediction of the normalized MSE

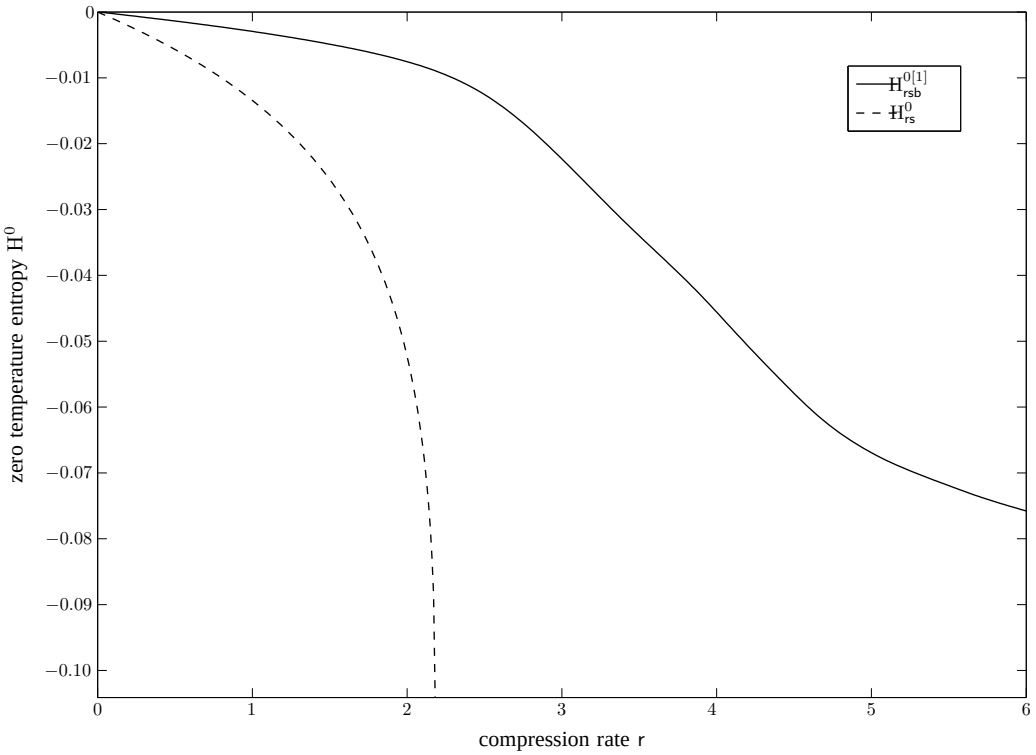


Fig. 10: $\mathsf{H}^0_{\mathsf{rs}}$ and $\mathsf{H}^{0[1]}_{\mathsf{rsb}}$ as functions of the compression rate considering the corresponding spin glass under the ℓ_0-norm recovery scheme. System setup is set to be same as the setup assumed in Fig. 8 and Fig. 9. The better approximation of the performance via the 1RSB ansatz is also visible in this figure.

at the compression rate r for a setup specified by the set $\mathbb{P}$. Consequently, the "RS break compression rate" $\mathsf{r}^{\mathsf{RS}}_{\mathsf{br}}(\cdot)$ for maximum deviation ϵ is given by

$$\mathsf{r}^{\mathsf{RS}}_{\mathsf{br}}(\mathbb{P};\epsilon) \coloneqq \max \mathbb{V}^{\mathsf{RS}}_{\mathsf{br}}(\mathbb{P};\epsilon). \tag{169}$$

In general, the set $\mathbb{P}$ includes several setup parameters such as sensing matrix and source's distribution, the sparsity factor, noise variance and estimation parameter. Considering a case with i.i.d. sensing matrix and sparse Gaussian source with a given sparsity factor α, the RS break compression rate is a function of snr and the estimation parameter λ, i.e., $\mathsf{r}^{\mathsf{RS}}_{\mathsf{br}}(\mathsf{snr},\lambda;\epsilon)$, where we define the source to noise power ratio snr as

$$\mathsf{snr} \coloneqq \frac{\mathsf{E}\, x^2}{\lambda_0} = \alpha\lambda_0^{-1}. \tag{170}$$

In this case, the RS ϵ-validity region $\mathbb{V}^{\mathsf{RS}}_{\mathsf{br}}(\mathsf{snr},\lambda;\epsilon)$ is the area enclosed by both the λ and snr axes as well as the $\mathsf{r}^{\mathsf{RS}}_{\mathsf{br}}(\mathsf{snr},\lambda;\epsilon)$ surface.

Fig. 11 illustrates the intersection of the RS ϵ-validity region and the planes $\mathsf{snr}=9$ and $\mathsf{snr}=12$ for $\epsilon=10^{-3}$. The break compression rate increases with respect to both λ and snr which agrees with the intuition. Moreover, $\mathsf{r}^{\mathsf{RS}}_{\mathsf{br}}(\mathsf{snr},\lambda;\epsilon)$ starts to saturate as λ grows. Another extreme case is when the estimation parameter tends to zero in

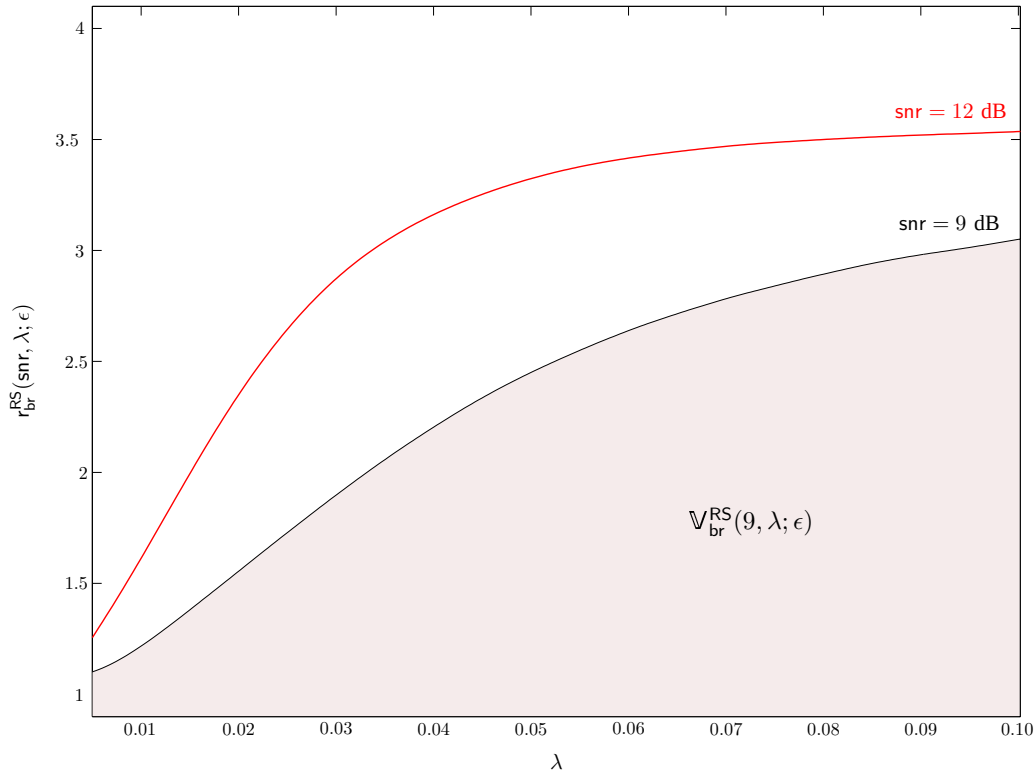


Fig. 11: $\mathsf{r}_{\mathsf{br}}^{\mathsf{RS}}(\mathsf{snr},\lambda;\epsilon)$ in terms of the estimation parameter λ for $\epsilon = 10^{-3}$, and $\mathsf{snr} = 9$ dB and $\mathsf{snr} = 12$ dB considering an i.i.d. matrix employed for sensing. The break compression rate starts to saturate as the estimation parameter grows.

which the MAP estimator reduces to

$$\mathbf{g}(\boldsymbol{y}) = \arg \min_{\|\boldsymbol{y}-\mathbf{A}\boldsymbol{v}\| \leq \epsilon_0} \|\boldsymbol{v}\|_0. \tag{171}$$

with $\epsilon_0 = \mathcal{O}(\frac{1}{\sqrt{\mathsf{snr}}})$. For this case, the break compression rate converges to the minimum compression rate $\mathsf{r} = 1$. This observation in the large snr limit agrees with the unstability of the RS ansatz reported in [53].

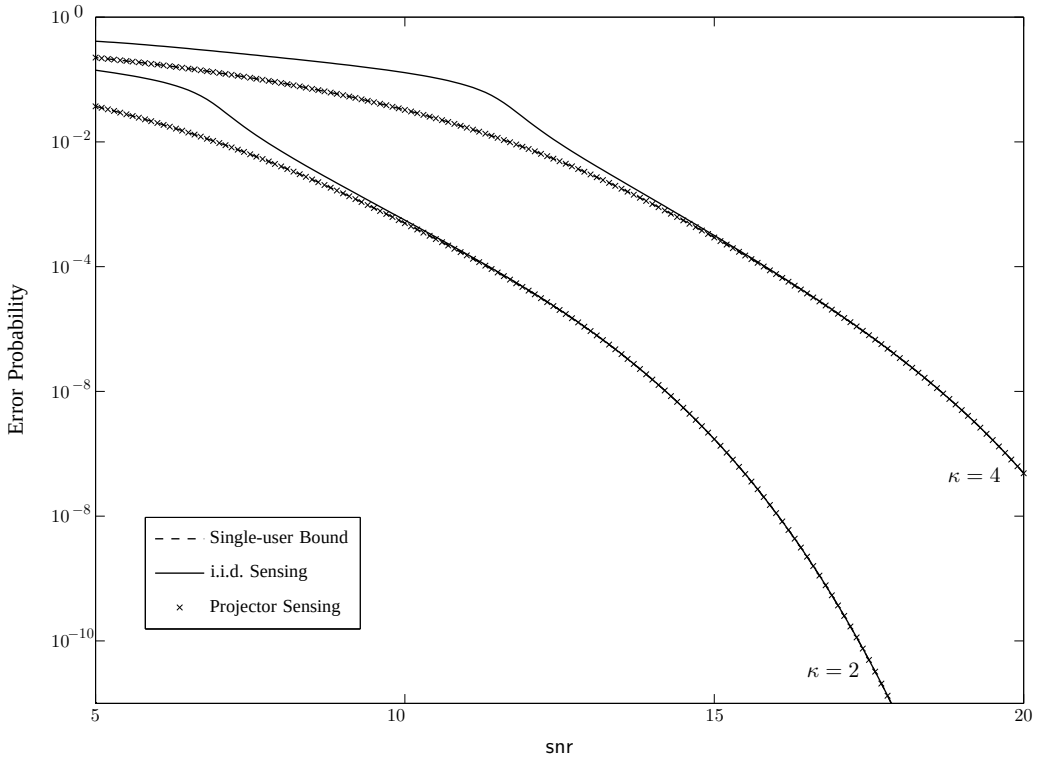


Fig. 12: The error probability versus snr when the ℓ_0 norm recovery scheme is employed and the compression rate is set to be $\mathsf{r} = 1$. The i.i.d. sensing reports deviation from the single-user bound within a moderate interval of snr while the projector sensing meets the single-user bound for almost every snr and alphabet size. Here, the sparsity factor and estimation parameter are considered to be $\alpha = 0.1$ and $\lambda = 0.1$, respectively.

C. Numerical Results for Finite Alphabet Sources

Considering a finite alphabet source with the nonzero outcomes given in (158), the boundary points in Example 4 become of the form

$$\left\{\pm\left(\frac{2k-1}{2}a(1+\lambda^{\mathsf{s}})\right)\right\} \tag{172}$$

for $k \in [1:\kappa]$. Moreover, for the LASSO and ℓ_0 norm recovery schemes, the boundary points read

$$\left\{\pm\left(\frac{2k-1}{2}a+\lambda^{\mathsf{s}}\right)\right\} \tag{173}$$

for $k \in [1:\kappa]$, and

$$\left\{\pm\left(\frac{1}{2}a+\frac{\lambda^{\mathsf{s}}}{a}\right), \pm\frac{2k-1}{2}a\right\} \tag{174}$$

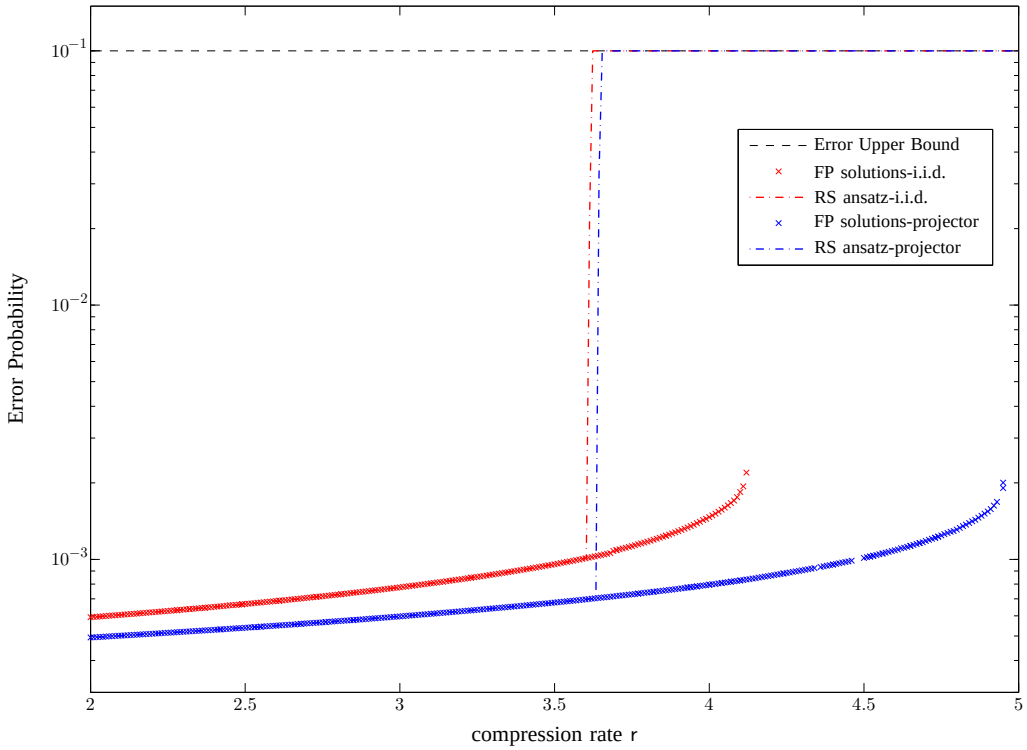


Fig. 13: Phase transition in the error probability with respect to the compression rate r when $\mathsf{snr} = 12$ dB. The sparsity factor and estimation parameter are considered to be $\alpha = 0.1$ and $\lambda = 0.1$ respectively, and $\kappa = 2$. The cross points indicate the solutions to the RS Fixed Point (FP) equations which do not lie on the error probability upper bound. The dashed lines show the RS ansätze in which the free energy meets the minimum value. As it is observed, in both the i.i.d. and projector sensing, the error probability reports a phase transition at a similar compression rate.

for $k \in [2 : \kappa]$, respectively. The source to noise power ratio snr is then defined as

$$\mathsf{snr} := \frac{\mathsf{E}\, x^2}{\lambda_0} = \frac{\alpha a^2(\kappa+1)(2\kappa+1)}{6\lambda_0}. \tag{175}$$

Fig. 12 shows the RS predicted error probability of the finite alphabet system as a function of snr for the unit compression rate when the ℓ_0 norm recovery scheme is employed. The cases with $\kappa = 2$ and $\kappa = 4$ are considered under both the i.i.d. and projector sensing. Here, the sparsity factor is set to be $\alpha = 0.1$ and the estimation parameter to be $\lambda = 0.1$. As the figure illustrates, for either sensing matrix, the error probability meets the single-user bound in a relatively large snr regime. The deviation from the single-user bound in the i.i.d. case, moreover, occurs in a larger interval of snr as κ grows. In contrast to the i.i.d. case, the coincidence occurs for almost every snr and κ when a projector sensing matrix is employed. This observation can be intuitively justified due to the orthogonality of the rows in this case.

As the compression rate increases, the projector matrix also starts to deviate form the single-user bound within a certain interval of snr. For larger rates, the error probability jumps to the upper bound of the single-user error probability. This reports a "phase transition" in the error probability with respect to the compression rate. More

precisely, for a given snr, the error probability jumps from the single-user bound to the upper bound of error probability at a certain compression rate. The transition rate corresponds to the maximum possible compression rate in which the ℓ_0 norm recovery scheme is able to recover the source vector from the noisy compressed observations and clearly increases as snr grows. Phase transitions in communication systems were reported in the literature for several examples such as turbo coding and Code Division Multiple Access (CDMA) systems [11], [69]; the phase transition here is similar to the one reported in [11].

Fig. 13 illustrates the phase transition for both the cases of i.i.d. and projector sensing when the ℓ_0 norm recovery scheme is employed. The source is assumed to be sparse with $\alpha = 0.1$, $\kappa = 2$ and $\mathsf{snr} = 12$ dB, and the estimation parameter is considered $\lambda = 0.1$. In order to find the transition rate, we have considered all the possible solutions of the RS saddle points using an exhaustive search and let the ansatz be the solution which returns the minimum free energy. The ansätze are indicated with dashed line in the figure. As one can see, the ansätze suddenly jump to the upper bound of the error probability at around $\mathsf{r} = 3.6$ in either case. The projector sensing, however, slightly outperforms the i.i.d. sensing within the interval of primary phase which extends the conclusion given for the sparse Gaussian sources in [32] to the sparse finite alphabet sources as well. In order to obtain a more accurate approximation of the performance and transition point, one may take RSB ansätze also into account. The RS ansatz, however, seems to give an accurate approximation for the specific setup considered here.

X. Conclusion

This manuscript considered the performance of the MAP estimator in the large-system limit with respect to a general distortion function. Taking a statistical mechanical approach, the replica method was employed to determine the asymptotic distortion of the system. We deviated from the earlier approaches, e.g., [15], [30]–[32], by evaluating the general replica ansatz of the corresponding spin glass. The general ansatz let us derive the RS, as well as the bRSB ansatz considering a large class of system matrices. The results recover the previous studies [15], [30]–[32] in special cases and justifies the uniqueness of the zero temperature entropy's expression under the bRSB assumption conjectured in [63].

The replica ansatz evaluated here led us to a more general form of the decoupling principle. In fact, invoking the general replica ansatz, it was shown by the moment method that for any tuple of input-output entries, the marginal joint distribution converges to the input-output empirical distribution asymptotically. This means that in the large-system limit, the marginal joint distribution of the entries determined by any replica ansatz decouples into a set of identical joint distributions. The form of the asymptotic decoupled distribution, however, depends on the structure imposed on the ansatz. For the bRSB ansatz, we showed that the vector-valued AWGN system estimated by a MAP estimator decouples into single-user MAP-estimated AWGN channels followed by some correlated impairment terms which intuitively model the interference of the system and vanish by reducing the bRSB assumption to RS. The general decoupling principle justified here confirms the conjecture that decoupling is a generic property of MAP estimators, since its validity relies only on the replica continuity assumption. Recent results in statistical mechanics have shown that failures in finding the exact solution via the replica method are mainly caused by the structure imposed on the ansatz, and not replica continuity [3], [5], [70]–[72].

The decoupling property enabled us to represent the equivalent "replica simulator" interpretation of the replica ansatz. In fact, the bRSB fixed point equations were shown to be completely described by the statistics of the corresponding decoupled system. Consequently, the bRSB ansatz was represented through the state evolution of a transition system which takes an initial set of ansatz parameters as the input and determines a new set of parameters via simulating the bRSB decoupled system as the output.

As an example of vector-valued MAP-estimated systems, we considered the noisy compressive sensing system and studied different sparse recovery schemes, including the linear, LASSO, and ℓ_0 norm minimization. The numerical investigation of the system showed that for sparse Gaussian sources, the performance of the linear and LASSO recovery schemes are accurately approximated by the RS ansatz within a large interval of compression rates. The RS prediction of the ℓ_0 norm scheme's performance, however, was observed to lack the stability within the moderate and high compression rates. As a result, the 1RSB ansatz for this scheme was considered which deviates from the RS ansatz significantly as the rate grows. For sparse finite alphabet sources, the RS prediction of the error probability reported a phase transition with respect to the compression rate. The numerical results, moreover, showed a better performance of the random projector sensing compared to i.i.d. in both the cases which were previously reported for sparse Gaussian sources in [32].

The current work can be pursued in several directions. As an example, the "replica simulator" introduced in Section VII can be studied further by methods developed in the context of transition systems. The analysis may result in proposing a new framework which simplifies the evaluation of fixed point equations. Another direction is the analysis of the conditional distribution of the correlated impairment terms in the bRSB decoupled system. The study can lead us to understand the necessary or sufficient conditions in which the RS ansatz gives an accurate approximation of the system's performance. Inspired by the Sherrington-Kirkpatrick model of spin glasses, for which the ∞RSB ansatz has been proved to be correct, our initial conjecture is that the exact solution for the cases exhibiting RSB is given by the ∞RSB ansatz. The latter study, furthermore, gives us some insights about the accuracy of the approximation given by a finite number of RSB steps.

XI. Acknowledgment

The authors would like to acknowledge German Research Foundation, Deutsche Forschungsgemeinschaft (DFG), for support of this work under the Grant No. MU 3735/2-1.

APPENDIX A
PROOF OF PROPOSITION IV.1

Starting from (43), we define the moment function $\mathsf{Z}(m)$ as in (44a). Therefore,

$$\mathsf{D}^{\mathsf{W}}(\hat{\boldsymbol{x}};\boldsymbol{x}) = \lim_{\beta\uparrow\infty}\lim_{n\uparrow\infty}\lim_{h\downarrow 0}\lim_{m\downarrow 0}\frac{1}{m}\frac{1}{n}\frac{\partial}{\partial h}\log \mathsf{Z}(m). \tag{176}$$

Taking the expectation with respect to the noise term first, the moment function is extended as

$$\mathsf{Z}(m) = \mathsf{E}_{\boldsymbol{x}}\mathsf{E}_{\mathbf{A}}\mathsf{E}_{\boldsymbol{z}}\sum_{\{\boldsymbol{v}_a\}} e^{-\beta\sum_{a=1}^{m}\mathcal{E}(\boldsymbol{v}_a|\boldsymbol{y},\mathbf{A})+hn\sum_{a=1}^{m}\mathsf{D}^{\mathsf{W}(n)}(\boldsymbol{v}_a;\boldsymbol{x})} \tag{177a}$$

$$= \mathsf{E}_{\boldsymbol{x}}\mathsf{E}_{\mathbf{A}}\mathsf{E}_{\boldsymbol{z}}\sum_{\{\boldsymbol{v}_a\}} e^{-\beta\sum_{a=1}^{m}\left\{\frac{1}{2\lambda}(\boldsymbol{x}-\boldsymbol{v}_a)^{\mathsf{T}}\mathbf{J}(\boldsymbol{x}-\boldsymbol{v}_a)+\frac{1}{\lambda}\boldsymbol{z}^{\mathsf{T}}\mathbf{A}(\boldsymbol{x}-\boldsymbol{v}_a)+\frac{1}{2\lambda}\|\boldsymbol{z}\|^2+u(\boldsymbol{v}_a)\right\}+hn\sum_{a=1}^{m}\mathsf{D}^{\mathsf{W}(n)}(\boldsymbol{v}_a;\boldsymbol{x})} \tag{177b}$$

$$\overset{\star}{=} \left(\frac{\lambda}{\lambda+m\beta\lambda_0}\right)^{\frac{k}{2}}\mathsf{E}_{\boldsymbol{x}}\mathsf{E}_{\mathbf{A}}\sum_{\{\boldsymbol{v}_a\}} e^{-\beta\left\{\sum_{a,b=1}^{m}\tilde{\boldsymbol{v}}_a^{\mathsf{T}}\mathbf{J}\tilde{\boldsymbol{v}}_b\zeta_{ab}+\sum_{a=1}^{m}u(\boldsymbol{v}_a)\right\}+hn\sum_{a=1}^{m}\mathsf{D}^{\mathsf{W}(n)}(\boldsymbol{v}_a;\boldsymbol{x})} \tag{177c}$$

where $\tilde{\boldsymbol{v}}_a = \boldsymbol{x}-\boldsymbol{v}_a$ for $a\in[1:m]$ is the unbiased[1] replica vector, $\mathbf{J}$ is the Gramian of the system matrix defined as $\mathbf{J}\coloneqq\mathbf{A}^{\mathsf{T}}\mathbf{A}$ and satisfies the properties stated in Section II, $\star$ comes from taking expectation over $\boldsymbol{z}$, and the factor ζ_{ab} is defined as

$$\zeta_{ab} \coloneqq \frac{1}{2\lambda}\left[\mathbf{1}\{a=b\}-\frac{\lambda_0}{\lambda+m\beta\lambda_0}\beta\right] \tag{178}$$

with λ_0 being the true noise variance as specified in Section II.

Remark A.1. Considering (177b), one could drop the term $\frac{1}{2\lambda}\|\boldsymbol{z}\|^2$, since it plays no rule in the optimization problem (2). More precisely, one could redefine the Hamiltonian in (10) to be

$$\mathcal{E}_{\text{new}}(\boldsymbol{v}|\boldsymbol{y},\mathbf{A}) = \mathcal{E}(\boldsymbol{v}|\boldsymbol{y},\mathbf{A})-\frac{1}{2\lambda}\|\boldsymbol{z}\|^2 \tag{179}$$

without loss of generality. In this case, the coefficient at the right hand side of (177c) reduces to 1, and ζ_{ab} reads

$$\zeta_{ab}^{\text{new}} \coloneqq \frac{1}{2\lambda}\left[\mathbf{1}\{a=b\}-\frac{\lambda_0}{\lambda}\beta\right]. \tag{180}$$

It is, however, clear from (177c) and (178) that as m tends to zero, both the approaches result in a same result.

Considering the expression in (177c), we define the random variable $\mathsf{Z}(m;\boldsymbol{x})$ as

$$\mathsf{Z}(m;\boldsymbol{x}) \coloneqq \mathsf{E}_{\mathbf{J}}\sum_{\{\boldsymbol{v}_a\}} e^{-\beta\left\{\sum_{a,b=1}^{m}\tilde{\boldsymbol{v}}_a^{\mathsf{T}}\mathbf{J}\tilde{\boldsymbol{v}}_b\zeta_{ab}+\sum_{a=1}^{m}u(\boldsymbol{v}_a)\right\}+hn\sum_{a=1}^{m}\mathsf{D}^{\mathsf{W}(n)}(\boldsymbol{v}_a;\boldsymbol{x})}. \tag{181}$$

Consequently, the moment function is given by taking the expectation over $\mathsf{Z}(m;\boldsymbol{x})$ with respect to $\boldsymbol{x}$ and multiplying with the scalar $\left(\frac{\lambda}{\lambda+m\beta\lambda_0}\right)^{\frac{k}{2}}$. However, we later on show that for almost all realizations of the source vector, $\mathsf{Z}(m;\boldsymbol{x})$ converges to a deterministic value, and therefore, the expectation with respect to $\boldsymbol{x}$ can be dropped. For $\mathsf{Z}(m;\boldsymbol{x})$,

[1]We call it unbiased since it expresses the deviation of the replicas from the source vector.

we have

$$\mathsf{Z}(m;\boldsymbol{x}) = \mathsf{E}_{\mathbf{J}} \sum_{\{\boldsymbol{v}_a\}} e^{-\beta \sum_{a,b=1}^{m} \tilde{\boldsymbol{v}}_a^{\mathsf{T}} \mathbf{J} \tilde{\boldsymbol{v}}_b \zeta_{ab}} \times e^{-\beta \sum_{a=1}^{m} u(\boldsymbol{v}_a) + hn \sum_{a=1}^{m} \mathsf{D}^{\mathbb{W}(n)}(\boldsymbol{v}_a;\boldsymbol{x})} \tag{182a}$$

$$= \sum_{\{\boldsymbol{v}_a\}} \left[\mathsf{E}_{\mathbf{J}} e^{-n\beta \mathrm{Tr}\{\mathbf{J}\mathbf{G}\}} \right] \times e^{-\beta \sum_{a=1}^{m} u(\boldsymbol{v}_a) + hn \sum_{a=1}^{m} \mathsf{D}^{\mathbb{W}(n)}(\boldsymbol{v}_a;\boldsymbol{x})} \tag{182b}$$

where $\mathbf{G}_{n\times n}$ is defined as

$$\mathbf{G} \coloneqq \frac{1}{n} \sum_{a,b=1}^{m} \tilde{\boldsymbol{v}}_b \tilde{\boldsymbol{v}}_a^{\mathsf{T}} \zeta_{a,b}. \tag{183}$$

Considering the eigendecomposition of the Gramian $\mathbf{J} = \mathbf{U}\mathbf{D}\mathbf{U}^{\mathsf{T}}$, the expectation in (182b) can be expressed in terms of a spherical integral where the integral measure is the probability measure of $\mathbf{U}$. Regarding the system setup specified in Section II, the matrix $\mathbf{U}$ is distributed over the orthogonal group $\mathbb{O}_n$ with Haar probability distribution. Therefore, the corresponding spherical integral is the so-called "Harish-Chandra" or "Itzykson & Zuber" integral. This integral has been extensively studied in the physics and mathematics literature, see for example [73], [74] and [55]. A brief discussion on the spherical integral and its closed form solution has been given in Appendix F. Invoking Theorem 1.2 and 1.7 in [56], as long as $\mathrm{rank}(\mathbf{G}) = \mathcal{O}(\sqrt{n})$[1], the expectation in (182b) can be written as

$$\mathsf{E}_{\mathbf{J}} e^{-n\beta \mathrm{Tr}\{\mathbf{J}\mathbf{G}\}} = e^{-n\left[\sum_{i=1}^{n} \int_0^{\beta\lambda_i^{\mathbf{G}}} \mathrm{R}_{\mathbf{J}}(-2\omega)\mathrm{d}\omega\right] + \epsilon_n} \tag{184}$$

with $\mathbf{G}$ being defined in (183), and $\epsilon_n \downarrow 0$ as $n \uparrow \infty$. In order to employ the above result and substitute it in (182b), we need to check the rank condition.

Lemma A.1. *Considering* $\mathbf{G}$ *to be defined as in* (183)*, the following argument holds.*

$$\mathrm{rank}(\mathbf{G}) = \mathcal{O}(\sqrt{n}). \tag{185}$$

■

Proof. First, we rewrite $\mathbf{G}$ as

$$\mathbf{G} = \frac{1}{2\lambda n} \left[\sum_{a=1}^{m} \tilde{\boldsymbol{v}}_a \tilde{\boldsymbol{v}}_a^{\mathsf{T}} - \beta \frac{\lambda_0}{\lambda + m\beta\lambda_0} (\sum_{a=1}^{m} \tilde{\boldsymbol{v}}_a)(\sum_{b=1}^{m} \tilde{\boldsymbol{v}}_b)^{\mathsf{T}} \right] \tag{186a}$$

$$= \frac{1}{2\lambda n} \tilde{\mathbf{V}} (\mathbf{I}_m - \beta \frac{\lambda_0}{\lambda + m\beta\lambda_0} \mathbf{1}_m) \tilde{\mathbf{V}}^{\mathsf{T}} \tag{186b}$$

where $\tilde{\mathbf{V}} = [\tilde{\boldsymbol{v}}_1, \ldots, \tilde{\boldsymbol{v}}_m]$ is an $n \times m$ matrix with the columns being the unbiased replicas. Then, by considering (186b), it is obvious that $\mathbf{G}$ could be, at most, of rank m. As Assumption 2 indicates, $\mathsf{Z}(m)$ analytically continues to the real axis, and the limit with respect to m is taken in a right neighborhood of 0. Therefore, for all values of

[1] $\mathcal{O}(\cdot)$ indicates the growth order with respect to composition, i.e., $\lim_{n\uparrow\infty} [f(n)]^{-1} \mathcal{O}(f(n)) = \mathsf{K} < \infty$.

n there exists a constant $\mathsf{K} \in \mathbb{R}^+$, such that $m \leq \mathsf{K}$. Consequently, one can write

$$\lim_{n\uparrow\infty} \frac{\operatorname{rank}(\mathbf{G})}{\sqrt{n}} \leq \lim_{n\uparrow\infty} \frac{m}{\sqrt{n}} \leq \lim_{n\uparrow\infty} \frac{\mathsf{K}}{\sqrt{n}} = 0 \tag{187}$$

which concludes that $\operatorname{rank}(\mathbf{G}) = \mathcal{O}(\sqrt{n})$. ▲

Lemma A.1 ensures that (184) always holds; therefore, noting the fact that $\mathbf{G}$ has only m non-zero eigenvalues, the expectation in the right hand side of (182b) reduces to

$$\mathsf{E}_{\mathbf{J}} e^{-n\beta \operatorname{Tr}\{\mathbf{JG}\}} = e^{-n\mathcal{G}(\mathbf{TQ}^{\mathrm{v}})+\epsilon_n} \tag{188}$$

where the function $\mathcal{G}(\cdot)$ is defined as

$$\mathcal{G}(\mathbf{M}) \coloneqq \int_0^{\beta} \operatorname{Tr}\{\mathbf{M}\mathrm{R}_{\mathbf{J}}(-2\omega\mathbf{M})\}\mathrm{d}\omega \tag{189}$$

for some square matrix $\mathbf{M}$, $\mathbf{T}$ is an $m \times m$ deterministic matrix given by

$$\mathbf{T} \coloneqq \frac{1}{2\lambda}\left[\mathbf{I}_m - \frac{\lambda_0}{\lambda + m\beta\lambda_0}\beta\mathbf{1}_m\right], \tag{190}$$

and $\mathbf{Q}^{\mathrm{v}}$ is the $m \times m$ "correlation matrix" defined as

$$\mathbf{Q}^{\mathrm{v}} = \frac{1}{n}\tilde{\mathbf{V}}^{\mathsf{T}}\tilde{\mathbf{V}}. \tag{191}$$

Remark A.2. Note that although $\mathbf{Q}^{\mathrm{v}}$ is symmetric, $\mathbf{TQ}^{\mathrm{v}}$ is not a symmetric matrix, in general; however, due to the symmetry of $\mathbf{G}$, the eigenvalues of $\mathbf{TQ}^{\mathrm{v}}$ are real, and therefore, the sequence of integrals over the real axis in (184) exists for all indices.

By substituting (188) in (182b), $\mathsf{Z}(m;\boldsymbol{x})$ is given as

$$\mathsf{Z}(m;\boldsymbol{x}) = \sum_{\{\boldsymbol{v}_a\}} e^{-n\mathcal{G}(\mathbf{TQ}^{\mathrm{v}})-\beta\sum_{a=1}^m u(\boldsymbol{v}_a)+hn\sum_{a=1}^m \mathsf{D}^{\mathbb{W}(n)}(\boldsymbol{v}_a;\boldsymbol{x})+\epsilon_n}. \tag{192}$$

In order to determine the sum in (192), we follow the technique which has been employed in [16] and [63]. We split the space of all replicas into subshells defined by the correlation matrices in which all the vectors of replicas in each subshell have a same correlation matrix. More precisely, for a given source vector $\boldsymbol{x}$, the subshell of the matrix $\mathbf{Q}_{m\times m}$ is defined as

$$\mathbb{S}(\mathbf{Q}) = \{\boldsymbol{v}_1, \ldots, \boldsymbol{v}_m | (\boldsymbol{x}-\boldsymbol{v}_a)^{\mathsf{T}}(\boldsymbol{x}-\boldsymbol{v}_b) = nq_{ab}\} \tag{193}$$

with $q_{ab} = [\mathbf{Q}]_{ab}$ denoting the entry (a,b) of $\mathbf{Q}$. The sum in (192) is determined first over each subshell, and then,

over all the subshells as the following.

$$\mathsf{Z}(m;\boldsymbol{x}) = \sum_{\{\boldsymbol{v}_a\}} \left[\int e^{-n\mathcal{G}(\mathbf{TQ})}\delta(\mathbf{Q}^{\mathrm{v}}-\mathbf{Q})\mathrm{d}\mathbf{Q}\right] e^{-\beta\sum_{a=1}^m u(\boldsymbol{v}_a)+hn\sum_{a=1}^m \mathsf{D}^{\mathbb{W}(n)}(\boldsymbol{v}_a;\boldsymbol{x})+\epsilon_n} \tag{194a}$$

$$= \int e^{-n\mathcal{G}(\mathbf{TQ})+\epsilon_n}\left[\sum_{\{\boldsymbol{v}_a\}}\delta(\mathbf{Q}^{\mathrm{v}}-\mathbf{Q})e^{-\beta\sum_{a=1}^m u(\boldsymbol{v}_a)+hn\sum_{a=1}^m \mathsf{D}^{\mathbb{W}(n)}(\boldsymbol{v}_a;\boldsymbol{x})}\right]\mathrm{d}\mathbf{Q} \tag{194b}$$

$$= \int e^{-n[\mathcal{G}(\mathbf{TQ})-\mathcal{I}(\mathbf{Q})]+\epsilon_n}\mathrm{d}\mathbf{Q} \tag{194c}$$

where $\mathrm{d}\mathbf{Q} \coloneqq \prod_{a,b=1}^m \mathrm{d}q_{ab}$, the integral is taken over $\mathbb{R}^{m\times m}$,

$$\delta(\mathbf{Q}^{\mathrm{v}}-\mathbf{Q}) \coloneqq \prod_{a,b=1}^m \delta(\tilde{\boldsymbol{v}}_a^{\mathsf{T}}\tilde{\boldsymbol{v}}_b - nq_{ab}), \tag{195}$$

and the term $e^{n\mathcal{I}(\mathbf{Q})}$ which determines the probability weight of the subshell $\mathbb{S}(\mathbf{Q})$ is defined as

$$e^{n\mathcal{I}(\mathbf{Q})} \coloneqq \sum_{\{\boldsymbol{v}_a\}}\delta(\mathbf{Q}^{\mathrm{v}}-\mathbf{Q})e^{-\beta\sum_{a=1}^m u(\boldsymbol{v}_a)+hn\sum_{a=1}^m \mathsf{D}^{\mathbb{W}(n)}(\boldsymbol{v}_a;\boldsymbol{x})}. \tag{196}$$

Remark A.3. One may define the subshells over the transferred correlation matrix $\mathbf{TQ}$ instead of correlation matrix $\mathbf{Q}$. In this case the subshells over $\mathbf{Q}$ defined in (193) only rotate in the m-dimensional space with respect to $\mathbf{T}$. The rotation, however, does not have any impact on the analysis.

The last step is to determine $e^{n\mathcal{I}(\mathbf{Q})}$. To do so, we represent the Dirac impulse function using its inverse Laplace transform. By defining s_{ab} as the complex frequency corresponding to $\delta(\tilde{\boldsymbol{v}}_a^{\mathsf{T}}\tilde{\boldsymbol{v}}_b - nq_{ab})$,

$$\delta(\tilde{\boldsymbol{v}}_a^{\mathsf{T}}\tilde{\boldsymbol{v}}_b - nq_{ab}) = \int e^{s_{ab}(\tilde{\boldsymbol{v}}_a^{\mathsf{T}}\tilde{\boldsymbol{v}}_b - nq_{ab})}\frac{\mathrm{d}s_{ab}}{2\pi\mathrm{j}} \tag{197}$$

where the integral is taken over the imaginary axis $\mathbb{J} = (t-\mathrm{j}\infty, t+\mathrm{j}\infty)$, for some $t\in\mathbb{R}$. Consequently, by defining the frequency domain correlation matrix $\mathbf{S}$ to be an $m\times m$ matrix with $[\mathbf{S}]_{ab} = s_{ab}$, (195) reads

$$\delta(\mathbf{Q}^{\mathrm{v}}-\mathbf{Q}) = \int e^{\sum_{a,b=1}^m s_{ab}(\tilde{\boldsymbol{v}}_a^{\mathsf{T}}\tilde{\boldsymbol{v}}_b - nq_{ab})}\mathrm{d}\mathbf{S} \tag{198a}$$

$$= \int \left[e^{-n\mathrm{Tr}\{\mathbf{S}^{\mathsf{T}}\mathbf{Q}\}}\right] e^{\sum_{a,b=1}^m s_{ab}\tilde{\boldsymbol{v}}_a^{\mathsf{T}}\tilde{\boldsymbol{v}}_b}\mathrm{d}\mathbf{S} \tag{198b}$$

with $\mathrm{d}\mathbf{S}$ being defined as $\mathrm{d}\mathbf{S} \coloneqq \prod_{a,b=1}^m \frac{\mathrm{d}s_{ab}}{2\pi\mathrm{j}}$, and the integral being taken over $\mathbb{J}^{m\times m}$. Substituting in (196), $e^{n\mathcal{I}(\mathbf{Q})}$ reduces to

$$e^{n\mathcal{I}(\mathbf{Q})} = \int e^{-n\mathrm{Tr}\{\mathbf{S}^{\mathsf{T}}\mathbf{Q}\}}\sum_{\{\boldsymbol{v}_a\}} e^{\sum_{a,b=1}^m s_{ab}\tilde{\boldsymbol{v}}_a^{\mathsf{T}}\tilde{\boldsymbol{v}}_b-\beta\sum_{a=1}^m u(\boldsymbol{v}_a)+hn\sum_{a=1}^m \mathsf{D}^{\mathbb{W}(n)}(\boldsymbol{v}_a;\boldsymbol{x})}\mathrm{d}\mathbf{S} \tag{199a}$$

$$= \int e^{-n\mathrm{Tr}\{\mathbf{S}^{\mathsf{T}}\mathbf{Q}\}}\ e^{n\mathcal{M}(\mathbf{S})}\mathrm{d}\mathbf{S} \tag{199b}$$

with $\mathcal{M}(\mathbf{S})$ being defined as

$$\mathcal{M}(\mathbf{S}) = \frac{1}{n} \log \sum_{\{\boldsymbol{v}_a\}} e^{\sum_{a,b=1}^{m} s_{ab} \tilde{\boldsymbol{v}}_a^{\mathsf{T}} \tilde{\boldsymbol{v}}_b - \beta \sum_{a=1}^{m} u(\boldsymbol{v}_a) + hn \sum_{a=1}^{m} \mathsf{D}^{\mathbb{W}(n)}(\boldsymbol{v}_a; \boldsymbol{x})}. \tag{200}$$

Thus, $\mathsf{Z}(m; \boldsymbol{x})$ finally reads

$$\mathsf{Z}(m; \boldsymbol{x}) = \int \int e^{-n\{\mathcal{G}(\mathbf{TQ}) + \mathrm{Tr}\{\mathbf{S}^{\mathsf{T}}\mathbf{Q}\} - \mathcal{M}(\mathbf{S})\} + \epsilon_n} \mathrm{d}\mathbf{S} \mathrm{d}\mathbf{Q}. \tag{201}$$

Consequently, one needs to evaluate the expectation of $\mathsf{Z}(m; \boldsymbol{x})$ with respect to $\boldsymbol{x}$, in order to determine the moment function $\mathsf{Z}(m)$. However, $\mathsf{Z}(m; \boldsymbol{x})$ for almost all realizations of $\boldsymbol{x}$ converges to a deterministic asymptotic as $n \uparrow \infty$, and thus, the expectation with respect to $\boldsymbol{x}$ can be dropped. To show the latter statement, we note that the only term in (201) which depends on $\boldsymbol{x}$ is $\mathcal{M}(\mathbf{S})$. Therefore, it is sufficient to study the convergence of $\mathcal{M}(\mathbf{S})$. Lemma A.2 justifies this property of $\mathcal{M}(\mathbf{S})$ using the law of large numbers, and the decoupling property of the functions $u(\cdot)$ and $\mathsf{d}(\cdot;\cdot)$.

Lemma A.2. *Consider the system specified in Section II, and let Assumption 2 hold. Then, as $n \uparrow \infty$, $\mathcal{M}(\mathbf{S})$ defined in (200) is given by*

$$\mathcal{M}(\mathbf{S}) = \mathsf{E}\left\{(1-\eta)\left[\log \sum_{\mathbf{v}} e^{(\mathbf{x}-\mathbf{v})^{\mathsf{T}}\mathbf{S}(\mathbf{x}-\mathbf{v}) - \beta u(\mathbf{v})}\right] + \eta\left[\log \sum_{\mathbf{v}} e^{(\mathbf{x}-\mathbf{v})^{\mathsf{T}}\mathbf{S}(\mathbf{x}-\mathbf{v}) - \beta u(\mathbf{v}) + h\eta^{-1}\mathsf{d}(\mathbf{v};\mathbf{x})}\right]\right\} \tag{202}$$

where $\mathbf{v}_{m\times 1} \in \mathbb{X}^m$, $\mathbf{x}_{m\times 1}$ is a vector with all the elements being the random variable x which is distributed with the source distribution p_x, the expectation is taken over p_x, and $\mathsf{d}(\mathbf{v};\mathbf{x})$ is defined as $\mathsf{d}(\mathbf{v};\mathbf{x}) := \sum_{a=1}^{m} \mathsf{d}(\mathrm{v}_a; \mathrm{x}_a)$. ■

Proof. Consider the decoupling property of the functions $u(\cdot)$ and $\mathsf{d}(\cdot;\cdot)$. Define the vector $\mathbf{v}_{m\times 1}$ over the support $\mathbb{X}^m$, and the coefficients $\{\mathsf{w}_i\}$ for $i \in [1:n]$ as

$$\mathsf{w}_i = \begin{cases} 0 & \text{if } i \notin \mathbb{W}(n) \\ |\mathbb{W}(n)|^{-1} & \text{if } i \in \mathbb{W}(n). \end{cases} \tag{203}$$

Then, $\mathcal{M}(\mathbf{S})$ reads

$$\mathcal{M}(\mathbf{S}) = \frac{1}{n} \log \sum_{\{\boldsymbol{v}_a\}} \prod_{i=1}^{n} e^{\sum_{a,b=1}^{m} s_{ab}(x_i - v_{ai})(x_i - v_{bi}) - \beta \sum_{a=1}^{m} u(v_{ai}) + hn \sum_{a=1}^{m} \mathsf{w}_i \mathsf{d}(v_{ai}; x_i)} \tag{204a}$$

$$= \frac{1}{n} \log \prod_{i=1}^{n} \sum_{\mathbf{v}} e^{\sum_{a,b=1}^{m} s_{ab}(x_i - \mathrm{v}_a)(x_i - \mathrm{v}_b) - \beta \sum_{a=1}^{m} u(\mathrm{v}_a) + hn \sum_{a=1}^{m} \mathsf{w}_i \mathsf{d}(\mathrm{v}_a; x_i)} \tag{204b}$$

$$= \frac{1}{n} \left[\sum_{i \notin \mathbb{W}} \mathcal{M}_0(\mathbf{S}; x_i) + \sum_{i \in \mathbb{W}} \mathcal{M}_1(\mathbf{S}; x_i)\right] \tag{204c}$$

where the functions $\mathcal{M}_0(\cdot;\cdot)$ and $\mathcal{M}_1(\cdot;\cdot)$ are defined as

$$\mathcal{M}_0(\mathbf{S};x_i)=\log\sum_{\mathbf{v}}e^{(\mathbf{x}-\mathbf{v})^{\mathsf{T}}\mathbf{S}(\mathbf{x}-\mathbf{v})-\beta u(\mathbf{v})} \tag{205a}$$

$$\mathcal{M}_1(\mathbf{S};x_i)=\log\sum_{\mathbf{v}}e^{(\mathbf{x}-\mathbf{v})^{\mathsf{T}}\mathbf{S}(\mathbf{x}-\mathbf{v})-\beta u(\mathbf{v})+h\frac{n}{|\mathbb{W}(n)|}\mathsf{d}(\mathbf{v};\mathbf{x})} \tag{205b}$$

where $\mathbf{x}_{m\times 1}$ is a vector with all the elements being x_i, and we define $\mathsf{d}(\mathbf{v};\mathbf{x})\coloneqq\sum_{a=1}^{m}\mathsf{d}(\mathrm{v}_a;\mathrm{x}_a)$ for compactness. As Assumption 2 suggests the limits with respect to m and n can be exchanged in (176); thus, one can consider the asymptotics of $\mathcal{M}(\mathbf{S})$ for a given m when n tends to its large limit. Regarding the fact that $\boldsymbol{x}$ is collected from an i.i.d. distribution, the term in the right hand side of (204c) converges to the expectation over the distribution p_x due to the law of large numbers; more precisely, as $n\uparrow\infty$

$$\frac{1}{n}\sum_{i\notin\mathbb{W}}\mathcal{M}_0(\mathbf{S};x_i)=\left[1-\frac{|\mathbb{W}(n)|}{n}\right]\frac{1}{n-|\mathbb{W}(n)|}\sum_{i\notin\mathbb{W}}\mathcal{M}_0(\mathbf{S};x_i)\longrightarrow(1-\eta)\ \mathsf{E}_x\mathcal{M}_0(\mathbf{S};x) \tag{206a}$$

$$\frac{1}{n}\sum_{i\in\mathbb{W}}\mathcal{M}_1(\mathbf{S};x_i)=\left[\frac{|\mathbb{W}(n)|}{n}\right]\frac{1}{|\mathbb{W}(n)|}\sum_{i\in\mathbb{W}}\mathcal{M}_1(\mathbf{S};x_i)\longrightarrow\eta\ \mathsf{E}_x\mathcal{M}_1(\mathbf{S};x) \tag{206b}$$

with η being defined as in (26). Substituting (206a) and (206b) in (204c), Lemma A.2 is concluded. ▲

Remark A.4. Considering Lemma A.2, it eventually says that the probability weight $e^{n\mathcal{I}(\mathbf{Q})}$ for a given correlation matrix $\mathbf{Q}$ converges to a deterministic weight as n tends to infinity. This statement equivalently states that for almost any given realization of the source vector, the correlation matrix converges to its expectation. In fact, considering the correlation matrix $\mathbf{Q}^{\mathrm{v}}$, as defined in (191), the entries are functions of $\boldsymbol{x}$, and therefore, variate randomly due to the source distribution for a given n. Lemma A.2, however, indicates that, as $n\uparrow\infty$, the entries converge to some deterministic asymptotics for almost any realization of $\boldsymbol{x}$. As an alternative approach, one could study the convergence property of the correlation matrix $\mathbf{Q}^{\mathrm{v}}$ by means of the law of large numbers first, and then, conclude Lemma A.2 by rewriting $\mathcal{M}(\mathbf{S})$ in proper way, and replacing it with the expectation using the fact that the probability weight $e^{n\mathcal{I}(\mathbf{Q})}$ needs to converge deterministically as $n\uparrow\infty$. Nevertheless, the approach taken here seems to be more straightforward.

Using Lemma A.2, we drop the expectation with respect to $\boldsymbol{x}$ in (177c). Replacing in (176), the asymptotic distortion is found by taking the limits. As Assumption 2 suggests, we exchange the order of the limits and take the limit with respect to n at first. Denoting that the probability measure defined with $e^{n\mathcal{I}(\mathbf{Q})}\mathrm{d}\mathbf{Q}$ satisfy the large deviation properties [61], we can use the saddle point approximation to evaluate the integral in (201) which says that as $n\uparrow\infty$

$$\mathsf{Z}(m)=\left(\frac{\lambda}{\lambda+m\beta\lambda_0}\right)^{\frac{k}{2}}\int\int e^{-n\{\mathcal{G}(\mathbf{TQ})+\mathrm{Tr}\{\mathbf{S}^{\mathsf{T}}\mathbf{Q}\}-\mathcal{M}(\mathbf{S})\}}\mathrm{d}\mathbf{S}\mathrm{d}\mathbf{Q}\doteq\mathsf{K}_n e^{-n\{\mathcal{G}(\mathbf{T}\tilde{\mathbf{Q}})+\mathrm{Tr}\{\tilde{\mathbf{S}}^{\mathsf{T}}\tilde{\mathbf{Q}}\}-\mathcal{M}(\tilde{\mathbf{S}})\}}, \tag{207}$$

where we drop ϵ_n given in (201) regarding the fact that it vanishes in the large limit. Here, $(\tilde{\mathbf{Q}},\tilde{\mathbf{S}})$ is the saddle point of the integrand function's exponent, K_n is a bounded coefficient, and $\doteq$ indicates the asymptotic equivalency in exponential scale defined as the following.

Definition A.1. The functions $a(\cdot)$ and $b(\cdot)$ defined over the non-bounded set $\mathbb{X}$ are said to be asymptotically equivalent in exponential scale, if

$$\lim_{n\uparrow\infty} \log|\frac{a(x_n)}{b(x_n)}| = 0. \tag{208}$$

for an unbounded sequence $\{x_n \in \mathbb{X}\}$. ■

As $n \uparrow \infty$, the mth moment can be replaced with its asymptotic equivalent in (176). Consequently, by substituting the equivalent term and exchanging the limits' order, we have

$$\mathsf{D}^{\mathsf{W}}(\hat{\boldsymbol{x}};\boldsymbol{x}) = \lim_{\beta\uparrow\infty}\lim_{m\downarrow 0}\lim_{h\downarrow 0}\lim_{n\uparrow\infty}\frac{1}{m}\frac{\partial}{\partial h}\left[-\mathcal{G}(\mathbf{T}\tilde{\mathbf{Q}}) - \mathrm{Tr}\{\tilde{\mathbf{S}}^{\mathsf{T}}\tilde{\mathbf{Q}}\} + \mathcal{M}(\tilde{\mathbf{S}}) + \frac{\log \mathsf{K}_n}{n}\right] \tag{209a}$$

$$\overset{\star}{=} \lim_{\beta\uparrow\infty}\lim_{m\downarrow 0}\lim_{h\downarrow 0}\frac{1}{m}\frac{\partial}{\partial h}\mathcal{M}(\tilde{\mathbf{S}}) \tag{209b}$$

$$= \lim_{\beta\uparrow\infty}\lim_{m\downarrow 0}\mathsf{E}\frac{\sum_{\mathbf{v}}\mathsf{d}(\mathbf{v};\mathbf{x})e^{(\mathbf{x}-\mathbf{v})^{\mathsf{T}}\tilde{\mathbf{S}}(\mathbf{x}-\mathbf{v})-\beta u(\mathbf{v})}}{m\sum_{\mathbf{v}}e^{(\mathbf{x}-\mathbf{v})^{\mathsf{T}}\tilde{\mathbf{S}}(\mathbf{x}-\mathbf{v})-\beta u(\mathbf{v})}} \tag{209c}$$

where $\star$ comes from the fact that K_n is bounded, and $\mathcal{G}(\mathbf{T}\tilde{\mathbf{Q}})$ and $\mathrm{Tr}\{\tilde{\mathbf{S}}^{\mathsf{T}}\tilde{\mathbf{Q}}\}$ are not functions of h.

The saddle point $(\tilde{\mathbf{Q}},\tilde{\mathbf{S}})$ is found by letting the derivatives of the exponent zero. Using the standard definition $\left[\frac{\partial}{\partial \mathbf{M}}\right]_{ab} \coloneqq \frac{\partial}{\partial[\mathbf{M}]_{ab}}$, the saddle point is given by the following fixed point equations.

$$\frac{\partial}{\partial \mathbf{Q}}\left[\mathcal{G}(\mathbf{T}\mathbf{Q}) + \mathrm{Tr}\{\mathbf{S}\mathbf{Q}\} - \mathcal{M}(\mathbf{S})\right]|_{(\tilde{\mathbf{Q}},\tilde{\mathbf{S}})} = 0 \tag{210a}$$

$$\frac{\partial}{\partial \mathbf{S}}\left[\mathcal{G}(\mathbf{T}\mathbf{Q}) + \mathrm{Tr}\{\mathbf{S}\mathbf{Q}\} - \mathcal{M}(\mathbf{S})\right]|_{(\tilde{\mathbf{Q}},\tilde{\mathbf{S}})} = 0. \tag{210b}$$

(210a) reduces to

$$\tilde{\mathbf{S}} = -\beta\mathbf{T}\mathrm{R}_{\mathbf{J}}(-2\beta\mathbf{T}\tilde{\mathbf{Q}}), \tag{211}$$

and (210b) results in

$$\tilde{\mathbf{Q}} = \mathsf{E}\frac{\sum_{\mathbf{v}}(\mathbf{x}-\mathbf{v})(\mathbf{x}-\mathbf{v})^{\mathsf{T}}e^{(\mathbf{x}-\mathbf{v})^{\mathsf{T}}\tilde{\mathbf{S}}(\mathbf{x}-\mathbf{v})-\beta u(\mathbf{v})}}{\sum_{\mathbf{v}}e^{(\mathbf{x}-\mathbf{v})^{\mathsf{T}}\tilde{\mathbf{S}}(\mathbf{x}-\mathbf{v})-\beta u(\mathbf{v})}}. \tag{212}$$

By replacing (211) in (209c) and (212), the expression for the asymptotic distortion and the saddle point correlation matrix can be considered as expectations over a conditional Boltzmann-Gibbs distribution $\mathrm{p}^{\beta}_{\mathbf{v}|\mathbf{x}}$ defined as

$$\mathrm{p}^{\beta}_{\mathbf{v}|\mathbf{x}}(\mathbf{v}|\mathbf{x}) \coloneqq \frac{e^{-\beta\left[(\mathbf{x}-\mathbf{v})^{\mathsf{T}}\mathbf{T}\mathrm{R}_{\mathbf{J}}(-2\beta\mathbf{T}\tilde{\mathbf{Q}})(\mathbf{x}-\mathbf{v})+u(\mathbf{v})\right]}}{\sum_{\mathbf{v}}e^{-\beta\left[(\mathbf{x}-\mathbf{v})^{\mathsf{T}}\mathbf{T}\mathrm{R}_{\mathbf{J}}(-2\beta\mathbf{T}\tilde{\mathbf{Q}})(\mathbf{x}-\mathbf{v})+u(\mathbf{v})\right]}} \tag{213}$$

which simplifies the expressions in (209c) and (212) to those given in Proposition IV.1.

In general the fixed point equation (212) can be satisfied with several saddle points, and therefore, multiple asymptotic distortions might be found. In this case, one should note that the valid solution is the one which minimizes the free energy of the spin glasses at the zero temperature, i.e., $\beta \uparrow \infty$. Using the mth moment, the free

energy of the system reads

$$\mathsf{F}(\beta) = -\lim_{n\uparrow\infty}\lim_{h\downarrow 0}\lim_{m\downarrow 0}\frac{1}{m}\frac{1}{\beta}\frac{1}{n}\log \mathsf{Z}(m) \tag{214a}$$

$$\stackrel{\star}{=} \lim_{m\downarrow 0}\lim_{h\downarrow 0}\frac{1}{\beta m}\left[\mathcal{G}(\mathbf{T}\tilde{\mathbf{Q}}) + \mathrm{Tr}\{\tilde{\mathbf{S}}^{\mathsf{T}}\tilde{\mathbf{Q}}\} - \mathcal{M}(\tilde{\mathbf{S}})\right] \tag{214b}$$

$$\stackrel{\dagger}{=} \lim_{m\downarrow 0}\frac{1}{m}\left[\frac{1}{\beta}\mathcal{G}(\mathbf{T}\tilde{\mathbf{Q}}) - \mathrm{Tr}\{\tilde{\mathbf{Q}}^{\mathsf{T}}\mathbf{T}\mathrm{R}_{\mathbf{J}}(-2\beta\mathbf{T}\tilde{\mathbf{Q}})\} - \frac{1}{\beta}\mathsf{E}\log\sum_{\mathbf{v}} e^{-\beta(\mathbf{x}-\mathbf{v})^{\mathsf{T}}\mathbf{T}\mathrm{R}_{\mathbf{J}}(-2\beta\mathbf{T}\tilde{\mathbf{Q}})(\mathbf{x}-\mathbf{v})-\beta u(\mathbf{v})}\right] \tag{214c}$$

where $\star$ comes from the facts that K_n is bounded and the limits with respect to m and n are supposed to exchange, and $\dagger$ is deduced from (211) and Lemma A.2. Finally by considering the definition of $\mathcal{G}(\cdot)$, Proposition IV.1 is concluded.

APPENDIX B
PROOF OF PROPOSITION V.1

Starting from Assumption 3, the replica correlation matrix is

$$\mathbf{Q} = \frac{\chi}{\beta}\mathbf{I}_m + q\mathbf{1}_m \tag{215}$$

for some non-negative real χ and q. Considering Definition IV.1, the Hamiltonian of the spin glass of replicas is given by

$$\mathcal{E}^{\mathrm{R}}(\mathbf{v}|\mathbf{x}) = (\mathbf{x}-\mathbf{v})^{\mathsf{T}}\mathbf{T}\mathrm{R}_{\mathbf{J}}(-2\beta\mathbf{T}\mathbf{Q})(\mathbf{x}-\mathbf{v}) + u(\mathbf{v}) \tag{216}$$

with $\mathbf{T}$ being defined in (49). Denoting $\mathbf{R} \coloneqq \mathbf{T}\mathrm{R}_{\mathbf{J}}(-2\beta\mathbf{T}\mathbf{Q})$, it is shown in Appendix E that $\mathbf{R}$ has the same structure as the correlation matrix; thus, one can write

$$\mathbf{R} = e\mathbf{I}_m - \beta\frac{f^2}{2}\mathbf{1}_m, \tag{217}$$

for some real f and e which are functions of χ and q. Denoting the eigendecomposition of $\mathbf{Q}$ as $\mathbf{Q} = \mathbf{V}\mathbf{D}^{\mathrm{Q}}\mathbf{V}^{\mathsf{T}}$, we have[1]

$$\mathbf{T} = \mathbf{V}\mathbf{D}^{\mathrm{T}}\mathbf{V}^{\mathsf{T}} \tag{218a}$$

$$\mathbf{R} = \mathbf{V}\mathbf{D}^{\mathrm{R}}\mathbf{V}^{\mathsf{T}} \tag{218b}$$

where $\mathbf{D}^{\mathrm{Q}}$, $\mathbf{D}^{\mathrm{T}}$ and $\mathbf{D}^{\mathrm{R}}$ are the diagonal matrices of eigenvalues. Therefore, we have

$$\mathbf{D}^{\mathrm{R}} = \mathbf{D}^{\mathrm{T}}\mathrm{R}_{\mathbf{J}}(-2\beta\mathbf{D}^{\mathrm{T}}\mathbf{D}^{\mathrm{Q}}) \tag{219}$$

which equivalently states that for $a \in [1:m]$

$$\lambda_a^{\mathbf{R}} = \lambda_a^{\mathbf{T}}\mathrm{R}_{\mathbf{J}}(-2\beta\lambda_a^{\mathbf{T}}\lambda_a^{\mathbf{Q}}) \tag{220}$$

with $\lambda_a^{\mathbf{R}}$, $\lambda_a^{\mathbf{Q}}$ and $\lambda_a^{\mathbf{T}}$ being the eigenvalue of $\mathbf{R}$, $\mathbf{Q}$ and $\mathbf{T}$ corresponding to the ath column of $\mathbf{V}$. The matrices $\mathbf{R}$, $\mathbf{Q}$ and $\mathbf{T}$ have two different corresponding eigenvalues, namely $\left\{e-\beta m\frac{f^2}{2}, \frac{\chi}{\beta}+mq, \frac{1}{2\lambda}\left[1-\frac{m\beta\lambda_0}{\lambda+m\beta\lambda_0}\right]\right\}$ which occur with multiplicity 1 and $\left\{e, \frac{\chi}{\beta}, \frac{1}{2\lambda}\right\}$ which occur with multiplicity $m-1$. Substituting in (220) and taking the limit when $m \downarrow 0$, e and f are found as

$$e = \frac{1}{2\lambda}\mathrm{R}_{\mathbf{J}}(-\frac{\chi}{\lambda}), \tag{221a}$$

$$f^2 = \frac{1}{\lambda^2}\frac{\partial}{\partial\chi}\left\{[\lambda_0\chi - \lambda q]\,\mathrm{R}_{\mathbf{J}}(-\frac{\chi}{\lambda})\right\}. \tag{221b}$$

[1]Note that $\mathbf{Q}$ is full-rank and symmetric.

To pursue the analysis, we rewrite the Hamiltonian using (217)

$$\mathcal{E}^{\mathsf{R}}(\mathbf{v}|\mathbf{x}) = e\|\mathbf{x}-\mathbf{v}\|^2 - \beta\frac{f^2}{2}\mathrm{Tr}\{(\mathbf{x}-\mathbf{v})(\mathbf{x}-\mathbf{v})^{\mathsf{T}}\mathbf{1}_m\} + u(\mathbf{v}), \tag{222}$$

and therefore, the partition function $\mathcal{Z}^{\mathsf{R}}(\beta|\mathbf{x})$ is given by

$$\mathcal{Z}^{\mathsf{R}}(\beta|\mathbf{x}) = \sum_{\{\mathrm{v}_a\}} e^{-\beta e\|\mathbf{x}-\mathbf{v}\|^2+\beta^2\frac{f^2}{2}\mathrm{Tr}\{(\mathbf{x}-\mathbf{v})(\mathbf{x}-\mathbf{v})^{\mathsf{T}}\mathbf{1}_m\}-\beta u(\mathbf{v})}. \tag{223}$$

Using the Gaussian integral, we have

$$e^{\beta^2\frac{f^2}{2}\mathrm{Tr}\{(\mathbf{x}-\mathbf{v})(\mathbf{x}-\mathbf{v})^{\mathsf{T}}\mathbf{1}_m\}} = \int e^{-\beta f\left[\sum_{a=1}^m(x-\mathrm{v}_a)\right]z}\mathrm{D}z, \tag{224}$$

and thus, the partition function reduces to

$$\mathcal{Z}^{\mathsf{R}}(\beta|\mathbf{x}) = \int\left[\sum_v e^{-\beta\left[e(x-v)^2+f(x-v)z+u(v)\right]}\right]^m \mathrm{D}z \tag{225}$$

with $v\in\mathbb{X}$. The parameters of the spin glass of replicas are then determined using the partition function. Starting with the normalized free energy, it reads

$$\mathsf{F}^{\mathsf{R}}(\beta,m) = -\frac{1}{\beta m}\mathsf{E}_x\log\int\left[\sum_v e^{-\beta\left[e(x-v)^2+f(x-v)z+u(v)\right]}\right]^m \mathrm{D}z. \tag{226}$$

Noting that $\int\mathrm{D}z$ takes expectation over the Gaussian distribution, one can use the Riesz equality in (42) to show that when m varies in a vicinity of 0

$$\mathsf{F}^{\mathsf{R}}(\beta,m) = -\frac{1}{\beta}\mathsf{E}\int\log\sum_v e^{-\beta\left[e(x-v)^2+f(x-v)z+u(v)\right]}\mathrm{D}z + \epsilon_m \tag{227}$$

where ϵ_m tends to 0 as $m\downarrow 0$ and the expectation is taken over $x\sim\mathrm{p}_x$. Consequently, as $m\downarrow 0$ the normalized free energy reads

$$\mathsf{F}^{\mathsf{R}}(\beta) = \lim_{m\downarrow 0}\mathsf{F}^{\mathsf{R}}(\beta,m) = -\frac{1}{\beta}\mathsf{E}\int\log\sum_v e^{-\beta\left[e(x-v)^2+f(x-v)z+u(v)\right]}\mathrm{D}z \tag{228}$$

The next parameters to be specified are χ and q. By determining the conditional distribution $\mathrm{p}^{\beta}_{\mathbf{v}|\mathbf{x}}$ and substituting in (50), the following fixed point equations are deduced

$$\left[\frac{\chi}{\beta}+q\right]m = \mathsf{E}_{\mathbf{x}}\sum_{\mathbf{v}}\|\mathbf{x}-\mathbf{v}\|^2\ \mathrm{p}^{\beta}_{\mathbf{v}|\mathbf{x}}(\mathbf{v}|\mathbf{x}), \tag{229a}$$

$$\left[\frac{\chi}{\beta}+mq\right]m = \mathsf{E}_{\mathbf{x}}\sum_{\mathbf{v}}\mathrm{Tr}\{(\mathbf{x}-\mathbf{v})(\mathbf{x}-\mathbf{v})^{\mathsf{T}}\mathbf{1}_m\}\ \mathrm{p}^{\beta}_{\mathbf{v}|\mathbf{x}}(\mathbf{v}|\mathbf{x}). \tag{229b}$$

where (229a) and (229b) are found by taking the trace and sum over all the entries of the both sides of (50), respectively. One can directly evaluate the right hand sides of (229a) and (229b); however, considering (223), it is

straightforward to show that

$$\mathsf{E}_{\mathbf{x}} \sum_{\mathbf{v}} \|\mathbf{x}-\mathbf{v}\|^2 \ \mathrm{p}^{\beta}_{\mathbf{v}|\mathbf{x}}(\mathbf{v}|\mathbf{x}) = m \frac{\partial}{\partial e} \mathsf{F}^{\mathsf{R}}(\beta, m), \tag{230a}$$

$$\mathsf{E}_{\mathbf{x}} \sum_{\mathbf{v}} \mathrm{Tr}\{(\mathbf{x}-\mathbf{v})(\mathbf{x}-\mathbf{v})^{\mathsf{T}} \mathbf{1}_m\} \ \mathrm{p}^{\beta}_{\mathbf{v}|\mathbf{x}}(\mathbf{v}|\mathbf{x}) = -\frac{m}{\beta f} \frac{\partial}{\partial f} \mathsf{F}^{\mathsf{R}}(\beta, m). \tag{230b}$$

After substituting and taking the limit $m \downarrow 0$, the fixed point equations finally read

$$\frac{\chi}{\beta} + q = \mathsf{E} \int \frac{\sum_v (v-x)^2 e^{-\beta\left[e(x-v)^2 + f(x-v)z + u(v)\right]}}{\sum_v e^{-\beta\left[e(x-v)^2 + f(x-v)z + u(v)\right]}} \mathrm{D}z \tag{231a}$$

$$\chi = \frac{1}{f} \mathsf{E} \int \frac{\sum_v (v-x) z e^{-\beta\left[e(x-v)^2 + f(x-v)z + u(v)\right]}}{\sum_v e^{-\beta\left[e(x-v)^2 + f(x-v)z + u(v)\right]}} \mathrm{D}z. \tag{231b}$$

with f and e defined in (221a) and (221b).

In order to determine the replicas' average distortion defined in (54) regarding the distortion function $\mathsf{d}(\cdot;\cdot)$, we replace the Hamiltonian by

$$\mathcal{E}^{\mathsf{R}}_h(\mathbf{v}|\mathbf{x}) = \mathcal{E}^{\mathsf{R}}(\mathbf{v}|\mathbf{x}) + h \sum_{a=1}^{m} \mathsf{d}(\mathrm{v}_a; x) \tag{232}$$

with $\mathcal{E}^{\mathsf{R}}(\mathbf{v}|\mathbf{x})$ given in (222), and take the steps as in (223)-(226) to find the modified form of the normalized free energy, i.e. $\mathsf{F}^{\mathsf{R}}(\beta, h, m)$. The replicas' average distortion is then evaluated as

$$\mathsf{D}^{\mathsf{R}}(\beta, m) = \frac{\partial}{\partial h} \mathsf{F}^{\mathsf{R}}(\beta, h, m)|_{h=0} \tag{233a}$$

$$= \mathsf{E} \int \frac{\sum_v \mathsf{d}(v; x) e^{-\beta\left[e(x-v)^2 + f(x-v)z + u(v)\right]}}{\sum_v e^{-\beta\left[e(x-v)^2 + f(x-v)z + u(v)\right]}} \mathrm{D}z. \tag{233b}$$

which does not depend on m, and thus, taking the limit $m \downarrow 0$ is not needed.

The last step is to take the zero temperature limit. Using the Laplace method of summation, as $\beta \uparrow \infty$ the fixed point equations reduce to

$$q = \mathsf{E} \int (\mathrm{g}-x)^2 \ \mathrm{D}z, \tag{234a}$$

$$\chi = \frac{1}{f} \mathsf{E} \int (\mathrm{g}-x) z \ \mathrm{D}z. \tag{234b}$$

with g being defined as

$$\mathrm{g} \coloneqq \arg\min_v \left[e(x-v)^2 + f(x-v)z + u(v)\right]. \tag{235}$$

Taking the same approach, the replicas' average distortion at zero temperature reads

$$\mathsf{D}^{\mathbb{W}} = \mathsf{E} \int \mathsf{d}(\mathrm{g}; x) \ \mathrm{D}z. \tag{236}$$

In order to avoid multiple solutions, we need to find the normalized free energy of the corresponding spin glass as given in Proposition IV.1. In fact, the fixed point equations in (234a) and (234b) may have different solutions, and therefore, the several asymptotics for the distortion can be obtained. In this case, the fixed point solution which

minimizes the zero temperature free energy of the system and its corresponding asymptotic distortion are taken. Substituting in Proposition IV.1, the free energy of the corresponding spin glass at the inverse temperature β is found as

$$\mathsf{F}(\beta) = \frac{1}{2\lambda}\left[\int_0^1 \mathrm{F}^{\beta}(\omega)\mathrm{d}\omega - \mathrm{F}^{\beta}(1)\right] + \mathsf{F}^{\mathsf{R}}(\beta) \tag{237}$$

where the function $\mathrm{F}^{\beta}(\cdot)$ is defined as

$$\mathrm{F}^{\beta}(\omega) = \frac{\chi}{\beta}\mathrm{R}_{\mathbf{J}}(-\frac{\chi}{\lambda}\omega) + \left[q - \frac{\lambda_0}{\lambda}\chi\right]\frac{\mathrm{d}}{\mathrm{d}\omega}\left[\omega\mathrm{R}_{\mathbf{J}}(-\frac{\chi}{\lambda}\omega)\right]. \tag{238}$$

By taking the limit as $\beta \uparrow \infty$, the zero temperature free energy reads

$$\mathsf{F}^{0} = \frac{1}{2\lambda}\left[\int_0^1 \mathrm{F}^{\infty}(\omega)\mathrm{d}\omega - \mathrm{F}^{\infty}(1)\right] + \mathsf{E}\int e(x-\mathrm{g})^2 + f(x-\mathrm{g})z + u(\mathrm{g})\ \mathrm{D}z \tag{239}$$

with g being defined as in (235) and $\mathrm{F}^{\infty}(\omega) \coloneqq \lim_{\beta\uparrow\infty}\mathrm{F}^{\beta}(\omega)$. By defining $\lambda^{\mathsf{s}} \coloneqq [2e]^{-1}$ and $\lambda_0^{\mathsf{s}} \coloneqq \left[4e^2\right]^{-1} f^2$ Proposition V.1 is concluded.

APPENDIX C
PROOF OF PROPOSITION VI.1

We take the same approach as in Appendix B. Considering the replica correlation matrix to be of the form

$$\mathbf{Q} = \frac{\chi}{\beta}\mathbf{I}_m + p\mathbf{I}_{\frac{m\beta}{\mu}} \otimes \mathbf{1}_{\frac{\mu}{\beta}} + q\mathbf{1}_m, \tag{240}$$

for some non-negative real χ, p, q, and μ, we need to evaluate the parameters of the spin glass of replicas defined in Definition IV.1. Starting with the Hamiltonian,

$$\mathcal{E}^{\mathsf{R}}(\mathbf{v}|\mathbf{x}) = (\mathbf{x}-\mathbf{v})^{\mathsf{T}}\mathbf{T}\mathrm{R}_{\mathbf{J}}(-2\beta\mathbf{T}\mathbf{Q})(\mathbf{x}-\mathbf{v}) + u(\mathbf{v}) \tag{241}$$

where $\mathbf{T}$ is given in (49). As discussed in Appendix E, for a given μ the matrix $\mathbf{R} \coloneqq \mathbf{T}\mathrm{R}_{\mathbf{J}}(-2\beta\mathbf{T}\mathbf{Q})$ is of the following form

$$\mathbf{R} = e\mathbf{I}_m - \beta\frac{g^2}{2}\mathbf{I}_{\frac{m\beta}{\mu}} \otimes \mathbf{1}_{\frac{\mu}{\beta}} - \beta\frac{f^2}{2}\mathbf{1}_m \tag{242}$$

where e, g and f can be found in terms of χ, p and q. Using the eigendecomposition of $\mathbf{R}$, $\mathbf{Q}$ and $\mathbf{T}$, it is then straightforward to show that for $a \in [1:m]$

$$\lambda_a^{\mathbf{R}} = \lambda_a^{\mathbf{T}}\mathrm{R}_{\mathbf{J}}(-2\beta\lambda_a^{\mathbf{T}}\lambda_a^{\mathbf{Q}}) \tag{243}$$

where $\lambda_a^{\mathbf{R}}$, $\lambda_a^{\mathbf{Q}}$ and $\lambda_a^{\mathbf{T}}$ denote the ath eigenvalues of $\mathbf{R}$, $\mathbf{Q}$ and $\mathbf{T}$, respectively. Regarding the structure of $\mathbf{Q}$ and $\mathbf{R}$, there are three different sets of corresponding eigenvalues for $\mathbf{R}$, $\mathbf{Q}$ and $\mathbf{T}$, namely

- $\left\{e - \mu\frac{g^2}{2} - m\beta\frac{f^2}{2}, \frac{\chi+\mu p}{\beta} + mq, \frac{1}{2\lambda}\left[1 - \frac{m\beta\lambda_0}{\lambda + m\beta\lambda_0}\right]\right\}$ with multiplicity 1,
- $\left\{e - \mu\frac{g^2}{2}, \frac{\chi+\mu p}{\beta}, \frac{1}{2\lambda}\right\}$ with multiplicity $m\beta\mu^{-1} - 1$, and
- $\left\{e, \frac{\chi}{\beta}, \frac{1}{2\lambda}\right\}$ with multiplicity $m - m\beta\mu^{-1}$.

Thus, by substituting in (243) and taking the limit when $m \downarrow 0$, e, g and f are given as

$$e = \frac{1}{2\lambda}\mathrm{R}_{\mathbf{J}}(-\frac{\chi}{\lambda}), \tag{244a}$$

$$g^2 = \frac{1}{\lambda\mu}\left[\mathrm{R}_{\mathbf{J}}(-\frac{\chi}{\lambda}) - \mathrm{R}_{\mathbf{J}}(-\frac{\chi+\mu p}{\lambda})\right], \tag{244b}$$

$$f^2 = \frac{1}{\lambda^2}\frac{\partial}{\partial\chi}\left\{[\lambda_0(\chi+\mu p) - \lambda q]\,\mathrm{R}_{\mathbf{J}}(-\frac{\chi+\mu p}{\lambda})\right\}. \tag{244c}$$

The next step is to evaluate the partition function. Substituting (242) in (241), the Hamiltonian reads

$$\mathcal{E}^{\mathsf{R}}(\mathbf{v}|\mathbf{x}) = e\|\mathbf{x}-\mathbf{v}\|^2 - \beta\frac{g^2}{2}\mathrm{Tr}\{(\mathbf{x}-\mathbf{v})(\mathbf{x}-\mathbf{v})^{\mathsf{T}}\mathbf{I}_{\frac{m\beta}{\mu}} \otimes \mathbf{1}_{\frac{\mu}{\beta}}\} - \beta\frac{f^2}{2}\mathrm{Tr}\{(\mathbf{x}-\mathbf{v})(\mathbf{x}-\mathbf{v})^{\mathsf{T}}\mathbf{1}_m\} + u(\mathbf{v}). \tag{245}$$

The partition function is then determined as in (52). Substituting in (52) and using the equalities

$$e^{\frac{1}{2}\beta^2 f^2 \mathrm{Tr}\{(\mathbf{x}-\mathbf{v})(\mathbf{x}-\mathbf{v})^\mathsf{T}\mathbf{1}_m\}} = \int e^{-\beta f\left[\sum_{a=1}^{m}(x-\mathrm{v}_a)\right]z_0}\mathrm{D}z_0, \tag{246a}$$

$$e^{\frac{1}{2}\beta^2 g^2 \mathrm{Tr}\{(\mathbf{x}-\mathbf{v})(\mathbf{x}-\mathbf{v})^\mathsf{T}\mathbf{I}_{\frac{m\beta}{\mu}}\otimes\mathbf{1}_{\frac{\mu}{\beta}}\}} = \prod_{k=0}^{\Xi}\int e^{-\beta g\left[\sum_{a=\varrho_k}^{\breve{\varrho}_k}(x-\mathrm{v}_a)\right]z_1}\mathrm{D}z_1, \tag{246b}$$

where $\varrho_k = k\mu\beta^{-1}+1$, $\breve{\varrho}_k = (k+1)\mu\beta^{-1}$, and $\Xi = m\beta\mu^{-1}-1$, the partition function is found as

$$\mathcal{Z}^{\mathsf{R}}(\beta;\mu|\mathbf{x}) = \int\left[\int\left[\sum_{v} e^{-\beta\left[e(x-v)^2+(fz_0+gz_1)(x-v)+u(v)\right]}\right]^{\frac{\mu}{\beta}}\mathrm{D}z_1\right]^{\frac{m\beta}{\mu}}\mathrm{D}z_0 \tag{247}$$

with $v\in\mathbb{X}$ where we denoted μ in the argument of the partition function to indicate that the expression is determined for a given μ. The normalized free energy of the spin glass of replicas then reads

$$\mathsf{F}^{\mathsf{R}}(\beta,m;\mu) = -\frac{1}{\beta m}\mathsf{E}_x\log\int\left[\int\left[\sum_{v} e^{-\beta\left[e(x-v)^2+(fz_0+gz_1)(x-v)+u(v)\right]}\right]^{\frac{\mu}{\beta}}\mathrm{D}z_1\right]^{\frac{m\beta}{\mu}}\mathrm{D}z_0. \tag{248}$$

Using the Riesz equality and taking the limit $m\downarrow 0$, the normalized free energy reduces to

$$\mathsf{F}^{\mathsf{R}}(\beta;\mu) = \lim_{m\downarrow 0}\mathsf{F}^{\mathsf{R}}(\beta,m;\mu) = -\frac{1}{\mu}\mathsf{E}\int\log\left\{\int\left[\sum_{v} e^{-\beta\left[e(x-v)^2+(fz_0+gz_1)(x-v)+u(v)\right]}\right]^{\frac{\mu}{\beta}}\mathrm{D}z_1\right\}\mathrm{D}z_0. \tag{249}$$

In order to find the fixed point equations, we use (50); therefore,

$$\left[\frac{\chi}{\beta}+q+p\right]m = \mathsf{E}_{\mathbf{x}}\sum_{\mathbf{v}}\|\mathbf{x}-\mathbf{v}\|^2\ \mathrm{p}^{\beta}_{\mathbf{v}|\mathbf{x}}(\mathbf{v}|\mathbf{x}), \tag{250a}$$

$$\left[\frac{\chi}{\beta}+\frac{\mu p}{\beta}+\frac{\mu q}{\beta}\right]m = \mathsf{E}_{\mathbf{x}}\sum_{\mathbf{v}}\mathrm{Tr}\{(\mathbf{x}-\mathbf{v})(\mathbf{x}-\mathbf{v})^\mathsf{T}\mathbf{I}_{\frac{m\beta}{\mu}}\otimes\mathbf{1}_{\frac{\mu}{\beta}}\}\ \mathrm{p}^{\beta}_{\mathbf{v}|\mathbf{x}}(\mathbf{v}|\mathbf{x}), \tag{250b}$$

$$\left[\frac{\chi}{\beta}+\frac{\mu p}{\beta}+mq\right]m = \mathsf{E}_{\mathbf{x}}\sum_{\mathbf{v}}\mathrm{Tr}\{(\mathbf{x}-\mathbf{v})(\mathbf{x}-\mathbf{v})^\mathsf{T}\mathbf{1}_m\}\ \mathrm{p}^{\beta}_{\mathbf{v}|\mathbf{x}}(\mathbf{v}|\mathbf{x}) \tag{250c}$$

where (250a), (250b) and (250c) are concluded by taking the trace, sum over the diagonal blocks and sum over all the entries of the both sides of (50), respectively. To evaluate the right hand sides of (250a)-(250c), we take the alternative approach and express the expectations as

$$\mathsf{E}_{\mathbf{x}}\sum_{\mathbf{v}}\|\mathbf{x}-\mathbf{v}\|^2\ \mathrm{p}^{\beta}_{\mathbf{v}|\mathbf{x}}(\mathbf{v}|\mathbf{x}) = m\frac{\partial}{\partial e}\mathsf{F}^{\mathsf{R}}(\beta,m;\mu), \tag{251a}$$

$$\mathsf{E}_{\mathbf{x}}\sum_{\mathbf{v}}\mathrm{Tr}\{(\mathbf{x}-\mathbf{v})(\mathbf{x}-\mathbf{v})^\mathsf{T}\mathbf{I}_{\frac{m\beta}{\mu}}\otimes\mathbf{1}_{\frac{\mu}{\beta}}\}\ \mathrm{p}^{\beta}_{\mathbf{v}|\mathbf{x}}(\mathbf{v}|\mathbf{x}) = -\frac{m}{\beta g}\frac{\partial}{\partial g}\mathsf{F}^{\mathsf{R}}(\beta,m;\mu), \tag{251b}$$

$$\mathsf{E}_{\mathbf{x}}\sum_{\mathbf{v}}\mathrm{Tr}\{(\mathbf{x}-\mathbf{v})(\mathbf{x}-\mathbf{v})^\mathsf{T}\mathbf{1}_m\}\ \mathrm{p}^{\beta}_{\mathbf{v}|\mathbf{x}}(\mathbf{v}|\mathbf{x}) = -\frac{m}{\beta f}\frac{\partial}{\partial f}\mathsf{F}^{\mathsf{R}}(\beta,m;\mu). \tag{251c}$$

Taking the derivatives and limit $m \downarrow 0$, the fixed point equations finally reduce to

$$\frac{\chi}{\beta} + q + p = \mathsf{E} \int \frac{\sum_v (v-x)^2 e^{-\beta\left[e(x-v)^2+(fz_0+gz_1)(x-v)+u(v)\right]}}{\sum_v e^{-\beta\left[e(x-v)^2+(fz_0+gz_1)(x-v)+u(v)\right]}} \tilde{\Lambda}^{\beta} \, \mathrm{D}z_1 \mathrm{D}z_0 \tag{252a}$$

$$\chi + \mu p + \mu q = \frac{1}{g} \mathsf{E} \int \frac{\sum_v (v-x) z_1 e^{-\beta\left[e(x-v)^2+(fz_0+gz_1)(x-v)+u(v)\right]}}{\sum_v e^{-\beta\left[e(x-v)^2+(fz_0+gz_1)(x-v)+u(v)\right]}} \tilde{\Lambda}^{\beta} \, \mathrm{D}z_1 \mathrm{D}z_0, \tag{252b}$$

$$\chi + \mu p = \frac{1}{f} \mathsf{E} \int \frac{\sum_v (v-x) z_0 e^{-\beta\left[e(x-v)^2+(fz_0+gz_1)(x-v)+u(v)\right]}}{\sum_v e^{-\beta\left[e(x-v)^2+(fz_0+gz_1)(x-v)+u(v)\right]}} \tilde{\Lambda}^{\beta} \, \mathrm{D}z_1 \mathrm{D}z_0 \tag{252c}$$

with $\tilde{\Lambda}^{\beta} \coloneqq \left[\int \Lambda^{\beta} \mathrm{D}z_1\right]^{-1} \Lambda^{\beta}$ and Λ^{β} being defined as

$$\Lambda^{\beta} \coloneqq \left[\sum_v e^{-\beta\left[e(x-v)^2+(fz_0+gz_1)(x-v)+u(v)\right]}\right]^{\frac{\mu}{\beta}}. \tag{253}$$

The replicas' average distortion regarding the distortion function $\mathsf{d}(\cdot;\cdot)$ is further determined by modifying the Hamiltonian as

$$\mathcal{E}_h^{\mathsf{R}}(\mathbf{v}|\mathbf{x}) = \mathcal{E}^{\mathsf{R}}(\mathbf{v}|\mathbf{x}) + h \sum_{a=1}^{m} \mathsf{d}(\mathrm{v}_a; x) \tag{254}$$

with $\mathcal{E}^{\mathsf{R}}(\mathbf{v}|\mathbf{x})$ given in (245), and taking the steps as in (245)-(248) to find the modified form of the normalized free energy, i.e. $\mathsf{F}^{\mathsf{R}}(\beta, h, m; \mu)$. The replicas' average distortion then reads

$$\mathsf{D}^{\mathsf{R}}(\beta;\mu) = \lim_{m\downarrow 0} \frac{\partial}{\partial h} \mathsf{F}^{\mathsf{R}}(\beta, h, m; \mu)|_{h=0} \tag{255a}$$

$$= \mathsf{E} \int \frac{\sum_v \mathsf{d}(v;x) e^{-\beta\left[e(x-v)^2+(fz_0+gz_1)(x-v)+u(v)\right]}}{\sum_v e^{-\beta\left[e(x-v)^2+(fz_0+gz_1)(x-v)+u(v)\right]}} \tilde{\Lambda}^{\beta} \, \mathrm{D}z_1 \mathrm{D}z_0. \tag{255b}$$

The analysis is concluded by taking the zero temperature limit. As $\beta \uparrow \infty$, (252a)-(252c) read

$$q + p = \mathsf{E} \int (\mathrm{g} - x)^2 \tilde{\Lambda} \mathrm{D}z_1 \mathrm{D}z_0, \tag{256a}$$

$$\chi + \mu q + \mu p = \frac{1}{g} \mathsf{E} \int (\mathrm{g} - x) z_1 \tilde{\Lambda} \mathrm{D}z_1 \mathrm{D}z_0, \tag{256b}$$

$$\chi + \mu p = \frac{1}{f} \mathsf{E} \int (\mathrm{g} - x) z_0 \tilde{\Lambda} \mathrm{D}z_1 \mathrm{D}z_0, \tag{256c}$$

where g is defined as

$$\mathrm{g} \coloneqq \arg\min_v \left[e(x-v)^2 + (fz_0 + gz_1)(x-v) + u(v)\right] \tag{257}$$

and $\tilde{\Lambda} \coloneqq \left[\int \Lambda \mathrm{D}z_1\right]^{-1} \Lambda$ with Λ denoting

$$\Lambda \coloneqq \lim_{\beta\uparrow\infty} \Lambda^{\beta} \tag{258a}$$

$$= e^{-\mu\left[e(x-\mathrm{g})^2+(fz_0+gz_1)(x-\mathrm{g})+u(\mathrm{g})\right]}. \tag{258b}$$

Moreover, the asymptotic distortion for a given μ reads

$$\mathsf{D}^{\mathbb{W}} = \mathsf{E} \int \mathsf{d}(\mathrm{g}; x)\tilde{\Lambda}\mathrm{D}z_1\mathrm{D}z_0. \tag{259}$$

(249) as well as (256a)-(259) are determined in terms of μ. Moreover, for a given μ, multiple solution to the fixed point equations can be found. Proposition IV.1 suggests us to choose the solution which minimizes the free energy. Therefore, one needs to find the optimal μ, and its corresponding χ, p and q, such that the free energy meets its minimum value. As the second law of thermodynamics is satisfied at any inverse temperature, we should initially search for the optimal μ considering a given β. We, then, find the corresponding χ, p, and q which minimize the zero temperature free energy. Using Proposition IV.1, the free energy at the inverse temperature β for a given μ is written as

$$\mathsf{F}(\beta;\mu) = \frac{1}{2\lambda}\left[\int_0^1 \mathrm{F}^{\beta}(\omega;\mu)\mathrm{d}\omega - \mathrm{F}^{\beta}(1;\mu)\right] + \mathsf{F}^{\mathsf{R}}(\beta;\mu) \tag{260}$$

where the function $\mathrm{F}^{\beta}(\cdot;\mu)$ is defined as

$$\mathrm{F}^{\beta}(\omega;\mu) = \frac{1}{\mu}\frac{\mathrm{d}}{\mathrm{d}\omega}\int_{\chi\omega}^{[\chi+\mu p]\omega} \mathrm{R}_{\mathbf{J}}(-\frac{t}{\lambda})\mathrm{d}t + \frac{\chi}{\beta}\mathrm{R}_{\mathbf{J}}(-\frac{\chi}{\lambda}\omega) + \left[q - \lambda_0\frac{\chi+\mu p}{\lambda}\right]\frac{\mathrm{d}}{\mathrm{d}\omega}\left[\omega\mathrm{R}_{\mathbf{J}}(-\frac{\chi+\mu p}{\lambda}\omega)\right]. \tag{261}$$

To find μ at the thermal equilibrium, we let

$$\frac{\partial}{\partial\mu}\mathsf{F}(\beta;\mu) = 0 \tag{262}$$

Using the equalities (244a)-(244c), (262) concludes that μ satisfies

$$\begin{aligned}\frac{1}{2\lambda}\left[p\mathrm{R}_{\mathbf{J}}(-\frac{\chi}{\lambda}) + q\mathrm{R}_{\mathbf{J}}(-\frac{\chi}{\lambda}) - q\mathrm{R}_{\mathbf{J}}(-\frac{\chi+\mu p}{\lambda})\right] &= \mathsf{F}^{\mathsf{R}}(\beta;\mu) + \frac{1}{2\lambda\mu}\int_{\chi}^{\chi+\mu p}\mathrm{R}_{\mathbf{J}}(-\frac{t}{\lambda})\mathrm{d}t \\ &+\mathsf{E}\frac{1}{\beta}\int\log\left[\sum_v e^{-\beta\left[e(x-v)^2+(fz_0+gz_1)(x-v)+u(v)\right]}\right]\tilde{\Lambda}^{\beta}\mathrm{D}z_1\mathrm{D}z_0\end{aligned} \tag{263}$$

which as $\beta\uparrow\infty$ reduces to

$$\frac{1}{2\lambda}\left[p\mathrm{R}_{\mathbf{J}}(-\frac{\chi}{\lambda}) + q\mathrm{R}_{\mathbf{J}}(-\frac{\chi}{\lambda}) - q\mathrm{R}_{\mathbf{J}}(-\frac{\chi+\mu p}{\lambda})\right] = \frac{1}{2\lambda\mu}\int_{\chi}^{\chi+\mu p}\mathrm{R}_{\mathbf{J}}(-\frac{t}{\lambda})\mathrm{d}t + \mathsf{E}\frac{1}{\mu}\int\log\tilde{\Lambda}\ \tilde{\Lambda}\mathrm{D}z_1\mathrm{D}z_0. \tag{264}$$

Denoting the solution to (264) by $\mu^{\star}$, the free energy of the corresponding spin glass is then given as $\mathsf{F}(\beta) = \mathsf{F}(\beta;\mu^{\star})$ which at the zero temperature reads

$$\mathsf{F}^0 = \frac{1}{2\lambda}\left[\int_0^1 \mathrm{F}^{\infty}(\omega)\mathrm{d}\omega - \mathrm{F}^{\infty}(1)\right] - \frac{1}{\mu}\mathsf{E}\int\log\left[\int\Lambda\mathrm{D}z_1\right]\ \mathrm{D}z_0 \tag{265}$$

with

$$\mathrm{F}^{\infty}(\omega) \coloneqq \lim_{\beta\uparrow\infty}\mathrm{F}^{\beta}(\omega;\mu^{\star}). \tag{266}$$

Finally by defining $\lambda^{\mathsf{s}} \coloneqq [2e]^{-1}$, $\lambda_0^{\mathsf{s}} \coloneqq \left[4e^2\right]^{-1} f^2$ and $\lambda_1^{\mathsf{s}} \coloneqq \left[4e^2\right]^{-1} g_1^2$, Proposition VI.1 is concluded.

APPENDIX D
PROOF OF PROPOSITION VI.3

The strategy here is to extend the approach in Appendix C to a general number of breaking steps. Following Appendix E and considering $\mathbf{Q}$ as

$$\mathbf{Q} = \frac{\chi}{\beta}\mathbf{I}_m + \sum_{\kappa=1}^{b} p_\kappa \mathbf{I}_{\frac{m\beta}{\mu_\kappa}} \otimes \mathbf{1}_{\frac{\mu_\kappa}{\beta}} + q\mathbf{1}_m, \tag{267}$$

the frequency domain correlation matrix $\mathbf{R} \coloneqq \mathbf{T}\mathrm{R}_{\mathbf{J}}(-2\beta\mathbf{T}\mathbf{Q})$ is written as

$$\mathbf{R} = e\mathbf{I}_m - \beta \sum_{\kappa=1}^{b} \frac{g_\kappa^2}{2} \mathbf{I}_{\frac{m\beta}{\mu_\kappa}} \otimes \mathbf{1}_{\frac{\mu_\kappa}{\beta}} - \beta\frac{f^2}{2}\mathbf{1}_m \tag{268}$$

considering a given vector $\boldsymbol{\mu} = [\mu_1, \ldots, \mu_b]^{\mathsf{T}}$, such that

$$\mu_{\kappa+1} = \vartheta_{\kappa+1}\mu_\kappa, \tag{269}$$

with $\{\vartheta_\kappa\}$ being non-negative integers, e, f and $\{g_\kappa\}$ are then found in terms of χ, q and $\{p_\kappa\}$ by letting

$$\lambda_a^{\mathbf{R}} = \lambda_a^{\mathbf{T}}\mathrm{R}_{\mathbf{J}}(-2\beta\lambda_a^{\mathbf{T}}\lambda_a^{\mathbf{Q}}) \tag{270}$$

for $a \in [1:m]$ where $\lambda_a^{\mathbf{R}}$, $\lambda_a^{\mathbf{Q}}$ and $\lambda_a^{\mathbf{T}}$ denote the ath corresponding eigenvalues of $\mathbf{R}$, $\mathbf{Q}$ and $\mathbf{T}$. As long as the constraint in (269) holds, $\mathbf{Q}$, $\mathbf{T}$ and $\mathbf{R}$ have $b+2$ different sets of corresponding eigenvalues specified by

- $\left\{e - \sum_{\kappa=1}^{b}\mu_\kappa\frac{g_\kappa^2}{2} - m\beta\frac{f^2}{2}, \frac{\chi}{\beta} + \sum_{\kappa=1}^{b}p_\kappa\frac{\mu_\kappa}{\beta} + mq, \frac{1}{2\lambda}\left[1 - \frac{m\beta\lambda_0}{\lambda + m\beta\lambda_0}\right]\right\}$ with multiplicity $\Theta_{b+1}(m) = 1$,
- $\left\{e - \sum_{\kappa=1}^{b}\mu_\kappa\frac{g_\kappa^2}{2}, \frac{\chi}{\beta} + \sum_{\kappa=1}^{b}p_\kappa\frac{\mu_\kappa}{\beta}, \frac{1}{2\lambda}\right\}$ with multiplicity $\Theta_b(m) = m\beta\mu_b^{-1} - 1$,
- $\left\{e - \sum_{\varsigma=1}^{\kappa}\mu_\varsigma\frac{g_\varsigma^2}{2}, \frac{\chi}{\beta} + \sum_{\varsigma=1}^{\kappa}p_\varsigma\frac{\mu_\varsigma}{\beta}, \frac{1}{2\lambda}\right\}$ with multiplicity $\Theta_\kappa(m) = m\beta\left(\mu_\kappa^{-1} - \mu_{\kappa+1}^{-1}\right)$ for $\kappa \in [1:b-1]$, and
- $\left\{e, \frac{\chi}{\beta}, \frac{1}{2\lambda}\right\}$ with multiplicity $\Theta_0(m) = m - m\beta\mu_1^{-1}$.

Substituting in (270) e, f and $\{g_\kappa\}$ for $\kappa \in [1:b]$ are determined in terms of χ, q and $\{p_\kappa\}$ as

$$e = \frac{1}{2\lambda}\mathrm{R}_{\mathbf{J}}(-\frac{\chi}{\lambda}), \tag{271a}$$

$$g_\kappa^2 = \frac{1}{\lambda\mu_\kappa}\left[\mathrm{R}_{\mathbf{J}}(-\frac{\tilde{\chi}_{\kappa-1}}{\lambda}) - \mathrm{R}_{\mathbf{J}}(-\frac{\tilde{\chi}_\kappa}{\lambda})\right], \tag{271b}$$

$$f^2 = \frac{1}{\lambda^2}\frac{\partial}{\partial\tilde{\chi}_b}\left\{[\lambda_0\tilde{\chi}_b - \lambda q]\,\mathrm{R}_{\mathbf{J}}(-\frac{\tilde{\chi}_b}{\lambda})\right\}. \tag{271c}$$

where we define $\tilde{\chi}_0 \coloneqq \chi$ and

$$\tilde{\chi}_\kappa \coloneqq \chi + \sum_{\varsigma=1}^{\kappa}\mu_\varsigma p_\varsigma \tag{272}$$

for $\kappa \in [1:b]$. The Hamiltonian of the spin glass of replicas is then determined as in (48). Substituting the Hamiltonian in (52) and using the equalities

$$e^{\frac{1}{2}\beta^2 f^2 \mathrm{Tr}\{(\mathbf{x}-\mathbf{v})(\mathbf{x}-\mathbf{v})^\mathsf{T}\mathbf{1}_m\}} = \int e^{-\beta f\left[\sum_{a=1}^m (x-\mathrm{v}_a)\right] z_0} \mathrm{D}z_0, \tag{273a}$$

$$e^{\frac{1}{2}\beta^2 g_\kappa^2 \mathrm{Tr}\{(\mathbf{x}-\mathbf{v})(\mathbf{x}-\mathbf{v})^\mathsf{T}\mathbf{I}_{\frac{m\beta}{\mu_\kappa}}\otimes \mathbf{1}_{\frac{\mu_\kappa}{\beta}}\}} = \prod_{k=0}^{\Xi_\kappa} \int e^{-\beta g_\kappa \left[\sum_{a=\varrho_k^\kappa}^{\breve{\varrho}_k^\kappa} (x-\mathrm{v}_a)\right] z_\kappa} \mathrm{D}z_\kappa, \tag{273b}$$

with $\varrho_k^\kappa = k\mu_\kappa\beta^{-1}+1$, $\breve{\varrho}_k^\kappa = (k+1)\mu_\kappa\beta^{-1}$, and $\Xi_\kappa = m\beta\mu_\kappa^{-1}-1$, the partition function finally reads

$$\mathcal{Z}^{\mathsf{R}}(\beta;\boldsymbol{\mu}|\mathbf{x}) = \int \left[\bigwedge_{\varsigma=2}^{b} \int \left[\int \left[\sum_v e^{-\beta\left[e(x-v)^2 + (fz_0 + \sum_{\kappa=1}^b g_\kappa z_\kappa)(x-v) + u(v)\right]} \right]^{\frac{\mu_1}{\beta}} \mathrm{D}z_1 \right]^{\frac{\mu_\varsigma}{\mu_{\varsigma-1}}} \mathrm{D}z_\varsigma \right]^{\frac{m\beta}{\mu_b}} \mathrm{D}z_0 \tag{274}$$

with $v \in \mathbb{X}$ where for the sequences $\{\xi_\varsigma\}$ and $\{z_\varsigma\}$ we define

$$\bigwedge_{\varsigma=1}^{b} \int \mathrm{F}^{\xi_\varsigma} \mathrm{D}z_\varsigma \coloneqq \int \left[\cdots \int \left[\int \mathrm{F}^{\xi_1} \mathrm{D}z_1 \right]^{\xi_2} \mathrm{D}z_2 \cdots \right]^{\xi_b} \mathrm{D}z_b. \tag{275}$$

Consequently, one evaluates the free energy as in (53) which by using the Riesz equality when $m \downarrow 0$ reduces to

$$\mathsf{F}^{\mathsf{R}}(\beta;\boldsymbol{\mu}) = -\frac{1}{\mu_b}\mathsf{E} \int \log \left\{ \bigwedge_{\varsigma=1}^{b} \int \left[\sum_v e^{-\beta\left[e(x-v)^2 + (fz_0 + \sum_{\kappa=1}^b g_\kappa z_\kappa)(x-v) + u(v)\right]} \right]^{\frac{\mu_\varsigma}{\mu_{\varsigma-1}}} \mathrm{D}z_\varsigma \right\} \mathrm{D}z_0 \tag{276}$$

where we have defined $\mu_0 = \beta$ for sake of compactness. The fixed point equations are, moreover, found via (50) where we have

$$\left[\frac{\chi}{\beta} + \sum_{\kappa=1}^b p_\kappa + q\right] m = \mathsf{E}_{\mathbf{x}} \sum_{\mathbf{v}} \|\mathbf{x}-\mathbf{v}\|^2 \ \mathrm{p}^\beta_{\mathbf{v}|\mathbf{x}}(\mathbf{v}|\mathbf{x}), \tag{277a}$$

$$\left[\frac{\tilde{\chi}_{\kappa-1}}{\beta} + \frac{\mu_\kappa}{\beta}\left(\sum_{\varsigma=\kappa}^b p_\varsigma + q\right)\right] m = \mathsf{E}_{\mathbf{x}} \sum_{\mathbf{v}} \mathrm{Tr}\{(\mathbf{x}-\mathbf{v})(\mathbf{x}-\mathbf{v})^\mathsf{T}\mathbf{I}_{\frac{m\beta}{\mu_\kappa}} \otimes \mathbf{1}_{\frac{\mu_\kappa}{\beta}}\} \ \mathrm{p}^\beta_{\mathbf{v}|\mathbf{x}}(\mathbf{v}|\mathbf{x}), \tag{277b}$$

$$\left[\frac{\tilde{\chi}_b}{\beta} + mq\right] m = \mathsf{E}_{\mathbf{x}} \sum_{\mathbf{v}} \mathrm{Tr}\{(\mathbf{x}-\mathbf{v})(\mathbf{x}-\mathbf{v})^\mathsf{T}\mathbf{1}_m\} \ \mathrm{p}^\beta_{\mathbf{v}|\mathbf{x}}(\mathbf{v}|\mathbf{x}) \tag{277c}$$

for $\kappa \in [1:b]$. (277a) and (277c) are found by taking trace and sum over all the entries from both sides of (50), respectively. (277b) is moreover concluded by adding up the entries over the diagonal blocks of size $\mu_\kappa\beta^{-1}$. The right hand sides of (277a)-(277c) can then be evaluated using the equalities

$$\mathsf{E}_{\mathbf{x}} \sum_{\mathbf{v}} \|\mathbf{x}-\mathbf{v}\|^2 \ \mathrm{p}^\beta_{\mathbf{v}|\mathbf{x}}(\mathbf{v}|\mathbf{x}) = m\frac{\partial}{\partial e}\mathsf{F}^{\mathsf{R}}(\beta, m; \boldsymbol{\mu}), \tag{278a}$$

$$\mathsf{E}_{\mathbf{x}} \sum_{\mathbf{v}} \mathrm{Tr}\{(\mathbf{x}-\mathbf{v})(\mathbf{x}-\mathbf{v})^\mathsf{T}\mathbf{I}_{\frac{m\beta}{\mu_\kappa}} \otimes \mathbf{1}_{\frac{\mu_\kappa}{\beta}}\} \ \mathrm{p}^\beta_{\mathbf{v}|\mathbf{x}}(\mathbf{v}|\mathbf{x}) = -\frac{m}{\beta g_\kappa}\frac{\partial}{\partial g_\kappa}\mathsf{F}^{\mathsf{R}}(\beta, m; \boldsymbol{\mu}), \tag{278b}$$

$$\mathsf{E}_{\mathbf{x}} \sum_{\mathbf{v}} \mathrm{Tr}\{(\mathbf{x}-\mathbf{v})(\mathbf{x}-\mathbf{v})^\mathsf{T}\mathbf{1}_m\} \ \mathrm{p}^\beta_{\mathbf{v}|\mathbf{x}}(\mathbf{v}|\mathbf{x}) = -\frac{m}{\beta f}\frac{\partial}{\partial f}\mathsf{F}^{\mathsf{R}}(\beta, m; \boldsymbol{\mu}). \tag{278c}$$

Thus, the fixed point equations are finally concluded as

$$\frac{\chi}{\beta}+\sum_{\kappa=1}^{b}p_\kappa+q=\mathsf{E}\int\frac{\sum_v(v-x)^2\ e^{-\beta\left[e(x-v)^2+(fz_0+\sum_{\kappa=1}^{b}g_\kappa z_\kappa)(x-v)+u(v)\right]}}{\sum_v e^{-\beta\left[e(x-v)^2+(fz_0+\sum_{\kappa=1}^{b}g_\kappa z_\kappa)(x-v)+u(v)\right]}}\prod_{\kappa=1}^{b}\tilde{\Lambda}_\kappa^\beta\ \mathrm{D}z_\kappa\mathrm{D}z_0 \tag{279a}$$

$$\tilde{\chi}_{\kappa-1}+\mu_\kappa\left(\sum_{\varsigma=\kappa}^{b}p_\varsigma+q\right)=\frac{1}{g_\kappa}\mathsf{E}\int\frac{\sum_v(v-x)z_\kappa\ e^{-\beta\left[e(x-v)^2+(fz_0+\sum_{\kappa=1}^{b}g_\kappa z_\kappa)(x-v)+u(v)\right]}}{\sum_v e^{-\beta\left[e(x-v)^2+(fz_0+\sum_{\kappa=1}^{b}g_\kappa z_\kappa)(x-v)+u(v)\right]}}\times$$

$$\times\prod_{\kappa=1}^{b}\tilde{\Lambda}_\kappa^\beta\ \mathrm{D}z_\kappa\mathrm{D}z_0 \tag{279b}$$

$$\tilde{\chi}_b=\frac{1}{f}\mathsf{E}\int\frac{\sum_v(v-x)z_0\ e^{-\beta\left[e(x-v)^2+(fz_0+\sum_{\kappa=1}^{b}g_\kappa z_\kappa)(x-v)+u(v)\right]}}{\sum_v e^{-\beta\left[e(x-v)^2+(fz_0+\sum_{\kappa=1}^{b}g_\kappa z_\kappa)(x-v)+u(v)\right]}}\prod_{\kappa=1}^{b}\tilde{\Lambda}_\kappa^\beta\ \mathrm{D}z_\kappa\mathrm{D}z_0. \tag{279c}$$

for $\kappa\in[1:b]$ in which we denote $\tilde{\Lambda}_\kappa^\beta:=\left[\int\Lambda_\kappa^\beta\mathrm{D}z_\kappa\right]^{-1}\Lambda_\kappa^\beta$ with Λ_1^β

$$\Lambda_1^\beta:=\left[\sum_v e^{-\beta\left[e(x-v)^2+(fz_0+\sum_{\kappa=1}^{b}g_\kappa z_\kappa)(x-v)+u(v)\right]}\right]^{\frac{\mu_1}{\beta}} \tag{280}$$

and $\{\Lambda_\kappa^\beta\}$ for $\kappa\in[2:b]$ being recursively defined as

$$\Lambda_\kappa^\beta:=\left[\int\Lambda_{\kappa-1}^\beta\ \mathrm{D}z_{\kappa-1}\right]^{\frac{\mu_\kappa}{\mu_{\kappa-1}}}. \tag{281}$$

The replicas' average distortion regarding the distortion function $\mathsf{d}(\cdot;\cdot)$ is further determined using the Hamiltonian modification technique employed in Appendix B and C. After modifying the Hamiltonian and taking the derivatives, the average distortion at the inverse temperature β is given by

$$\mathsf{D}^{\mathsf{R}}(\beta;\boldsymbol{\mu})=\mathsf{E}\int\frac{\sum_v\mathsf{d}(v;x)e^{-\beta\left[e(x-v)^2+(fz_0+\sum_{\kappa=1}^{b}g_\kappa z_\kappa)(x-v)+u(v)\right]}}{\sum_v e^{-\beta\left[e(x-v)^2+(fz_0+\sum_{\kappa=1}^{b}g_\kappa z_\kappa)(x-v)+u(v)\right]}}\prod_{\kappa=1}^{b}\tilde{\Lambda}_\kappa^\beta\ \mathrm{D}z_\kappa\mathrm{D}z_0. \tag{282}$$

Finally, by taking the limit $\beta\uparrow\infty$, we find the asymptotic distortion as

$$\mathsf{D}^{\mathsf{W}}=\mathsf{E}\int\mathsf{d}(\mathrm{g};x)\prod_{\kappa=1}^{b}\tilde{\Lambda}_\kappa\ \mathrm{D}z_\kappa\mathrm{D}z_0 \tag{283}$$

where g is defined as

$$\mathrm{g}:=\arg\min_v\left[e(x-v)^2+(fz_0+\sum_{\kappa=1}^{b}g_\kappa z_\kappa)(x-v)+u(v)\right], \tag{284}$$

and $\tilde{\Lambda}_\kappa$ denotes the limiting factor $\tilde{\Lambda}_\kappa^\infty$. Considering the definition of $\tilde{\Lambda}_\kappa^\beta$, $\tilde{\Lambda}_\kappa$ reads $\tilde{\Lambda}_\kappa = \left[\int \Lambda_\kappa \mathrm{D}z_\kappa\right]^{-1} \Lambda_\kappa$ with

$$\Lambda_1 \coloneqq e^{-\mu_1 \left[e(x-\mathrm{g})^2 + (fz_0 + \sum_{\kappa=1}^{b} g_\kappa z_\kappa)(x-\mathrm{g}) + u(\mathrm{g})\right]} \tag{285}$$

and $\{\Lambda_\kappa\}$ for $\kappa \in [2:b]$

$$\Lambda_\kappa \coloneqq \left[\int \Lambda_{\kappa-1}\ \mathrm{D}z_{\kappa-1}\right]^{\frac{\mu_\kappa}{\mu_{\kappa-1}}}. \tag{286}$$

Moreover, the fixed point equations reduce to

$$\sum_{\kappa=1}^{b} p_\kappa + q = \mathsf{E} \int (\mathrm{g}-x)^2 \prod_{\kappa=1}^{b} \tilde{\Lambda}_\kappa\ \mathrm{D}z_\kappa \mathrm{D}z_0, \tag{287a}$$

$$\tilde{\chi}_{\kappa-1} + \mu_\kappa \left(\sum_{\varsigma=\kappa}^{b} p_\varsigma + q\right) = \frac{1}{g_\kappa} \mathsf{E} \int (\mathrm{g}-x) z_\kappa \prod_{\kappa=1}^{b} \tilde{\Lambda}_\kappa\ \mathrm{D}z_\kappa \mathrm{D}z_0, \tag{287b}$$

$$\tilde{\chi}_b = \frac{1}{f} \mathsf{E} \int (\mathrm{g}-x) z_0 \prod_{\kappa=1}^{b} \tilde{\Lambda}_\kappa\ \mathrm{D}z_\kappa \mathrm{D}z_0, \tag{287c}$$

for $\kappa \in [1:b]$.

As in the 1RSB ansatz, we set $\boldsymbol{\mu}$ to be the extreme point of the free energy at a given inverse temperature β, in order to satisfy the second law of thermodynamics. The solution needs to be found over the set of non-negative real vectors which satisfy the constraint in (269). The parameters of the ansatz, however, are finally taken such that the zero temperature free energy is minimized.

Using Proposition IV.1, the free energy of the corresponding spin glass for a given vector $\boldsymbol{\mu}$ is written as

$$\mathsf{F}(\beta;\boldsymbol{\mu}) = \frac{1}{2\lambda}\left[\int_0^1 \mathrm{F}^\beta(\omega;\boldsymbol{\mu})\mathrm{d}\omega - \mathrm{F}^\beta(1;\boldsymbol{\mu})\right] + \mathsf{F}^{\mathsf{R}}(\beta;\boldsymbol{\mu}) \tag{288}$$

where the function $\mathrm{F}^\beta(\cdot;\boldsymbol{\mu})$ is defined as

$$\mathrm{F}^\beta(\omega;\boldsymbol{\mu}) = \sum_{\kappa=1}^{b} \frac{1}{\mu_\kappa} \frac{\mathrm{d}}{\mathrm{d}\omega} \int_{\tilde{\chi}_{\kappa-1}\omega}^{\tilde{\chi}_\kappa \omega} \mathrm{R}_{\mathbf{J}}(-\frac{t}{\lambda})\mathrm{d}t + \frac{\chi}{\beta}\mathrm{R}_{\mathbf{J}}(-\frac{\chi}{\lambda}\omega) + \left[q - \frac{\lambda_0}{\lambda}\tilde{\chi}_b\right] \frac{\mathrm{d}}{\mathrm{d}\omega}\left[\omega \mathrm{R}_{\mathbf{J}}(-\frac{\tilde{\chi}_b}{\lambda}\omega)\right]. \tag{289}$$

Therefore, the vector $\boldsymbol{\mu}^\star$, for a given β, is set as

$$\boldsymbol{\mu}^\star = \arg\min_{\boldsymbol{\mu}} \mathsf{F}(\beta;\boldsymbol{\mu}) \tag{290}$$

with $\boldsymbol{\mu} \in \mathbb{S}_{\boldsymbol{\mu}}$ where $\mathbb{S}_{\boldsymbol{\mu}}$ is the set of non-negative real vectors satisfying the constraint in (269). By substituting (271a)-(271c) in (289), $\boldsymbol{\mu}^\star$ reduces to

$$\boldsymbol{\mu}^\star = \arg\min_{\boldsymbol{\mu}} \left\{\frac{1}{2\lambda}\left[\int_0^1 \mathrm{F}^\beta(\omega;\boldsymbol{\mu})\mathrm{d}\omega\right] + \mathsf{F}^{\mathsf{R}}(\beta;\boldsymbol{\mu}) - e\Delta(\boldsymbol{\mu})\right\} \tag{291}$$

with $\boldsymbol{\mu} \in \mathbb{S}_{\boldsymbol{\mu}}$ where $\Delta(\cdot)$ reads

$$\Delta(\boldsymbol{\mu}) \coloneqq \frac{1}{e}\left\{\sum_{\kappa=1}^{b} \frac{1}{\mu_\kappa}\left[\tilde{e}_\kappa \tilde{\chi}_\kappa - \tilde{e}_{\kappa-1}\tilde{\chi}_{\kappa-1}\right] + \left[\frac{\tilde{e}_0\tilde{\chi}_0}{\beta} + \tilde{e}_b q - \frac{f^2}{2}\tilde{\chi}_b\right]\right\} \tag{292}$$

with $\tilde{e}_0 \coloneqq e$ and

$$\tilde{e}_\kappa \coloneqq e - \sum_{\varsigma=1}^{\kappa} \mu_\varsigma \frac{g_\varsigma^2}{2} \tag{293}$$

for $\kappa \in [1:b]$. The vector $\boldsymbol{\mu}^\star$ is then determined such that it minimizes the free energy . Finally by taking the limit $\beta \uparrow \infty$, the zero temperature free energy is evaluated as

$$\mathsf{F}^0 = \frac{1}{2\lambda}\left[\int_0^1 \mathrm{F}^\infty(\omega)\mathrm{d}\omega - \mathrm{F}^\infty(1)\right] - \frac{1}{\mu_b}\mathsf{E}\int \log\left[\int \Lambda_b \mathrm{D}z_b\right]\mathrm{D}z_0 \tag{294}$$

where we define

$$\mathrm{F}^\infty(\omega) \coloneqq \lim_{\beta\uparrow\infty} \mathrm{F}^\beta(\omega;\boldsymbol{\mu}^\star). \tag{295}$$

Denoting $\lambda^{\mathsf{s}} \coloneqq [2e]^{-1}$, $\lambda_0^{\mathsf{s}} \coloneqq \left[4e^2\right]^{-1} f^2$ and $\lambda_\kappa^{\mathsf{s}} \coloneqq \left[4e^2\right]^{-1} g_\kappa^2$ for $\kappa \in [1:b]$, and defining the sequence $\{\zeta_\kappa\}$ such that $\zeta_0 = 1$ and

$$\zeta_\kappa \coloneqq 1 - \sum_{\varsigma=1}^{\kappa} \mu_\varsigma \frac{\lambda_\varsigma^{\mathsf{s}}}{\lambda^{\mathsf{s}}} \tag{296}$$

for $\kappa \in [1:b]$, Proposition VI.3 is concluded.

APPENDIX E
GENERAL RSB FREQUENCY DOMAIN CORRELATION MATRIX

Consider the spin glass of replicas defined in Definition IV.1, the Hamiltonian reads

$$\mathcal{E}^{\mathsf{R}}(\mathbf{v}|\mathbf{x}) = (\mathbf{x}-\mathbf{v})^{\mathsf{T}}\mathbf{R}(\mathbf{x}-\mathbf{v}) + u(\mathbf{v}). \tag{297}$$

where $\mathbf{R} \coloneqq \mathbf{T}\mathrm{R}_{\mathbf{J}}(-2\beta\mathbf{TQ})$ is referred to as the "frequency domain correlation matrix". In this appendix, we show that under the general RSB assumption on $\mathbf{Q}$, including the RS case, the frequency domain correlation matrix has the same structure with different scalar coefficients. To show that, let the correlation matrix be of the form

$$\mathbf{Q} = q_0\mathbf{I}_m + \sum_{i=1}^{b} q_i \mathbf{I}_{\frac{m}{\xi_i}} \otimes \mathbf{1}_{\xi_i} + q_{b+1}\mathbf{1}_m \tag{298}$$

for some integer b where $q_0, q_{b+1} \neq 0$. (298) represents the bRSB as well as RS structures by setting the coefficients correspondingly. Considering $\mathbf{T}$ as defined in (49), $\mathbf{TQ}$ is then written as

$$\mathbf{TQ} = \frac{1}{2\lambda}\left[\mathbf{Q} - \frac{\beta\lambda_0}{\lambda + m\beta\lambda_0}\mathbf{1}_m\mathbf{Q}\right]. \tag{299}$$

Defining the vector $\boldsymbol{u}_{m\times 1}$ as a vector with all entries equal to 1, it is clear that $\boldsymbol{u}$ is an eigenvector of $\mathbf{Q}$, and therefore, by denoting the eigendecomposition of $\mathbf{Q}$ as $\mathbf{V}\mathbf{D}^{\mathrm{Q}}\mathbf{V}^{\mathsf{T}}$, $\mathbf{1}_m$ reads

$$\mathbf{1}_m = \boldsymbol{u}\boldsymbol{u}^{\mathsf{T}} = \mathbf{V}\mathbf{D}^{1}\mathbf{V}^{\mathsf{T}} \tag{300}$$

where $\mathbf{D}^1$ is a diagonal matrix in which all the diagonal entries expect the entry corresponding to the eigenvector $\boldsymbol{u}$ are zero. Consequently, (299) reduces to

$$\mathbf{TQ} = \frac{1}{2\lambda}\mathbf{V}\left[\mathbf{D}^{\mathrm{Q}} - \frac{\beta\lambda_0}{\lambda + m\beta\lambda_0}\mathbf{D}^{1}\mathbf{D}^{\mathrm{Q}}\right]\mathbf{V}^{\mathsf{T}} \tag{301}$$

which states that $\mathbf{TQ}$ and $\mathbf{Q}$ span the same eigenspace. The eigenvalues of $\mathbf{TQ}$ and $\mathbf{Q}$ are also distributed with the same frequencies. In fact, as the eigenvalue corresponding to $\boldsymbol{u}$ occurs with multiplicity 1, the second term on the right hand side of (299) does not change the distribution of eigenvalues and only modifies the eigenvalue corresponding to $\boldsymbol{u}$. Therefore, $\mathbf{TQ}$ can be also represented as in (298) with different scalar coefficient.

To extend the scope of the analysis to $\mathbf{R}$, we note that the function $\mathrm{R}_{\mathbf{J}}(\cdot)$ is strictly increasing for any $\mathrm{F}_{\mathbf{J}}$ different from the single mass point CDF[1] [63]. Consequently, the eigenvalues' distribution remains unchanged, and thus,

$$\mathbf{R} = r_0\mathbf{I}_m + \sum_{i=1}^{b} r_i \mathbf{I}_{\frac{m}{\xi_i}} \otimes \mathbf{1}_{\xi_i} + r_{b+1}\mathbf{1}_m. \tag{302}$$

for some real $\{r_i\}$. In the case that $\mathrm{F}_{\mathbf{J}}$ is the single mass point CDF, the R-transform becomes a constant function which results in $\mathrm{R}_{\mathbf{J}}(-2\beta\mathbf{TQ}) = \mathsf{K}\mathbf{I}_m$ for some constant K. Therefore, $\mathbf{R} = \mathsf{K}\mathbf{T}$ which is again represented as in (302) by setting $r_i = 0$ for $i \in [1:b]$. This concludes that $\mathbf{R}$ has the same structure as $\mathbf{Q}$ for any $\mathrm{F}_{\mathbf{J}}$.

[1] In the single mass point CDF, we have $\mathrm{F}_{\mathbf{J}}(\lambda) = \mathbf{1}\{\lambda \geq \mathsf{K}\}$ for some real constant K.

APPENDIX F
ASYMPTOTICS OF SPHERICAL INTEGRAL

Consider μ_n^ζ to be the Haar measure on the orthogonal group $\mathbb{O}_n$ for $\zeta = 1$, and on the unitary group $\mathbb{U}_n$ for $\zeta = 2$. Let $\mathbf{G}_n$ and $\mathbf{D}_n$ be $n \times n$ matrices; then, the integral of the form

$$\mathrm{I}_n^\zeta(\mathbf{G}_n, \mathbf{D}_n) \coloneqq \int e^{n\mathrm{Tr}\{\mathbf{U}\mathbf{G}_n\mathbf{U}^\dagger\mathbf{D}_n\}} \mathrm{d}\mu_n^\zeta(\mathbf{U}), \tag{303}$$

is known as the "spherical integral". This integral has been extensively studied in the mathematics literature, as well as physics where it is often called "Harish-Chandra" or "Itzykson & Zuber" integral. In a variety of problems, such as ours, the evaluation of spherical integrals in asymptotic regime is interesting, and therefore, several investigations have been done on this asymptotics. In [55], the asymptotics of the integral has been investigated when the matrices $\mathbf{G}_n$ and $\mathbf{D}_n$ have n distinct eigenvalues with converging spectrums, and under some assumptions, a closed form formula has been given; however, the final formula in [55] is too complicated and hard to employ. In [56], the authors showed that, for a low-rank $\mathbf{G}_n$, the asymptotics of the integral can be written directly in terms of the R-transform corresponding to the asymptotic eigenvalue distribution of $\mathbf{D}_n$. As long as the replica analysis is being considered, we can utilize the result from [56], since the number of replicas can be considered to be small enough.

In [56], Theorem 1.2, it is shown that when $\mathbf{G}_n$ is a rank-one matrix, under the assumption that the spectrum of $\mathbf{D}_n$ asymptotically converges to a deterministic CDF $\mathrm{F}_{\mathbf{D}}$ with compact and finite length support, the asymptotics of the integral can be written in terms of the R-transform $\mathrm{R}_{\mathbf{D}}(\cdot)$ as

$$\lim_{n\uparrow\infty} \frac{1}{n} \log \mathrm{I}_n^\zeta(\mathbf{G}_n, \mathbf{D}_n) = \int_0^\theta \mathrm{R}_{\mathbf{D}}(\frac{2\omega}{\zeta}) \mathrm{d}\omega, \tag{304}$$

in which θ denotes the single nonzero eigenvalue of $\mathbf{G}_n$. The authors further showed in Theorem 1.7 that in the case of $\mathrm{rank}(\mathbf{G}_n) = \mathcal{O}(\sqrt{n})$, under the same assumption as in Theorem 1.2, the spherical integral asymptotically factorizes into product of rank-one integrals, and therefore,

$$\lim_{n\uparrow\infty} \frac{1}{n} \log \mathrm{I}_n^\zeta(\mathbf{G}_n, \mathbf{D}_n) = \sum_{i=1}^m \int_0^{\theta_i} \mathrm{R}_{\mathbf{D}}(\frac{2\omega}{\zeta}) \mathrm{d}\omega, \tag{305}$$

with $\{\theta_i\}$ denoting the nonzero eigenvalues of $\mathbf{G}_n$ for $i \in [1:m]$, and $m = \mathrm{rank}(\mathbf{G}_n)$.

In Appendix A, one can employ (305) in order to evaluate the asymptotics over the system matrix consistent to the system setup illustrated in Section II. Moreover, by using the above discussion, the investigations in Appendix A can be extended to the case of complex variables. More about the spherical integral and its asymptotics can be found in [56], and the references therein.

REFERENCES

[1] S. F. Edwards and P. W. Anderson, "Theory of spin glasses," *Journal of Physics F: Metal Physics*, vol. 5, no. 5, p. 965, 1975.

[2] L. Pastur and M. Shcherbina, "Absence of self-averaging of the order parameter in the Sherrington-Kirkpatrick model," *Journal of Statistical Physics*, vol. 62, no. 1-2, pp. 1–19, 1991.

[3] F. Guerra and F. L. Toninelli, "The thermodynamic limit in mean field spin glass models," *Communications in Mathematical Physics*, vol. 230, no. 1, pp. 71–79, 2002.

[4] ——, "The infinite volume limit in generalized mean field disordered models," *arXiv preprint cond-mat/0208579*, 2002.

[5] S. B. Korada and N. Macris, "Tight bounds on the capacity of binary input random CDMA systems," *Information Theory, IEEE Transactions on*, vol. 56, no. 11, pp. 5590–5613, 2010.

[6] N. Merhav, *Statistical physics and information theory*. Now Publishers Inc, 2010.

[7] M. Mézard and G. Parisi, "A replica analysis of the travelling salesman problem," *Journal de Physique*, vol. 47, no. 8, pp. 1285–1296, 1986.

[8] Y. Fu and P. W. Anderson, "Application of statistical mechanics to NP-complete problems in combinatorial optimisation," *Journal of Physics A: Mathematical and General*, vol. 19, no. 9, p. 1605, 1986.

[9] H. Nishimori, *Statistical physics of spin glasses and information processing: an introduction*. Clarendon Press, 2001, no. 111.

[10] A. Montanari, "Turbo codes: The phase transition," *The European Physical Journal B-Condensed Matter and Complex Systems*, vol. 18, no. 1, pp. 121–136, 2000.

[11] T. Tanaka, "A statistical-mechanics approach to large-system analysis of CDMA multiuser detectors," *Information Theory, IEEE Transactions on*, vol. 48, no. 11, pp. 2888–2910, 2002.

[12] ——, "Average-case analysis of multiuser detectors," 2001.

[13] D. Guo and S. Verdú, "Multiuser detection and statistical mechanics," in *Communications, Information and Network Security*. Springer, 2003, pp. 229–277.

[14] R. R. Müller, "Channel capacity and minimum probability of error in large dual antenna array systems with binary modulation," *IEEE Transactions on Signal Processing*, vol. 51, no. 11, pp. 2821–2828, 2003.

[15] D. Guo and S. Verdú, "Randomly spread CDMA: Asymptotics via statistical physics," *Information Theory, IEEE Transactions on*, vol. 51, no. 6, pp. 1983–2010, 2005.

[16] R. Müller, D. Guo, and A. L. Moustakas, "Vector precoding for wireless MIMO systems and its replica analysis," *Selected Areas in Communications, IEEE Journal on*, vol. 26, no. 3, pp. 530–540, 2008.

[17] D. Guo, D. Baron, and S. Shamai, "A single-letter characterization of optimal noisy compressed sensing," in *Communication, Control, and Computing, 2009. Allerton 2009. 47th Annual Allerton Conference on*. IEEE, 2009, pp. 52–59.

[18] D. Guo, S. Verdú, and L. K. Rasmussen, "Asymptotic normality of linear multiuser receiver outputs," *Information Theory, IEEE Transactions on*, vol. 48, no. 12, pp. 3080–3095, 2002.

[19] D. N. Tse and S. V. Hanly, "Linear multiuser receivers: Effective interference, effective bandwidth and user capacity," *Information Theory, IEEE Transactions on*, vol. 45, no. 2, pp. 641–657, 1999.

[20] D. N. Tse and O. Zeitouni, "Linear multiuser receivers in random environments," *Information Theory, IEEE Transactions on*, vol. 46, no. 1, pp. 171–188, 2000.

[21] Y. C. Eldar and A. M. Chan, "On the asymptotic performance of the decorrelator," *Information Theory, IEEE Transactions on*, vol. 49, no. 9, pp. 2309–2313, 2003.

[22] S. Verdú and S. Shamai, "Spectral efficiency of CDMA with random spreading," *Information Theory, IEEE Transactions on*, vol. 45, no. 2, pp. 622–640, 1999.

[23] J. Zhang, E. K. Chong, and D. N. Tse, "Output MAI distributions of linear MMSE multiuser receivers in DS-CDMA systems," *Information Theory, IEEE Transactions on*, vol. 47, no. 3, pp. 1128–1144, 2001.

[24] A. M. Tulino and S. Verdú, "Random matrix theory and wireless communications," *Communications and Information theory*, vol. 1, no. 1, pp. 1–182, 2004.

[25] R. R. Müller, G. Alfano, B. M. Zaidel, and R. de Miguel, "Applications of large random matrices in communications engineering," *arXiv preprint arXiv:1310.5479*, 2013.

[26] D. Guo, L. K. Rasmussen, and T. J. Lim, "Linear parallel interference cancellation in long-code CDMA multiuser detection," *Selected Areas in Communications, IEEE Journal on*, vol. 17, no. 12, pp. 2074–2081, 1999.

[27] S. Shamai and S. Verdú, "The impact of frequency-flat fading on the spectral efficiency of CDMA," *Information Theory, IEEE Transactions on*, vol. 47, no. 4, pp. 1302–1327, 2001.

[28] R. R. Müller and W. H. Gerstacker, "On the capacity loss due to separation of detection and decoding," *Information Theory, IEEE Transactions on*, vol. 50, no. 8, pp. 1769–1778, 2004.

[29] R. R. Müller, "On channel capacity, uncoded error probability, ML-detection, and spin glasses," in *Proc. Workshop on Concepts in Information Theory*. pp. 79–81, Breisach, Germany, June 2002.

[30] S. Rangan, A. K. Fletcher, and V. Goyal, "Asymptotic analysis of MAP estimation via the replica method and applications to compressed sensing," in *IEEE Transactions on Information Theory*, 2012, pp. 1902–1923.

[31] A. M. Tulino, G. Caire, S. Verdu, and S. Shamai, "Support recovery with sparsely sampled free random matrices," *Information Theory, IEEE Transactions on*, vol. 59, no. 7, pp. 4243–4271, 2013.

[32] M. Vehkaperä, Y. Kabashima, and S. Chatterjee, "Analysis of regularized LS reconstruction and random matrix ensembles in compressed sensing," *IEEE Transactions on Information Theory*, vol. 62, no. 4, pp. 2100–2124, 2016.

[33] D. L. Donoho, "Compressed sensing," *Information Theory, IEEE Transactions on*, vol. 52, no. 4, pp. 1289–1306, 2006.

[34] E. J. Candès, J. Romberg, and T. Tao, "Robust uncertainty principles: Exact signal reconstruction from highly incomplete frequency information," *Information Theory, IEEE Transactions on*, vol. 52, no. 2, pp. 489–509, 2006.

[35] E. J. Candes and T. Tao, "Near-optimal signal recovery from random projections: Universal encoding strategies?" *Information Theory, IEEE Transactions on*, vol. 52, no. 12, pp. 5406–5425, 2006.

[36] D. L. Donoho and X. Huo, "Uncertainty principles and ideal atomic decomposition," *Information Theory, IEEE Transactions on*, vol. 47, no. 7, pp. 2845–2862, 2001.

[37] M. Elad and A. M. Bruckstein, "A generalized uncertainty principle and sparse representation in pairs of bases," *Information Theory, IEEE Transactions on*, vol. 48, no. 9, pp. 2558–2567, 2002.

[38] D. L. Donoho and M. Elad, "Optimally sparse representation in general (nonorthogonal) dictionaries via ℓ_1 minimization," *Proceedings of the National Academy of Sciences*, vol. 100, no. 5, pp. 2197–2202, 2003.

[39] R. Tibshirani, "Regression shrinkage and selection via the LASSO," *Journal of the Royal Statistical Society. Series B (Methodological)*, pp. 267–288, 1996.

[40] S. S. Chen, D. L. Donoho, and M. A. Saunders, "Atomic decomposition by basis pursuit," *SIAM review*, vol. 43, no. 1, pp. 129–159, 2001.

[41] D. Needell and J. A. Tropp, "Cosamp: Iterative signal recovery from incomplete and inaccurate samples," *Applied and Computational Harmonic Analysis*, vol. 26, no. 3, pp. 301–321, 2009.

[42] W. Dai and O. Milenkovic, "Subspace pursuit for compressive sensing signal reconstruction," *Information Theory, IEEE Transactions on*, vol. 55, no. 5, pp. 2230–2249, 2009.

[43] T. T. Cai and L. Wang, "Orthogonal matching pursuit for sparse signal recovery with noise," *Information Theory, IEEE Transactions on*, vol. 57, no. 7, pp. 4680–4688, 2011.

[44] D. Donoho and J. Tanner, "Counting faces of randomly projected polytopes when the projection radically lowers dimension," *Journal of the American Mathematical Society*, vol. 22, no. 1, pp. 1–53, 2009.

[45] D. L. Donoho and J. Tanner, "Counting the faces of randomly-projected hypercubes and orthants, with applications," *Discrete & computational geometry*, vol. 43, no. 3, pp. 522–541, 2010.

[46] ——, "Precise undersampling theorems," *Proceedings of the IEEE*, vol. 98, no. 6, pp. 913–924, 2010.

[47] M. Bayati and A. Montanari, "The dynamics of message passing on dense graphs, with applications to compressed sensing," *IEEE Transactions on Information Theory*, vol. 57, no. 2, pp. 764–785, 2011.

[48] E. Bolthausen, "On the high-temperature phase of the sherrington-kirkpatrick model," in *Seminar at EURANDOM, Eindhoven*, 2009.

[49] G. Reeves and M. Gastpar, "The sampling rate-distortion tradeoff for sparsity pattern recovery in compressed sensing," *IEEE Transactions on Information Theory*, vol. 58, no. 5, pp. 3065–3092, 2012.

[50] Y. Wu and S. Verdú, "Optimal phase transitions in compressed sensing," *Information Theory, IEEE Transactions on*, vol. 58, no. 10, pp. 6241–6263, 2012.

[51] F. Krzakala, M. Mézard, F. Sausset, Y. Sun, and L. Zdeborová, "Statistical-physics-based reconstruction in compressed sensing," *Physical Review X*, vol. 2, no. 2, p. 021005, 2012.

[52] Y. Kabashima, T. Wadayama, and T. Tanaka, "Statistical mechanical analysis of a typical reconstruction limit of compressed sensing," *arXiv preprint arXiv:1001.4298*, 2010.

[53] ——, "A typical reconstruction limit for compressed sensing based on ℓ_p-norm minimization," *Journal of Statistical Mechanics: Theory and Experiment*, vol. 2009, no. 09, p. L09003, 2009.

[54] C.-K. Wen, J. Zhang, K.-K. Wong, J.-C. Chen, and C. Yuen, "On sparse vector recovery performance in structurally orthogonal matrices via LASSO," *arXiv preprint arXiv:1410.7295*, 2014.

[55] A. Guionnet and O. Zeitouni, "Large deviations asymptotics for spherical integrals," *Journal of functional analysis*, vol. 188, no. 2, pp. 461–515, 2002.

[56] A. Guionnet, M. Maı *et al.*, "A fourier view on the R-transform and related asymptotics of spherical integrals," *Journal of functional analysis*, vol. 222, no. 2, pp. 435–490, 2005.

[57] N. I. Akhiezer, *The classical moment problem: and some related questions in analysis*. Oliver & Boyd, 1965, vol. 5.

[58] B. Simon, "The classical moment problem as a self-adjoint finite difference operator," *Advances in Mathematics*, vol. 137, no. 1, pp. 82–203, 1998.

[59] A. Bereyhi, R. Müller, and H. Schulz-Baldes, "RSB decoupling property of MAP estimators," in *Information Theory Workshop (ITW), 2016 IEEE*. IEEE, 2016, pp. 379–383.

[60] F. Riesz, "Sur les valeurs moyennes des fonctions," *Journal of the London Mathematical Society*, vol. 1, no. 2, pp. 120–121, 1930.

[61] A. Dembo and O. Zeitouni, *Large deviations techniques and applications*. Springer Science & Business Media, 2009, vol. 38.

[62] M. Mezard and A. Montanari, *Information, physics, and computation*. Oxford University Press, 2009.

[63] B. M. Zaidel, R. Müller, A. L. Moustakas, and R. de Miguel, "Vector precoding for gaussian MIMO broadcast channels: Impact of replica symmetry breaking," *Information Theory, IEEE Transactions on*, vol. 58, no. 3, pp. 1413–1440, 2012.

[64] G. Parisi, "A sequence of approximated solutions to the SK model for spin glasses," *Journal of Physics A: Mathematical and General*, vol. 13, no. 4, p. L115, 1980.

[65] M. N. Hansen and E. M. Schmidt, *Algorithms and data structures: transition systems*. Datalogisk Institut, Aarhus Universitet, 2003.

[66] A. Finkel and P. Schnoebelen, "Fundamental structures in well-structured infinite transition systems," in *LATIN'98: Theoretical Informatics*. Springer, 1998, pp. 102–118.

[67] R. Couillet and M. Debbah, *Random matrix methods for wireless communications*. Cambridge University Press, 2011.

[68] A. L. Moustakas and S. H. Simon, "On the outage capacity of correlated multiple-path MIMO channels," *Information Theory, IEEE Transactions on*, vol. 53, no. 11, pp. 3887–3903, 2007.

[69] D. Agrawal and A. Vardy, "The turbo decoding algorithm and its phase trajectories," *IEEE Transactions on Information Theory*, vol. 47, no. 2, pp. 699–722, 2001.

[70] M. Talagrand, *Spin glasses: a challenge for mathematicians: cavity and mean field models*. Springer Science & Business Media, 2003, vol. 46.

[71] F. Guerra and F. L. Toninelli, "Quadratic replica coupling in the Sherrington–Kirkpatrick mean field spin glass model," *Journal of Mathematical Physics*, vol. 43, no. 7, pp. 3704–3716, 2002.

[72] F. Guerra, "Broken replica symmetry bounds in the mean field spin glass model," *Communications in mathematical physics*, vol. 233, no. 1, pp. 1–12, 2003.

[73] Harish-Chandra, "Differential operators on a semisimple Lie algebra," *American Journal of Mathematics*, pp. 87–120, 1957.

[74] C. Itzykson and J.-B. Zuber, "The planar approximation. II," *Journal of Mathematical Physics*, vol. 21, no. 3, pp. 411–421, 1980.